

# Identifying Network Ties from Panel Data: Theory and an Application to Tax Competition\*

Áureo de Paula

Imran Rasul

Pedro CL Souza<sup>†</sup>

October 2019

## Abstract

Social interactions determine many economic behaviors, but information on social ties does not exist in most publicly available and widely used datasets. We present results on the identification of social networks from observational panel data that contains no information on social ties between agents. In the context of a canonical social interactions model, we provide sufficient conditions under which the social interactions matrix, endogenous and exogenous social effect parameters are all globally identified. While this result is relevant across different estimation strategies, we then describe how high-dimensional estimation techniques can be used to estimate the interactions model based on the Adaptive Elastic Net GMM method. We employ the method to study tax competition across US states. We find the identified social interactions matrix implies tax competition differs markedly from the common assumption of competition between geographically neighboring states, providing further insights for the long-standing debate on the relative roles of factor mobility and yardstick competition in driving tax setting behavior across states. Most broadly, our identification and application show the analysis of social interactions can be extended to economic realms where no network data exists. *JEL Codes: C31, D85, H71.*

---

\*We gratefully acknowledge financial support from the ESRC through the Centre for the Microeconomic Analysis of Public Policy (RES-544-28-0001), the Centre for Microdata Methods and Practice (RES-589-28-0001) and the Large Research Grant ES/P008909/1 and from the ERC (SG338187). We thank Edo Aioldi, Luis Alvarez, Oriana Bandiera, Larry Blume, Yann Bramoullé, Stephane Bonhomme, Vasco Carvalho, Gary Chamberlain, Andrew Chesher, Christian Dustmann, Sérgio Firpo, Jean-Pierre Florens, Eric Gautier, Giacomo de Giorgi, Matthew Gentzkow, Stefan Hoderlein, Bo Honoré, Matt Jackson, Dale Jorgensen, Christian Julliard, Maximilian Kasy, Miles Kimball, Thibaut Lamadon, Simon Sokbae Lee, Arthur Lewbel, Tong Li, Xiadong Liu, Elena Manresa, Charles Manski, Marcelo Medeiros, Angelo Mele, Francesca Molinari, Pepe Montiel, Andrea Moro, Whitney Newey, Ariel Pakes, Eleonora Pattachini, Michele Pelizzari, Martin Pesendorfer, Christiern Rose, Adam Rosen, Bernard Salanie, Olivier Scaillet, Sebastien Sieglöch, Pasquale Schiraldi, Tymon Sloczynski, Kevin Song, John Sutton, Adam Szeidl, Thiago Tachibana, Elie Tamer, and seminar and conference participants for valuable comments. We also thank Tim Besley and Anne Case for comments and sharing data. Previous versions of this paper were circulated as “Recovering Social Networks from Panel Data: Identification, Simulations and an Application.” All errors remain our own. Simulation and estimation codes are available upon request.

<sup>†</sup>de Paula: University College London, CeMMAP and IFS, a.paula@ucl.ac.uk; Rasul: University College London and IFS, i.rasul@ucl.ac.uk; Souza: Warwick University, pedro.souza@warwick.ac.uk

# 1 Introduction

In many economic environments, behavior is shaped by social interactions between agents. In individual decision problems, social interactions have been key to understanding outcomes as diverse as educational test scores, the demand for financial assets, and technology adoption (Sacerdote, 2001; Bursztyn *et al.*, 2014; Conley and Udry, 2010). In macroeconomics, the structure of firm’s production and credit networks propagate shocks, or help firms to learn (Acemoglu *et al.*, 2012; Chaney, 2014). In political economy, ties between jurisdictions are key to understanding tax setting behavior (Tiebout, 1956; Shleifer, 1985; Besley and Case, 1994).

Underpinning all these bodies of research is some measurement of the underlying social ties between agents. However, information on social ties does not exist in most publicly available and widely used datasets. To overcome this limitation, studies of social interaction either *postulate* ties based on common observables or homophily, or *elicit* data on networks. However, it is increasingly recognized that postulated and elicited networks remain imperfect solutions to the fundamental problem of missing data on social ties, because of econometric concerns that arise with either method, or simply because of the cost of collecting network data.<sup>1</sup>

Two consequences are that: (i) classes of problems in which social interactions occur are understudied, because social networks data is missing or too costly to collect; (ii) there is no way to validate social interactions analysis in contexts where ties are postulated. In this paper we tackle this challenge by deriving sufficient conditions under which global identification of the *entire structure* of social networks is obtained, using only observational panel data that itself contains *no* information on network ties. Our identification results allow the study of social interactions without data on social networks, and the validation of structures of social interaction where social ties have hitherto been postulated.

A researcher is assumed to have panel data on individuals  $i = 1, \dots, N$  for instances  $t = 1, \dots, T$ . An instance refers to a specific observation for  $i$  and need not correspond to a time period (for example if  $i$  refers to a firm,  $t$  could refer to market  $t$ ). The outcome of interest for individual  $i$  in instance  $t$  is  $y_{it}$  and is generated according to a canonical structural model of social interactions:<sup>2</sup>

$$y_{it} = \rho_0 \sum_{j=1}^N W_{0,ij} y_{jt} + \beta_0 x_{it} + \gamma_0 \sum_{j=1}^N W_{0,ij} x_{jt} + \alpha_i + \alpha_t + \epsilon_{it} \quad (1)$$

---

<sup>1</sup>As detailed in de Paula (2017), elicited networks are often self-reported, and can introduce error for the outcome of interest. Network data can be censored if only a limited number of links can feasibly be reported. Incomplete survey coverage of nodes in a network may lead to biased aggregate network statistics. Chandrasekhar and Lewis (2016) show that even when nodes are randomly sampled from a network, partial sampling leads to non-classical measurement error, and biased estimation. Collecting social network data is also a time and resource intensive process. In response to these concerns, a nascent strand of literature explores cost-effective alternatives to full elicitation to recover aggregate network statistics (Breza *et al.*, 2017).

<sup>2</sup>Blume *et al.* (2015) present micro-foundations based on non-cooperative games of incomplete information for individual choice problems, that result in this estimating equation for a class of social interaction models.

Outcome  $y_{it}$  depends on the outcome of other individuals to whom  $i$  is socially tied,  $y_{jt}$ , and  $x_{jt}$  includes characteristics of those individuals (or lagged values of  $y_{it}$ ).  $W_{0,ij}$  measures how the outcome and characteristics of  $j$  causally impact the outcome for  $i$ . As outcomes for all individuals obey equations analogous to (1), the system of equations can be written in matrix notation where the structure of interactions is captured by the adjacency matrix, denoted  $W_0$ . Our approach allows for unobserved heterogeneity across individuals  $\alpha_i$  and common shocks to all individuals  $\alpha_t$ . This framework encompasses the classic linear-in-means specification of Manski (1993). In his terminology,  $\rho_0$  and  $\gamma_0$  capture endogenous and exogenous social effects, and  $\alpha_t$  captures correlated effects. The distinction between endogenous and exogenous peer effects is critical, as only the former generates social multiplier effects.

Manski’s seminal contribution set out the reflection problem of separately identifying endogenous, exogenous and correlated effects in linear models. However, it has been somewhat overlooked that he also set out another challenge on the identification of the social network in the first place.<sup>3</sup> This is the problem we tackle and so expand the scope of identification beyond  $\rho_0$ ,  $\beta_0$  and  $\gamma_0$ . Our point of departure from much of the literature is to therefore presume  $W_0$  is *entirely unknown* to the researcher. We derive sufficient conditions under which all the entries in  $W_0$ , and the endogenous and exogenous social effect parameters,  $\rho_0$  and  $\gamma_0$ , are globally identified. By identifying the social interactions matrix  $W_0$ , our results allow the recovery of aggregate network characteristics such as the degree distribution and patterns of homophily, as well as node-level statistics such as the strength of social interactions between nodes, and the centrality of nodes. This is useful because such aggregate and node-level statistics often map back to underlying models of social interaction (Ballester *et al.*, 2006; Jackson *et al.*, 2017; de Paula, 2017).

The mathematical strategy for our identification result is new and fundamentally different from those employed elsewhere in this nascent literature (and does not rely on requirements on network sparsity). However it delivers sufficient conditions that are mild, and relate to existing results on the identification of social effects parameters when  $W_0$  is known (Bramoullé *et al.*, 2009; De Giorgi *et al.*, 2010; Blume *et al.*, 2015). Our identification result is also useful in other estimation contexts, such as when a researcher has partial knowledge of  $W_0$ , or in navigating between priors on reduced-form (later denoted  $\Pi$ ) and structural (later denoted  $\theta$ ) parameters in a Bayesian framework, thus avoiding issues raised in Kline and Tamer (2016).

Global identification is a necessary requirement for consistency of extremum estimators such as those based on GMM (Hansen 1982; Newey and McFadden 1994). Our identification analysis thus

---

<sup>3</sup>Manski (1993) highlights difficulties (and potential restrictions) for identifying  $\rho_0$ ,  $\beta_0$  and  $\gamma_0$  when all individuals interact with each other, and when this is observed by the researcher. In (1), this corresponds to  $W_{0,ij} = N^{-1}$ , for  $i, j = 1, \dots, N$ . At the same time, he states (p. 536), “I have presumed that researchers know how individuals form reference groups and that individuals correctly perceive the mean outcomes experienced by their supposed reference groups. There is substantial reason to question these assumptions (...) If researchers do not know how individuals form reference groups and perceive reference-group outcomes, then it is reasonable to ask whether observed behavior can be used to infer these unknowns (...) The conclusion to be drawn is that informed specification of reference groups is a necessary prelude to analysis of social effects.”

provides primitives for this important condition. To estimate the model, we employ the Adaptive Elastic Net GMM method (Caner and Zhang, 2014) because this allows us to deal with a potentially high-dimensional parameter vector (in comparison to the time dimension in the data) including all the entries of the social interactions matrix  $W_0$ , though other estimation protocols may also be entertained (e.g., using Bayesian methods or a priori information as previously alluded).<sup>4</sup>

We showcase the method using Monte Carlo simulations based on stylized random network structures as well as real world networks. In each case, we take a fixed network structure  $W_0$ , and simulate panel data as if the data generating process were given by (1). We then apply the method on the simulated panel data to recover estimates of all elements in  $W_0$ , as well as the endogenous and exogenous social effect parameters  $(\rho_0, \gamma_0)$ . The networks considered vary in size, complexity, and their aggregate and node-level features. Despite this heterogeneity, we find the method to perform well in all simulations. In a reasonable dimension of panel data  $T$  and with varying node numbers across simulations ( $N$ ), we find the true network structure  $W_0$  is well recovered. For each simulated network, the majority of true links are correctly identified even for  $T = 5$ , and the proportion of true non-links (zeroes in  $W_0$ ) captured correctly as zeros is over 85% even when  $T = 5$ . Both proportions rapidly increase with  $T$ . *A fortiori*, we estimate aggregate and node-level statistics of each network, demonstrating the accurate recovery of key players in networks for example. Furthermore, biases in the estimation of endogenous and exogenous effects parameters  $(\hat{\rho}, \hat{\gamma})$  fall quickly with  $T$  and are close to zero for large sample sizes.

In the final part of our analysis, we apply the method to shed new light on a classic real world social interactions problem: tax competition between US states. The literatures in political economy and public economics have long recognized the behavior of state governors might be influenced by decisions made in ‘neighboring’ states. The typical empirical approach has been to postulate the relevant neighbors as being geographically contiguous states. Our approach allows us to infer the set of economic neighbors determining social interactions in tax setting behavior from panel data on outcomes and covariates alone. In this application, the panel data dimensions cover mainland US states,  $N = 48$ , for years 1962-2015,  $T = 53$ .

We find the identified network structure of tax competition to differ markedly from the common assumption of competition between geographic neighbors. The identified network has fewer edges than the geography-based network, that gets reflected in the far lower clustering coefficient in the identified network than in the geographic network (.026 versus .194). With the recovered social

---

<sup>4</sup>The elastic net was introduced by Zou and Hastie, 2005 in part to circumvent difficulties faced by alternative estimation protocols (e.g., LASSO) when the number of parameters,  $p$ , exceeds the number of observations,  $n$  (where  $p$  and  $n$  follow the notation in that paper). Whereas the theoretical results on the large sample properties of elastic net estimators usually have not exploited sparsity, several articles have demonstrated its performance in data scenarios where this occurs. For example, Zou and Hastie, 2005 consider an application to leukemia classification where  $p = 7,129$  and  $n = 72$  (see their Section 6) and Zou and Zhang, 2009 explore a scenario where  $p = 1,000$  and  $n = 200$ . The favourable performance of the elastic net in these cases also relates to the literature on the ‘effective number of parameters’ (or ‘effective degrees of freedom’) in the estimation of sparse models (Tibshirani and Taylor, 2012). In Section 3 we provide an informal calculation for the minimum number of time periods such that penalized estimation is feasible in our context.

interactions matrix we establish, beyond geography, what covariates correlate to the existence of ties between states and the strength of those ties. We identify non-adjacent states that influence tax setting and, more broadly, we establish that social interactions are highly asymmetric: some states – such as Delaware, a well known low-tax state – are especially focal in driving tax setting in other jurisdictions. We use all these results to shed new light on the main hypotheses for social interactions in tax setting: factor mobility and yardstick competition (Tiebout, 1956; Shleifer, 1985; Besley and Case, 1994).

Our paper contributes to the literature on the identification of social interactions models. The first generation of papers studied the case where  $W_0$  is known, so only the endogenous and exogenous social effects parameters need to be identified. It is now established that if the known  $W_0$  differs from the linear-in-means example,  $\rho_0$  and  $\gamma_0$  can be identified (Bramoullé *et al.*, 2009; De Giorgi *et al.*, 2010). Intuitively, identification in those cases can use peers-of-peers, that are not necessarily connected to individual  $i$  and can be used to leverage variation from exclusion restrictions in (1), or can use groups of different sizes within which all individuals interact among each other (Lee, 2007). Bramoullé *et al.* (2009) show these conditions are met if  $I, W_0$  and  $W_0^2$  are linearly independent, which is shown to hold generically by Blume *et al.* (2015). However, as made precise in Section 2, the linear algebraic arguments employed in Bramoullé *et al.* (2009) or Blume *et al.* (2015) do not apply when  $W_0$  is unobserved and other arguments have to be used instead.<sup>5</sup>

Our paper builds on these papers by studying the problem where  $W_0$  is entirely unknown to the researcher. In so doing, we open up the study of social interactions to the many realms where complete social network data does not actually exist. Closely related to our work, Blume *et al.* (2015) investigate the case when  $W_0$  is *partially* observed. Specifically, Blume *et al.* (2015, Theorem 6) show that if two individuals are *known* to not be directly connected, the parameters of interest in a model related to (1) can be identified. An alternative approach is taken in Blume *et al.* (2011, Theorem 7): they suggest a parameterization of  $W_0$  according to a pre-specified distance between nodes. We do not impose such restrictions, but note that partial observability of  $W_0$  (as in Blume *et al.*, 2015) or placing additional structure on  $W_0$  (as in Blume *et al.*, 2011) is complementary to our approach as it reduces the number of parameters in  $W_0$  to be retrieved.

Bonaldi *et al.* (2015) and Manresa (2016) estimate models like (1) when  $W_0$  is not observed, but where  $\rho_0$  is restricted to be zero so there are no endogenous social effects. They use sparsity-inducing methods from the statistics literature, but the presence of  $\rho_0$  in our case complicates identification non-trivially because it introduces issues of simultaneity that we address.

Rose (2015) also presents related identification results for linear models like (1). Assuming sparsity of the neighborhood structure, Rose (2015) offers identification conditions under rank restrictions on sub-matrices of the reduced form coefficient matrix from a regression of outcomes ( $y_{it}$ )

---

<sup>5</sup>Alternative identification approaches when  $W_0$  is known focus on higher moments (variances and covariances across individuals) of outcomes (de Paula, 2017), and rely on additional restrictions on the higher moments of  $\epsilon_{it}$ . We also note that (1) is a spatial autoregressive model. There,  $W_0$  is also typically assumed known. Anselin (2010) reviews this literature.

on covariates ( $x_{it}$ ). Intuitively, given two observationally equivalent systems, sparsity guarantees the existence of pairs that are not connected in either. Since observationally equivalent systems are linked via the reduced-form coefficient matrix, this pair allows one to identify certain parameters in the model. Having identified those parameters, Rose (2015) shows that one can proceed to identify other aspects of the structure (see also Gautier and Rose, 2016). This is related to the ideas in Blume *et al.* (2015, Theorem 6), who show identification results can be leveraged if individuals are *known* not to be connected. Our main identification results presented in the next section do *not* rely on properties of sparse networks, and make use of plausible and intuitive conditions, whereas the auxiliary rank conditions necessary in Rose (2015) may be computationally complex to verify. More recently, Lewbel *et al.* (2019) propose an estimation strategy for the parameters  $\rho_0$ ,  $\beta_0$  and  $\gamma_0$  of model (1) in the absence of network links if many different groups are able to be observed.

Finally, in the statistics literature, Lam and Souza (2019) study the penalized estimation of model (1) when  $W_0$  is not observed, assuming the model and social interactions are identified. The statistical literature on graphical models has investigated the estimation of neighborhoods defined by the covariance structure of the random variables at hand (Meinshausen and Buhlmann, 2006). This corresponds to a model where  $y_t = (I - \rho_0 W_0)^{-1} \epsilon_t$  is jointly normal (abstracting from covariates). On a graph with  $N$  nodes corresponding to the variables in the model, an edge between two nodes (variables)  $i$  and  $j$  is absent when these two variables are conditionally independent given the other nodes. In this Gaussian model, this corresponds to a zero  $ij$  entry in the inverse covariance matrix for  $y_t$  (see, e.g., Yuan and Lin, 2007, p. 19). In the model above, the inverse covariance matrix is  $(I - \rho_0 W_0)^\top \Sigma_\epsilon^{-1} (I - \rho_0 W_0)$ , where  $\Sigma_\epsilon$  is the variance covariance structure for  $\epsilon_t$ . The discovery of zero entries in this matrix is not equivalent to the identification of  $W_0$  as we study, and involves  $\Sigma_\epsilon$  (as do identification strategies using higher moments when  $W_0$  is known).<sup>6</sup> Related studies in the statistics literature also focus on higher moments and define neighborhoods differently (Diebold and Yilmaz, 2015; Rothenhäusler *et al.*, 2015).

Our conclusions discuss how our approach can be modified, and assumptions weakened, to integrate in partial knowledge of  $W_0$ . We also discuss the next steps required to simultaneously identify models of network formation and the structure of social interactions.

The paper is organized as follows. Section 2 presents our core result: the sufficient conditions under which the social interactions matrix, endogenous and exogenous social effects are globally identified. Section 3 describes the high-dimensional estimation techniques used, based on the Adaptive Elastic Net GMM method and presents simulation results from stylized and real-world networks. Section 4 applies our methods to study tax competition between US states. Section 5 concludes. The Appendix provides proofs and further details on estimation and simulations.

---

<sup>6</sup>In fact, Meinshausen and Buhlmann (2006)'s neighborhood estimates (as also Lam and Souza (2019)'s) rely on (penalized) regressions of  $y_{it}$  on  $y_{1t}, \dots, y_{i-1,t}, y_{i+1,t}, \dots, y_{N,t}$ , which do not address the econometric endogeneity in estimating  $W_0$ .

## 2 Identification

### 2.1 Setup

Consider a researcher with panel data covering  $i = 1, \dots, N$  individuals repeatedly observed over  $t = 1, \dots, T$  instances. We consider that the number of individuals  $N$  in the network is fixed, but potentially large. The aim is to use this data to identify a social interactions model, with no data on actual social ties being available. For expositional ease, we first consider identification in a simpler version of the canonical model in (1), where we drop individual-specific ( $\alpha_i$ ) and time-constant fixed effects ( $\alpha_t$ ), and assume  $x_{it}$  is a one-dimensional regressor for individual  $i$  and instance  $t$ . Of course, we later extend the analysis to include individual-specific and time-constant fixed effects, and also allow for multidimensional covariates  $x_{k,it}$ ,  $k = 1, \dots, K$ . We adopt the subscript “0” to denote parameters generating the data, and non-subscripted parameters are generic values in the parameter space:

$$y_{it} = \rho_0 \sum_{j=1}^N W_{0,ij} y_{jt} + \beta_0 x_{it} + \gamma_0 \sum_{j=1}^N W_{0,ij} x_{jt} + \epsilon_{it}. \quad (2)$$

As outcomes for all individuals  $i = 1, \dots, N$  obey equations analogous to (2), the system of equations can be more compactly written in matrix notation as:

$$y_t = \rho_0 W_0 y_t + \beta_0 x_t + \gamma_0 W_0 x_t + \epsilon_t. \quad (3)$$

The vector of outcomes  $y_t = (y_{1t}, \dots, y_{Nt})'$  assembles the individual outcomes in instance  $t$ ; the vector  $x_t$  does the same with individual characteristics.  $y_t$ ,  $x_t$  and  $\epsilon_t$  have dimension  $N \times 1$ , the social interactions matrix  $W_0$  is  $N \times N$ , and  $\rho_0$ ,  $\beta_0$ , and  $\gamma_0$  are scalar parameters. We do not make any distributional assumptions on  $\epsilon_t$  beyond  $\mathbb{E}(\epsilon_t | x_t) = 0$  (or  $\mathbb{E}(\epsilon_t | z_t) = 0$  for an appropriate instrumental variable  $z_t$  if  $x_t$  is also endogenous). We assume the network structure is predetermined and constant, and that the number of individuals  $N$  is fixed. The network structure  $W_0$  is a parameter to be identified and estimated.<sup>7</sup>

A regression of outcomes on covariates corresponds, then, to the reduced form for (3),

$$y_t = \Pi_0 x_t + \nu_t, \quad (4)$$

with  $\Pi_0 = (I - \rho_0 W_0)^{-1}(\beta_0 I + \gamma_0 W_0)$  and  $\nu_t \equiv (I - \rho_0 W_0)^{-1} \epsilon_t$ . If  $W_0$  is observed, Bramoullé *et al.* (2009) note that a structure  $(\rho, \beta, \gamma)$  that is observationally equivalent to  $(\rho_0, \beta_0, \gamma_0)$  is such that  $(I - \rho_0 W_0)^{-1}(\beta_0 I + \gamma_0 W_0) = (I - \rho W_0)^{-1}(\beta I + \gamma W_0)$ . This equation can be written as a

---

<sup>7</sup>A related set of papers instead focuses on the distribution of networks generating the pattern in data and aims to estimate aggregate network effects. Souza (2014) offers several identification and estimation results in this spirit. In particular, he infers the network distribution within a certain class of statistical network formation models from outcome data from many groups, such as classrooms, in few time periods. We instead concentrate on estimating the set of links for one group of size  $N$  followed over  $t = 1, \dots, T$  instances.

linear equation in  $I, W_0$  and  $W_0^2$  and identification is established if those matrices are linearly independent. If  $W_0$  is not observed, the putative unobserved structure now comprises  $W$  and an observationally equivalent parameter vector will instead satisfy  $(I - \rho_0 W_0)^{-1}(\beta_0 I + \gamma_0 W_0) = (I - \rho W)^{-1}(\beta I + \gamma W)$ . Following the strategy in Bramoullé *et al.* (2009) would lead to an equation in  $I, W, W_0$  and  $W W_0$ , and the insights obtained in that paper then do *not* carry over for the case we study when  $W_0$  is unknown.

We establish identification of the structural parameters of the model, including the social interactions matrix  $W_0$ , from the coefficients matrix  $\Pi_0$ . Without data on the network  $W_0$ , we treat it as an additional parameter in an otherwise standard model relating outcomes and covariates. Our identification strategy relies on how changes in covariates  $x_{it}$  reverberate through the system and impact  $y_{it}$ , as well as outcomes for other individuals. These are summarized by the entries of the coefficient matrix  $\Pi_0$ , which, in turn, encode information about  $W_0$  and  $(\rho_0, \beta_0, \gamma_0)$ . A non-zero partial effect  $x_{it}$  of  $y_{jt}$  indicates the existence of direct *or* indirect links between  $i$  and  $j$ . When  $\rho_0 = 0$  (and  $\Pi_0 = \beta_0 I + \gamma_0 W_0$ ), only direct links would produce such a correlation. When  $\rho \neq 0$ , both direct and indirect connections may generate a non-zero response but distant connections will lead to a lower response. Our results formally determine sufficient conditions to precisely disentangle these forces.

We first set out five assumptions underpinning our main identification results. Three of these are entirely standard in the social interactions. A fourth is a normalization required to separately identify  $(\rho_0, \gamma_0)$  from  $W_0$ , and the fifth is closely related to known results on the identification of  $(\rho_0, \gamma_0)$  when  $W_0$  is known (Bramoullé *et al.*, 2009). These Assumptions (A1-A5) deliver an identified set of up to two points.

Our first assumption explicitly states that no individual affects himself and is a standard condition in social interaction models:

$$(A1) \quad (W_0)_{ii} = 0, \quad i = 1, \dots, N.$$

With Assumption (A1), we can omit elements on the diagonal of  $W_0$  from the parameter space. We thus can denote a generic parameter vector as  $\theta = (W_{12}, \dots, W_{N,N-1}, \rho, \gamma, \beta)' \in \mathbb{R}^m$ , where  $m = N(N-1) + 3$ , and  $W_{ij}$  is the  $(i, j)$ -th element of  $W$ . Reduced-form parameters can be tied back to the structural model (3) by letting  $\Pi : \mathbb{R}^m \rightarrow \mathbb{R}^{N^2}$  define the relation between structural and reduced-form parameters:

$$\Pi(\theta) = (I - \rho W)^{-1}(\beta I + \gamma W),$$

where  $\theta \in \mathbb{R}^m$ , and  $\Pi_0 \equiv \Pi(\theta_0)$ .

As  $\epsilon_t$  (and, consequently,  $\nu_t$ ) is mean-independent from  $x_t$ ,  $\mathbb{E}[\epsilon_t | x_t] = 0$ , the matrix  $\Pi_0$  can be identified as the linear projection of  $y_t$  on  $x_t$ . We do not impose additional distributional assumptions on the disturbance term, except for conditions that allow us to identify the reduced-



form parameters in (4). If  $x_t$  is endogenous, i.e.  $\mathbb{E}[\epsilon_t|x_t] \neq 0$ , a vector of instrumental variables  $z_t$  may still be used to identify  $\Pi_0$ . In either case, identification of  $\Pi_0$  requires variation of the regressor across individuals  $i$  and through instances  $t$ . In other words, either  $\mathbb{E}[x_t x_t']$  (if exogeneity holds) or  $\mathbb{E}[x_t z_t']$  (otherwise) are full-rank.

Our next assumption controls the propagation of shocks and guarantees they die as they reverberate through the network. This provides adequate stability in the system, and is closely related to the concept of stationarity in network models. It implies the maximum eigenvalue norm of  $\rho_0 W_0$  is less than one. It also ensures  $(I - \rho_0 W_0)$  is a non-singular matrix, and so the variance of  $y_t$  exists, the transformation  $\Pi(\theta_0)$  is well-defined, and the Neumann expansion  $(I - \rho_0 W_0)^{-1} = \sum_{j=0}^{\infty} (\rho_0 W_0)^j$  is appropriate.

(A2)  $\sum_{j=1}^N |\rho_0 (W_0)_{ij}| < 1$  for every  $i = 1, \dots, N$ ,  $\|W_0\| < C$  for some positive  $C \in \mathbb{R}$  and  $|\rho_0| < 1$ .

We next assume that network effects do not cancel out, another standard assumption.

(A3)  $\beta_0 \rho_0 + \gamma_0 \neq 0$ .

The need for this assumption can be shown by expanding the expression for  $\Pi(\theta_0)$ , which is possible by (A2):

$$\Pi(\theta_0) = \beta_0 I + (\rho_0 \beta_0 + \gamma_0) \sum_{k=1}^{\infty} \rho_0^{k-1} W_0^k. \quad (5)$$

If Assumption (A3) were violated,  $\beta_0 \rho_0 + \gamma_0 = 0$  and  $\Pi_0 = \beta_0 I$  so the endogenous and exogenous effects balance each other out, and network effects are altogether eliminated in the reduced form.<sup>8</sup>

Identification of the social effects parameters  $(\rho_0, \gamma_0)$  requires that at least one row of  $W_0$  adds to a fixed and known number. Otherwise,  $\rho_0$  and  $\gamma_0$  cannot be separately identified from  $W_0$ . Clearly, no such condition would be required if  $W_0$  was observed.

(A4) There is an  $i$  such that  $\sum_{j=1, \dots, N} (W_0)_{ij} = 1$ .

Letting  $W_y \equiv \rho_0 W_0$  and  $W_x \equiv \gamma_0 W_0$  denote the matrices that summarize the influence of peers' outcomes (the endogenous social effects) and characteristics on one's outcome (the exogenous social effects), respectively, the assumption above can be seen as a normalization. In this case,  $\rho_0$  and  $\gamma_0$  represent the row-sum for individual  $i$  in  $W_y$  and  $W_x$ , respectively.<sup>9</sup> In line with the literature, we

---

<sup>8</sup>One important case is when networks do not determine outcomes, which we interpret as  $\rho_0 = \gamma_0 = 0$  or with  $W_0$  representing the empty network. From equation (5), it is clear that if  $\Pi(\theta_0)$  is *not* diagonal with constant entries, then it must be that  $(\rho_0 \beta_0 + \gamma_0) \neq 0$ , which implies that  $\rho_0 \neq 0$  or  $\gamma_0 \neq 0$ , and also that  $W_0$  is non-empty. Taken together, this suggests that the observation that  $\Pi(\theta_0)$  is not diagonal is sufficient to ensure that network effects are present and Assumption (A3) is not violated.

<sup>9</sup>An alternative to Assumption (A4) is to impose the normalization on the parameters. For example, one could normalize  $\rho^* = 1$  and allow the network to be rescaled accordingly. In this case,  $W^* = \rho_0 W_0$  would be identified instead. Also  $W_x = \frac{\gamma_0}{\rho_0} W^*$  so  $\gamma_0$  would be identified relative to  $\rho_0$ .  $W_y$  and  $W_x$  are unchanged.

maintain that the same  $W_0$  governs the structure of both endogenous ( $W_y$ ) and exogenous ( $W_x$ ) effects. We later discuss relaxing this assumption when more than one regressor is used.

Our final assumption provides for a specific kind of network asymmetry. We require the diagonal of  $W_0^2$  not to be constant as one of our sufficient conditions for identification.

(A5) There exists  $l, k$  such that  $(W_0^2)_{ll} \neq (W_0^2)_{kk}$ , i.e. the diagonal of  $W_0^2$  is not proportional to  $\iota$ , where  $\iota$  is the  $N \times 1$  vector of ones.

In unweighted networks, the diagonal of the square of the social interactions matrix captures the number of reciprocated links for each individual or, in the case of undirected networks, the popularity of those individuals. Assumption (A5) hence intuitively suggests differential popularity across individuals in the social network.

This assumption is related to the network asymmetry condition proposed elsewhere, such as in Bramoullé *et al.* (2009). They show that when  $W_0$  is known, the structural model (2) is identified if  $I$ ,  $W_0$ , and  $W_0^2$  are linearly independent. Given the remaining assumptions, this condition is satisfied if (A5) is satisfied, but the converse is *not* true: one can construct examples in which  $I$ ,  $W_0$ , and  $W_0^2$  are linearly independent when  $W_0^2$  has a constant diagonal, so that  $\Pi_0$  does not pin down  $\theta_0$ . The strengthening of this hypothesis is the formal price to pay for the social interactions matrix  $W_0$  being unknown to the researcher.<sup>10</sup>

Before proceeding to our formal results, we provide a very simple illustration to shed light on how the assumptions above come together to provide identification. Suppose the observed reduced-form matrix is,

$$\Pi_0 = \frac{1}{455} \begin{bmatrix} 275 & 310 & 0 \\ 310 & 275 & 0 \\ 0 & 0 & 182 \end{bmatrix},$$

and that, following (A4), the first row is normalized to one. From the third row and column of  $\Pi_0$ , we see there is no path of any length connecting the individual in row 3 to or from those in rows 1

---

<sup>10</sup>To see the strength of the assumption of Bramoullé *et al.* (2009) when  $W_0$  is known, choose constants  $c_1$ ,  $c_2$ , and  $c_3$  such that  $c_1 I + c_2 W_0 + c_3 W_0^2 = 0$ . Focusing on diagonal elements of this condition, we see that if the diagonal of  $W_0^2$  is not proportional to the diagonal of  $I$ , then  $c_1 = c_3 = 0$  because  $\text{diag}(W_0) = 0$ . It follows that  $c_2 = 0$  if at least one (off-diagonal) element of  $W_0$  is non-zero. However, the converse is not true, so that if Assumptions A1-A5 do not hold, one can construct examples where  $\Pi_0$  does not pin down  $\theta_0$ . Take, for instance,  $N = 5$  with  $\theta_0$  and  $\theta$  where  $\beta = \beta_0 = 1$ ,  $\rho = 1.5$ ,  $\rho_0 = 0.5$ ,  $\gamma = -2.5$ ,  $\gamma_0 = 0.5$ ,

$$W_0 = \begin{bmatrix} 0 & 0.5 & 0 & 0 & 0.5 \\ 0.5 & 0 & 0.5 & 0 & 0 \\ 0 & 0.5 & 0 & 0.5 & 0 \\ 0 & 0 & 0.5 & 0 & 0.5 \\ 0.5 & 0 & 0 & 0.5 & 0 \end{bmatrix} \quad \text{and} \quad W = \begin{bmatrix} 0 & 0 & 0.5 & 0.5 & 0 \\ 0 & 0 & 0 & 0.5 & 0.5 \\ 0.5 & 0 & 0 & 0 & 0.5 \\ 0.5 & 0.5 & 0 & 0 & 0 \\ 0 & 0.5 & 0.5 & 0 & 0 \end{bmatrix}.$$

Both  $W$  and  $W_0$  violate (A5) ( $(W^2)_{kk} = (W_0^2)_{kk} = 0.5$  for any  $k$ ), and  $\rho$  violates (A2). Nonetheless,  $I, W_0$  and  $W_0^2$  are linearly independent and, likewise, so are  $I, W$ , and  $W^2$ . In this case, *both* parameter sets produce  $\Pi = (I - \rho_0 W_0)^{-1}(\beta_0 I + \gamma_0 W_0) = (I - \rho W)^{-1}(\beta I + \gamma W)$ . This arises even as  $W$  and  $W_0$  represent very different network structures: any pair connected under  $W$  is not connected under  $W_0$  and *vice-versa*.

or 2 since her outcome is not affected by their covariates and their outcomes are not affected by her covariates. In other words, individual 3 is isolated and  $(W_0)_{13} = (W_0)_{23} = (W_0)_{31} = (W_0)_{32} = 0$ . On the other hand, individuals 1 and 2 cannot be isolated as their covariates are correlated with the other individual's outcome, reflecting (A5).<sup>11</sup> Due to the row-sum normalization of the first row,  $(W_0)_{12} = 1$ . Using (A3), it can be seen that  $W_0$  is symmetric if  $\Pi_0$  is symmetric. We thus find that  $(W_0)_{21} = 1$ . This and (A1) map all elements of  $W_0$ , and thus,

$$W_0 = \begin{bmatrix} 0 & 1 & 0 \\ 1 & 0 & 0 \\ 0 & 0 & 0 \end{bmatrix}.$$

As the third individual is isolated, she will be only be affected by her exogenous  $x_i$  and not by endogenous or exogenous peer effects. Hence the (3,3) element of  $\Pi_0$  is equal to  $\beta_0 = \frac{182}{455} = .4$ . To find  $\rho_0$ , note that  $(I - \rho_0 W_0)\Pi_0 = \beta_0 I + \gamma_0 W_0$ . Hence focussing on the (1,1) elements of the matrices above, we find that  $\frac{275}{455} - \rho_0 \frac{310}{455} = .4$ , implying  $\rho_0 = .3$  (complying with (A2)). Finally,  $\gamma_0$  is identified from entry (1,2), giving  $\gamma_0 = \frac{310}{455} - .3 \frac{275}{455} = .5$ .

## 2.2 Main Identification Results

Under the relatively mild assumptions above, we can begin to identify parameters related to the network. These results are then useful for our main identification theorems. Let  $\lambda_{0j}$  denote an eigenvalue of  $W_0$  with corresponding eigenvector  $v_{0,j}$  for  $j = 1, \dots, N$ . Assumptions (A2) and (A3) allow us to identify the eigenvectors of  $W_0$  directly from the reduced form. As  $|\rho_0| < 1$ :

$$\begin{aligned} \Pi_0 v_{0,j} &= \beta_0 v_{0,j} + (\rho_0 \beta_0 + \gamma_0) \sum_{k=1}^{\infty} \rho_0^{k-1} W_0^k v_{0,j} \\ &= \left[ \beta_0 + (\rho_0 \beta_0 + \gamma_0) \sum_{k=1}^{\infty} \rho_0^{k-1} \lambda_{0,j}^k \right] v_{0,j} \\ &= \frac{\beta_0 + \gamma_0 \lambda_{0,j}}{1 - \rho_0 \lambda_{0,j}} v_{0,j}. \end{aligned} \tag{6}$$

The infinite sum converges as  $|\rho_0 \lambda_{0,j}| < 1$  by (A2). The equation above implies that  $v_{0,j}$  is also an eigenvector of  $\Pi_0$  with associated eigenvalue  $\lambda_{\Pi,j} = \frac{\beta_0 + \gamma_0 \lambda_{0,j}}{1 - \rho_0 \lambda_{0,j}}$ . The fact that eigenvectors of  $\Pi_0$  are also eigenvectors of  $W_0$  has a useful implication: eigencentralities may be identified from the reduced form, even when  $W_0$  is not identified. As detailed in de Paula (2017) and Jackson *et al.* (2017), such eigencentralities often play an important role in empirical work as they allow a

<sup>11</sup>If on the other hand,  $(W_0)_{ij} = 0.5, i \neq j$  in violation of (A5) and all agents were connected, the model would not be identified.

mapping back to underlying models of social interaction.<sup>12</sup>

Now let  $\Theta \equiv \{\theta \in \mathbb{R}^m : \text{Assumptions (A1)-(A5) are satisfied}\}$  be the structural parameter space of interest. Our first theorem establishes local identification of the mapping. A parameter point  $\theta_0$  is locally identifiable if there exists a neighborhood of  $\theta_0$  containing no other  $\theta$  which is observationally equivalent. Using classical results in Rothenberg (1971), we show that our assumptions are sufficient to ensure that the Jacobian of  $\Pi$  relative to  $\theta$  is non-singular, which, in turn, suffices to establish local identification.

**Theorem 1.** *Assume (A1)-(A5).  $\theta_0 \in \Theta$  is locally identifiable.*

An immediate consequence of local identification is that the set  $\{\theta \in \Theta : \Pi(\theta) = \Pi(\theta_0)\}$  is discrete (i.e. its elements are isolated points). The following corollary establishes that  $\Pi$  is a proper function, i.e. the inverse image  $\Pi^{-1}(K)$  of any compact set  $K \subset \mathbb{R}^{N^2}$  is also compact (Krantz and Parks, 2013, p. 124). Since it is discrete, the identified set must be finite.

**Corollary 1.** *Assume (A1)-(A5). Then  $\Pi(\cdot)$  is a proper mapping. Moreover, the set  $\{\theta : \Pi(\theta) = \Pi(\theta_0)\}$  is finite.*

Under additional assumptions, the identified set is at most a singleton in each of the partitioning sets  $\Theta_- \equiv \Theta \cap \{\rho\beta + \gamma < 0\}$  and  $\Theta_+ \equiv \Theta \cap \{\rho\beta + \gamma > 0\}$ .<sup>13</sup> Since  $\Theta = \Theta_- \cup \Theta_+$ , if the sign of  $\rho_0\beta_0 + \gamma_0$  is unknown, the identified set contains, at most, two elements. In the theorem that follows, we show global identification only for  $\theta \in \Theta_+$ , since arguments are mirrored for  $\theta \in \Theta_-$ .

**Theorem 2.** *Assume (A1)-(A5), then for every  $\theta \in \Theta_+$  we have  $\Pi(\theta) = \Pi(\theta_0) \Rightarrow \theta = \theta_0$ . That is,  $\theta_0$  is globally identified with respect to the set  $\Theta_+$ .*

Similar arguments apply if Theorem 2 instead were to be restricted to  $\theta \in \Theta_-$ . The proof of the corollary below is immediate and therefore omitted.

**Corollary 2.** *Assume (A1)-(A5). If  $\rho_0\beta_0 + \gamma_0 > 0$ , then the identified set contains at most one element, and similarly if  $\rho_0\beta_0 + \gamma_0 < 0$ . Hence, if the sign of  $\rho_0\beta_0 + \gamma_0$  is unknown, the identified set contains, at most, two elements.<sup>14</sup>*

<sup>12</sup>To identify the eigencentralities, we identify the eigenvector that corresponds to the dominant eigenvalue. If  $W_0$  is non-negative and irreducible, this is the (unique) eigenvector with strictly positive entries, by the Perron-Frobenius Theorem for non-negative matrices (see Horn and Johnson, 2013, p.534).

<sup>13</sup>The global inversion results we use are related to, but different from, those used by Komunjer (2012), Lee and Lewbel (2013) and Chiappori *et al.* (2015). Those authors use variations on a classical inversion result of Hadamard. In contrast, we employ results on the cardinality of the pre-image of a function, relying on less stringent assumptions. Specifically, while the classical Hadamard result requires that the image of the function be simply-connected (Theorem 6.2.8 of Krantz and Parks, 2013), the results we rely on do not.

<sup>14</sup>Under some special conditions, the mirror image of  $\theta_0$  can be characterized from equation (5). If  $-W_0$  satisfies Assumption (A4), we may set  $\rho^* = -\rho_0$ ,  $\beta^* = \beta_0$ ,  $\gamma^* = -\gamma_0$  and  $W^* = -W_0$ . Then  $\rho_0\beta_0 + \gamma_0 = -(\rho^*\beta^* + \gamma^*)$ . Also note that  $\sum_{k=1}^{\infty} \rho_0^{k-1} W_0^k = -\sum_{k=1}^{\infty} (\rho^*)^{k-1} (W^*)^k$ , and so  $(\rho_0\beta_0 + \gamma_0) \sum_{k=1}^{\infty} \rho_0^{k-1} W_0^k = (\rho^*\beta^* + \gamma^*) \sum_{k=1}^{\infty} (\rho^*)^{k-1} (W^*)^k$ . It follows that  $\Pi(\theta_0) = \Pi(\theta^*)$ , where  $\theta^* = (\rho^*, \beta^*, \gamma^*, W^*)$ .

We now turn our attention to the problem of identifying the sign of  $\rho_0\beta_0 + \gamma_0$  from the observation of  $\Pi_0$ . This would then allow us to establish global identification using Theorem 2. It is apparent from (5) that if  $\rho_0 > 0$  and  $(W_0)_{ij} \geq 0$ , for all  $i, j = \{1, \dots, N\}$  the off-diagonal elements of  $\Pi_0$  identify the sign of  $\rho_0\beta_0 + \gamma_0$ .

**Corollary 3.** *Assume (A1)-(A5). If  $\rho_0 > 0$  and  $(W_0)_{ij} \geq 0$ , the model is globally identified.*

Real world applications often suggest endogenous social interactions are positive ( $\rho_0 > 0$ ), in which case global identification is fully established by Corollary 3. On the other hand, if  $\rho_0 < 0$  (which is so if outcomes are strategic substitutes, for example),  $\rho_0^k$  in (5) alternates signs with  $k$ , and the off-diagonal elements no longer carry the sign of  $\rho_0\beta_0 + \gamma_0$ . Nonetheless, if  $W_0$  is non-negative and irreducible (i.e., not permutable into a block-triangular matrix or, equivalently, a strongly connected social network), the model is also identifiable without further restrictions on  $\rho_0$ :

**Corollary 4.** *Assume (A1)-(A5),  $(W_0)_{ij} \geq 0$  and  $W_0$  is irreducible. If  $W_0$  has at least two real eigenvalues or  $|\rho_0| < \sqrt{2}/2$ , then the model is globally identified.*

Corollary 4 holds if there are at least two real eigenvalues, or if  $\rho_0$  is appropriately bounded. Since  $W_0$  is non-negative, it has at least one real eigenvalue, by the Perron-Frobenius Theorem. If  $W_0$  is symmetric, for example, its eigenvalues are all real, and Corollary 4 holds. It also holds if  $(W_0)_{ij} \leq 0$ , as we can re-write the model as  $\rho W_0 = -\rho|W_0|$  where  $|W_0|$ , is the matrix whose entries are the absolute values of the entries in  $W_0$ . In any case, the bound on  $|\rho_0|$  is sufficient and holds in most (if not all) empirical estimates we are aware of obtained from either elicited or postulated networks, and in our application on tax competition.

## 2.3 Extensions

### 2.3.1 Individual Fixed Effects

We observe outcomes for  $i = 1, \dots, N$  individuals repeatedly through  $t = 1, \dots, T$  instances. If  $t$  corresponds to time, it is natural to think of there being unobserved heterogeneity across individuals,  $\alpha_i$ , to be accounted for when estimating  $\Pi_0$ . The structural model (2) is then,

$$y_{it} = \rho_0 \sum_{j=1}^N W_{0,ij} y_{jt} + \beta_0 x_{it} + \gamma_0 \sum_{j=1}^N W_{0,ij} x_{jt} + \alpha_i + \epsilon_{it},$$

which can be written in matrix form as,

$$y_t = \rho_0 W_0 y_t + x_t \beta_0 + W_0 x_t \gamma_0 + \alpha^* + \epsilon_t,$$

where  $\alpha^*$  is the vector of fixed effects. Individual-specific and time-constant fixed effects can be eliminated using the standard subtraction of individual time averages. Defining  $\bar{y}_t = T^{-1} \sum_{t=1}^T y_t$ ,  $\bar{x}_t = T^{-1} \sum_{t=1}^T x_t$  and  $\bar{\epsilon}_t = T^{-1} \sum_{t=1}^T \epsilon_t$ ,

$$y_t - \bar{y}_t = \rho_0 W_0 (y_t - \bar{y}_t) + (x_t - \bar{x}_t) \beta_0 + W_0 (x_t - \bar{x}_t) \gamma_0 + \epsilon_t - \bar{\epsilon}_t,$$

if  $W_0$  does not change with time. Identification from the reduced form follows from previous theorems, since  $\Pi_0$  is unchanged when regressing  $y_t - \bar{y}_t$  on  $x_t - \bar{x}_t$ .<sup>15</sup>

### 2.3.2 Common Shocks

We next allow for unobserved common shocks to all individuals in the network in the same instance  $t$ . Such correlated effects  $\alpha_t$  can confound the identification of social interactions. As we have not placed any distributional assumption on the covariance matrix of the disturbance term, our analysis readily incorporates correlated effects that are orthogonal to  $x_t$ . When this is not the case, one possibility is to model the corrected effects  $\alpha_t$  explicitly. The model then is,

$$y_t = \rho_0 W_0 y_t + x_t \beta_0 + \gamma_0 W_0 x_t + \alpha_t \iota + \epsilon_t,$$

where  $\alpha_t$  is a scalar capturing shocks in the network common to all individuals. Let  $\Pi_{01} = (I - \rho_0 W_0)^{-1}$  and  $\Pi_{02} = (\beta_0 I + \gamma_0 W_0)$  such that  $\Pi_0 = \Pi_{01} \Pi_{02}$ . The reduced-form model is,

$$y_t = \Pi_0 x_t + \alpha_t \Pi_{01} \iota + v_t.$$

We propose a transformation to eliminate the correlated effects: exclude the individual-invariant  $\alpha_t$ , subtracting the mean of the variables at a given period (global differencing). For this purpose, define  $H = \frac{1}{n} \iota \iota'$ . We note that in empirical and theoretical work it is customary to strengthen Assumption (A4) and require that *all* rows of  $W_0$  sum to one if no individual is isolated (see for example Blume *et al.*, 2015). This strengthened assumption is usually referred to as row-sum normalization, and is stated below:

(A4') For all  $i = 1, \dots, N$  we have that  $\sum_{j=1, \dots, N} (W_0)_{ij} = 1$ .

This can be written compactly as  $W_0 \iota = \iota$ . In this case,  $W_0$  can be interpreted as the normalized adjacency matrix. Under row-sum normalization we have that,

$$\begin{aligned} (I - H) y_t &= (I - H) (I - \rho_0 W_0)^{-1} (\beta_0 I + \gamma_0 W_0) x_t + (I - H) (I - \rho_0 W_0)^{-1} \epsilon_t \\ &= (I - H) \Pi_0 x_t + (I - H) v_t, \end{aligned}$$

---

<sup>15</sup>As is the case in panel data, this would require strict exogeneity ( $\mathbb{E}[\epsilon_s | x_t] = 0$  for any  $s$  and  $t$ ) or predetermined errors ( $\mathbb{E}[\epsilon_s | x_t] = 0$  for  $s \geq t$ ) so that the matrix  $\Pi_0$  can be consistently estimated.

because  $(I - H)(I - \rho_0 W_0)^{-1} \alpha_t \iota = 0$  if Assumption (A4') holds. It then follows that  $\tilde{\Pi}_0 = (I - H)\Pi_0$  is identified. The next proposition shows that, under row-sum normalization of  $W_0$ ,  $\Pi_0$  is identified from  $\tilde{\Pi}_0$  (and, as a consequence, the previous results immediately apply).

**Proposition 1.** *If  $W_0$  is diagonalizable and row-sum normalized,  $\Pi_0$  is identified from  $\tilde{\Pi}_0$ .*

Under row-sum normalization of  $W_0$ , a common group-level shock affects individuals homogeneously since  $(I - \rho_0 W_0)^{-1} \alpha_t \iota = \alpha_t (I + \rho_0 W_0 + \rho_0^2 W_0^2 + \dots) \iota = \frac{\alpha_t}{1 - \rho_0} \iota$ , which is a vector with no variation across entries. Consequently, global differencing eliminates correlated effects and  $(I - H)(I - \rho_0 W_0)^{-1} \alpha_t \iota = (I - \rho_0 W_0)^{-1} \alpha_t (I - H) \iota = 0$ . In the absence of row-sum normalization, global differencing does not ensure that correlated effects are eliminated. To see this, note that  $(I - \rho_0 W_0)^{-1}$  is no longer row-sum normalized and, crucially,  $\alpha_t (I - \rho_0 W_0)^{-1} \iota$  is not a vector with constant entries.

The next proposition makes this point formally, that the stronger Assumption (A4') is *necessary* to eliminate group-level shocks, by showing it is not possible to construct a data transformation that eliminates group effects in the absence of row-sum normalization.

**Proposition 2.** *Define  $r_{W_0} = (I - \rho_0 W_0)^{-1} \iota$ . If in space  $\Theta = \{\theta \in \mathbb{R}^m : \text{Assumptions (A1)-(A5) are satisfied}\}$  there are  $N$  matrices  $W_0^{(1)}, \dots, W_0^{(N)}$  such that  $[r_{W_0^{(1)}} \dots r_{W_0^{(N)}}]$  has rank  $N$ , then the only transformation such that  $(I - \tilde{H})(I - \rho_0 W_0)^{-1} \iota = 0$  is  $\tilde{H} = I$ .*

It is useful to be able to test for row-sum normalization (A4') as it enables common shocks to be accounted for in the social interactions model. This is possible as,

$$\begin{aligned} \Pi_0 \iota &= \beta_0 \iota + (\rho_0 \beta_0 + \gamma_0) \sum_{k=1}^{\infty} \rho_0^{k-1} W_0^k \iota \\ &= \left[ \beta_0 + (\rho_0 \beta_0 + \gamma_0) \sum_{k=1}^{\infty} \rho_0^{k-1} \right] \iota \\ &= \frac{\beta_0 + \gamma_0}{1 - \rho_0} \iota. \end{aligned} \tag{7}$$

The last equality follows from the observation that, under row-normalization of  $W_0$ ,  $W_0^k \iota = W_0 \iota = \iota$ ,  $k > 0$ . This implies  $\Pi_0$  has constant row-sums, which suggests row-sum normalization is testable. In the Appendix we derive a Wald test statistic to do so.<sup>16</sup>

<sup>16</sup>For ease of explanation, in the Appendix we derive the test under the asymptotic distribution of the OLS estimator. The test generally holds with minor adjustments for estimators with known asymptotic distributions.

### 2.3.3 Multivariate Covariates

Next allowing for multivariate  $x_t$  of dimension  $n \times k$ , the reduced-form model (4) is,

$$y_t = \sum_{k=1}^K \Pi_{0,k} x_{k,t} + \nu_t,$$

where  $\Pi_{0,k} = (I - \rho_0 W_0)^{-1} (\beta_{0,k} + \gamma_{0,k} W_0)$ ,  $x_{k,t}$  refers to the  $k$ -th column of  $x_t$ , and  $\beta_{0,k}$  and  $\gamma_{0,k}$  select the  $k$ -th element of  $K$ -dimensional  $\beta_0$  and  $\gamma_0$ , respectively. The previous identification results then apply sequentially to each  $\Pi_{0,k}$ ,  $k = 1, \dots, K$ . In fact, we only then need to maintain  $W_x = \gamma_0 W_0$  for one covariate. It is therefore possible to allow the structure of endogenous and exogenous social effects to differ for  $K - 1$  of the covariates. With  $K$  covariates, equation (3) is,

$$y_t = \rho_0 W_0 y_t + \sum_{k=1}^K \beta_{0,k} x_t + \sum_{k=1}^K \gamma_{0,k} W_{0,k} x_{k,t} + \epsilon_t.$$

Let  $W_{0,k} = W_0$  be the case for  $k = 1$ . Then, having identified  $\rho_0$  and  $W_0$  from  $\Pi_{1,0}$ ,

$$(I - \rho_0 W_0) \Pi_{0,k} = \beta_{0,k} I + \gamma_{0,k} W_{0,k},$$

for  $k = 2, \dots, K$ . The parameter  $\beta_{0,k}$  then corresponds to the diagonal elements of  $(I - \rho_0 W_0) \Pi_{0,k}$  and the off-diagonal entries correspond to the off-diagonal elements of  $\gamma_{0,k} W_{0,k}$ . If Assumption (A4) holds for every  $k = 1, \dots, K$ , we can identify  $\gamma_{0,k}$  and thus  $W_{0,k}$  for every  $k = 1, \dots, K$ .<sup>17</sup>

## 3 Implementation

We now transition from our core identification results to their practical implementation. As this is a high-dimensional estimation problem, our preferred approach makes use of the Adaptive Elastic Net GMM (Caner and Zhang, 2014), that is based on the penalized GMM objective function. Given the identification results presented in Section 2, the populational version of the GMM objective function will be uniquely minimized at the true parameter vector.

After setting out the estimation procedure, we showcase the method using Monte Carlo simulations based both on stylized random network structures as well as real world networks. In each case, we take a fixed network structure  $W_0$ , and simulate panel data as if the data generating process were given by (1). We apply the method on the simulated panel data to recover estimates of all elements in  $W_0$ , as well as the endogenous and exogenous social effect parameters.

---

<sup>17</sup>Blume *et al.* (2015) also study the case in which the social structure mediating endogenous and exogenous social effects might differ. When  $W_x$  is known and there is partial knowledge of the endogenous social interaction matrix  $W_0$ , they show that the parameters of the model can be identified (their Theorem 6). Analogously, when there are enough unconnected nodes in each of the social interaction matrices represented by  $W_x$  and  $W_0$ , and the identity of those nodes is known, identification is also (generically) possible (their Theorem 7).



### 3.1 Estimation

The parameter vector to be estimated is high-dimensional:  $\theta = (W_{12}, \dots, W_{N,N-1}, \rho, \gamma, \beta)' \in \mathbb{R}^m$ , where  $m = N(N-1) + 3$  and  $W_{ij}$  is the  $(i, j)$ -th element of the  $N \times N$  social interactions matrix  $W_0$ . To be clear, in a network with  $N$  individuals, there are  $N(N-1)$  potential interactions because individuals could interact with everyone else but herself (which would violate Assumption A1). As a consequence, even with a modest  $N$ , there are many more parameters to estimate and  $m$  is large. For example, a network with  $N = 50$  implies more than two thousand parameters to estimate. While we consider  $N$  (and thus  $m$ ) is fixed, we still refer to  $\theta$  as high-dimensional. OLS estimation requires  $m \ll NT (\Rightarrow N \ll T)$ , so many more time periods than individuals: a requirement often met in finance data sets (van Vliet, 2018) or in other fields (see, e.g., Section 4.2 in Rothenhäusler *et al.*, 2015). Instead, to estimate a large number of parameters with limited data we utilize high-dimensional estimation methods, that are the focus of a rapidly growing literature. However, the identification results presented in Section 2 apply more broadly and irrespective of the estimation procedure.

Sparsity is a key assumption underlying all high-dimensional estimation techniques. In the context of social interactions, we say that  $W_0$  is sparse if  $\tilde{m}$ , the number of non-zero elements of  $W_0$ , is such that  $\tilde{m} \ll NT$ . The notion of sparsity thus depends on the number of time periods: although  $N$  and  $m$  are fixed,  $\tilde{m}$  itself can grow with  $T$ . Sparsity corresponds to assuming that individuals influence or are influenced by a small number of others, relative to the overall size of the potential network and the time horizon in the data. As such, sparsity is typically *not* a binding constraint in social networks analysis.<sup>18</sup>

In the estimation of sparse models, the “effective number of parameters” (or “effective degrees of freedom”) relates to the number of variables with non-zero estimated coefficients (Tibshirani and Taylor, 2012). In the context of the current social network model (and the Elastic Net estimator on which the estimation strategy below builds on), this is approximately equivalent to the density of the network times the number of parameters  $m$ . We then require this number to be smaller than  $T$ . Implicitly, this calculation provides a rough assessment on the minimum required  $T$ . For example, with  $N = 30$  and a network with 2% of potential links in place, this implies  $T$  should be larger than 18.

Finally, to reiterate, our identification results themselves do *not* depend on the sparsity of networks. In particular, Assumptions A1 to A5 *do not* impose restrictions on the number of links

---

<sup>18</sup>For example, common stylized networks are sparse, such as: (i) star: all individuals receive spillovers from the same individual; (ii) lattice: each individual is a source of spillover only to one other individual; (iii) interactions in pairs or triads or small groups, such as those described by De Giorgi *et al.* (2010); and (iv) small world networks (Watts, 1999). Prominent real world economic networks are also sparse. For example, in individual-level elicited data from *AddHealth* on teenage friendships (defined as reciprocated nominations), the density of links is around 2% of all feasible links. In firm-level data, the density of production networks in the US is less than 1% of all feasible links (Atalay *et al.*, 2011).

in  $W_0$ , or  $\tilde{m}$ .<sup>19</sup>

Our preferred approach estimates the interaction matrix in the reduced form while penalizing and imposing sparsity on the structural object  $W_0$ . We impose sparsity and penalization in the structural-form matrix  $W_0$  because this is a weaker requirement than imposing sparsity and penalization in the reduced-form matrix  $\Pi_0$ .<sup>20</sup> To accomplish this, we make use of the Adaptive Elastic Net GMM (Caner and Zhang, 2014), that is based on the penalized GMM objective function,

$$G_{NT}(\theta, p) \equiv g_{NT}(\theta)' M_T g_{NT}(\theta) + p_1 \sum_{\substack{i,j=1 \\ i \neq j}}^N |W_{i,j}| + p_2 \sum_{\substack{i,j=1 \\ i \neq j}}^N |W_{i,j}|^2 \quad (8)$$

where  $\theta = (W_{1,2}, \dots, W_{N,N-1}, \rho, \gamma, \beta)'$  with dimension  $m = N(N-1) + 3$ , and  $p_1$  and  $p_2$  are the penalization terms. The term  $g_{NT}(\theta)' M_T g_{NT}(\theta)$  is the unpenalized GMM objective function with moment conditions based on the orthogonality between the structural disturbance term and the covariates:  $g_{NT}(\theta) = \sum_{t=1}^T [x_{1t}e_t(\theta)' \cdots x_{Nt}e_t(\theta)']'$ ,  $e_t(\theta) = y_t - (I - \rho W)^{-1}(\beta I + \gamma W)x_t$ . There are  $q \equiv N^2$  moment conditions since  $x_{it}$  is orthogonal to  $e_{jt}$ , for each  $i, j = 1, \dots, N$ . Hence the GMM weight matrix  $M_T$  is of dimension  $N^2 \times N^2$ , symmetric, and positive definite. For simplicity, we use  $M_T = I_{N^2 \times N^2}$ . Note that if  $x_t$  is econometrically endogenous, one can also exploit moment conditions with respect to available instrumental variables.<sup>21</sup>

Given the identification results presented in Section 2, if  $\theta \neq \theta_0$  and does not belong to the identified set, then  $\Pi(\theta) \neq \Pi(\theta_0)$ . Consequently, the populational version of the GMM objective function is uniquely minimized at the true parameter vector  $\theta_0$ .

The penalization terms in (8) is what makes this different from a standard GMM problem. The first term,  $p_1 \sum_{i,j=1, i \neq j}^N |W_{i,j}|$ , penalizes the sum of the absolute values of  $W_{ij}$ , i.e. the sum of the strength of links, for all node-pairs. The second term,  $p_2 \sum_{i,j=1, i \neq j}^N |W_{i,j}|^2$ , penalizes the sum of the square of the parameters. This term has been shown to provide better model-selection properties, especially when explanatory variables are correlated (Zou and Zhang, 2009). The first stage estimate is,

$$\tilde{\theta}(p) = (1 + p_2/T) \cdot \arg \min_{\theta \in \mathbb{R}^p} G_{NT}(\theta, p) \quad (9)$$

where  $(1 + p_2/T)$  is a bias-correction term also used by Caner and Zhang (2014).

<sup>19</sup>If  $N \rightarrow \infty$ , Assumption A2 would imply vanishing  $(W_0)_{ij}$  entries. As highlighted previously, we consider  $N$  to be fixed, in line with many practical applications. Furthermore, Assumption A2 is used to represent inverse matrices as Neumann series in our identification results. What is necessary for this to hold is that a sub-multiplicative norm on  $\rho W$  be less than one. Here we use a specific norm (i.e., the maximum row sum norm), but other (induced) norms are also possible (i.e., the 2-norm or the 1-norm) (see Horn and Johnson, 2013, Chapter 5.6).

<sup>20</sup>Note that even if  $W$  is sparse,  $\Pi$  may not be sparse. In Appendix B.1, we show that  $[\Pi_0]_{ij} = 0$  if, and only if, there are no paths between  $i$  and  $j$  in  $W_0$ , and so the pair is not connected. So sparsity in  $\Pi_0$  is understood as  $W_0$  being ‘sparsely connected’, which is a stronger assumption than sparsity in  $W_0$ .

<sup>21</sup>For expositional ease, we describe estimation in the context of the reduced form model (4), thereby abstaining from individual fixed or correlated effects. As the GMM estimator uses moments between the structural disturbance terms and covariates, this endogeneity is built into the estimation procedure.

Depending on the choice of  $p_1$ , some  $W_{i,j}$ 's will be estimated as exact zeros. A larger share of parameters will be estimated as zeros if  $p_1$  increases. The penalization also shrinks non-zero estimates towards zero. A second (adaptive) step provides improvements by re-weighting the penalization by the inverse of the first-step estimates (Zou, 2006):

$$\hat{\theta}(p) = (1 + p_2/T) \cdot \arg \min_{\theta \in \mathbb{R}^p} \left\{ g_{NT}(\theta)' M_T g_{NT}(\theta) + p_1^* \sum_{\substack{\{i,j:\tilde{W}_{i,j} \neq 0, \\ i,j=1,\dots,N, \\ i \neq j\}}} \frac{|W_{i,j}|}{|\tilde{W}_{i,j}|^\gamma} + p_2 \sum_{\substack{\{i,j:\tilde{W}_{i,j} \neq 0, \\ i,j=1,\dots,N, \\ i \neq j\}}} |W_{i,j}|^2 \right\}, \quad (10)$$

where  $\tilde{W}_{i,j}$  is the  $(i, j)$ -th element of the first-step estimate of  $W$ , and we follow Caner and Zhang (2014) to set  $\gamma = 2.5$ . Elements  $\tilde{W}_{i,j}$  estimated as zeros in the first stage are kept as zero in the second stage, because  $\tilde{W}_{i,j} = 0$  implies the effective penalization is infinite. We write  $p = (p_1, p_1^*, p_2)$  as the final set of penalization parameters. Conditional on  $p$ , the estimate of the Adaptive Elastic Net GMM procedure is  $\hat{\theta}(p)$ . Finally, we update the estimates of  $\rho_0$ ,  $\beta_0$  and  $\gamma_0$  on a regression using peers-of-peers as instruments, similar to Bramoullé *et al.* (2009), but using the network as estimated in (10). This final step is not necessary but performs better in small samples. As in Caner and Zhang (2014, p. 35), the penalization parameters  $p$  are chosen by the BIC criterion. This balances model fit with the number of parameters included in the model.<sup>22</sup>

In Appendix B.2 we provide further implementation details, including the choice of initial conditions. Of course, other estimation methods are available and our identification results do not hinge on any particular estimator. Our aim is to demonstrate the practical feasibility of using the Adaptive Elastic Net estimator, rather than claim it is the optimal estimator.<sup>23</sup> Indeed, in Appendix B.3 we show how OLS can also be used to estimate  $\theta$  if  $T$  is sufficiently large. This makes precise the benefits of penalized estimation for any given  $T$  and highlights that sparsity is not required for our identification results.

## 3.2 Simulations

We showcase the method using Monte Carlo simulations based both on stylized random network structures as well as real world networks. We describe the simulation procedures, results and

---

<sup>22</sup>Following Caner and Zhang, 2014, the choice of  $p$ , which we denote as  $\hat{p}$ , is the one that minimizes

$$\text{BIC}(p) = \log \left[ g_{NT}(\hat{\theta}(p))' M_T g_{NT}(\hat{\theta}(p)) \right] + A(\hat{\theta}(p)) \cdot \frac{\log T}{T}$$

where  $A(\hat{\theta}(p))$  counts the number of non-zero coefficients among  $\{W_{1,2}, \dots, W_{N,N-1}\}$ . (See also Zou *et al.*, 2007.)

<sup>23</sup>For example, Manresa (2016) also relies on a Lasso-related methodology but restricts  $\rho_0$  to be zero and so ignores endogenous social effects. If instrumental variables are available, Lam and Souza (2016) propose estimating (1) directly using the Adaptive Lasso and exploiting sparsity of the estimated  $W_0$ . Gautier and Rose (2016) extend the (identification-robust) Self-Tuning Instrumental Variable estimator in Gautier and Tsybakov (2014).

robustness checks in more detail in the Appendix. Here we just provide a brief overview to highlight how well the method works to recover social networks even in relatively short panels.

For each simulated network, we take a fixed network structure  $W_0$ , and simulate panel data as if the data generating process were given by (1). We then apply the method on the simulated panel data to recover estimates of all elements in  $W_0$ , as well as the endogenous and exogenous social effect parameters  $(\rho_0, \gamma_0)$ . Our result identifies entries in  $W_0$  and so naturally recovers links of varying strength. It is long recognized that link strength might play an important role in social interactions (Granovetter, 1973). Data limitations often force researchers to postulate some ties to be weaker than others (say, based on interaction frequency). In contrast, our approach identifies the continuous strength of ties,  $W_{0,ij}$ , where  $W_{0,ij} > 0$  implies node  $j$  influences node  $i$ .

The stylized networks we consider are a random network, and a political party network in which two groups of nodes each cluster around a central node. The real world networks we consider are the high-school friendship network in Coleman (1964) from a small high school in Illinois, and one of the village networks elicited in Banerjee *et al.* (2013) from rural Karnataka, India. These networks vary in size, complexity, and their aggregate and node-level features. All four networks are also sparse. For the stylized networks, we first assess the performance of the estimator for a fixed network size,  $N = 30$ . We simulate the real-world networks using non-isolated nodes in each (so  $N = 70$  and  $65$  respectively).<sup>24</sup>

Despite the heterogeneity across network scenarios, the method performs well in all simulations. Figure A1 shows the simulation results. Each Panel presents a different metric as we vary  $T$  for each simulated network. Panel A shows that for each network, the proportion of zero entries in  $W_0$  correctly estimated as zeros is above 90% even when exploiting a small number of time periods ( $T = 5$ ). The proportion approaches 100% as  $T$  grows. Conversely, Panel B shows the proportion of non-zeros entries estimated as non-zeros is also high for small  $T$ . It is above 70% from  $T = 5$  for the Erdos-Renyi network, being at least 85% across networks for  $T = 25$ , and increasing as  $T$  grows. As discussed above, the Adaptive Elastic Net estimator is better in recovering true zero entries because it is a well-known feature that shrinkage estimators tend to shrink small parameters to zero.

Panels C and D show that for each simulated network, the mean absolute deviation between estimated and true networks for  $\hat{W}$  and  $\hat{\Pi}$  falls quickly with  $T$  and is close zero for large sample sizes. Finally, Panels E and F show that biases in the endogenous and exogenous social effects parameters,  $\hat{\rho}$  and  $\hat{\gamma}$ , also fall quickly in  $T$ . The fact that biases are not zero is as expected for small  $T$ , being analogous to well-known results for autoregressive time series models.<sup>25</sup>

In the Appendix we show the robustness of the simulation results to: (i) varying network sizes and node definitions in the real work network of Banerjee *et al.* (2013); (ii) alternative parameter

<sup>24</sup>As in Bramoullé *et al.*, 2009, we exclude isolated nodes because they do not conform with row-sum normalization.

<sup>25</sup>The bias in spatial auto-regressive models with small number of observations *even when the network is observed* is similarly documented by Mizruchi and Neuman (2008), Farber *et al.* (2009), Smith (2009), Neuman and Mizruchi (2010), and Wang *et al.* (2014).

choices and richening up the structure of shocks across nodes. We also demonstrate the gains from using the Adaptive Elastic Net GMM estimator over alternative estimators, such as the Adaptive Lasso estimator and OLS.

## 4 Application: Tax Competition Between US States

Our identification result can be used to shed new light on a classic social interactions problem: tax competition between US states (Wilson, 1999). Since the seminal empirical studies in tax competition between jurisdictions (Case *et al.*, 1989; Case *et al.*, 1993), it has been well-recognized that defining competing ‘neighbors’ is the central empirical challenge, and theory cannot resolve the issue. Two mechanisms have been argued to drive the structure of interactions across jurisdictions: factor mobility and yardstick competition.

On factor mobility, Tiebout (1956) first argued that labor and capital can move in response to differential tax rates across jurisdictions. Factor mobility leads naturally to the postulated social interactions matrix being: (i) geographic neighbors given labor mobility; and (ii) jurisdictions with similar economic or demographic characteristics, given capital mobility (Case *et al.*, 1989).<sup>26</sup>

A second mechanism occurs through political economy channels (Shleifer, 1985). In particular, yardstick competition between jurisdictions is driven by voters making comparisons between states to learn about their own politician’s quality. Besley and Case (1995) formalize the idea in a model where voters use taxes set by governors in neighboring states to infer their own governor’s quality. This generates informational externalities across jurisdictions, forcing incumbents into yardstick competition, where their tax setting behavior is determined by what other incumbents do. Yardstick competition leads naturally to the postulated interactions matrix corresponding to a matrix of ‘political neighbors’: other states that voters make comparisons to.

This application shows the practical use of our approach to recover social interactions in a setting in which the number of nodes and time periods is relatively low: the data covers mainland US states,  $N = 48$ , for years 1962-2015,  $T = 53$ . Our approach identifies the structure of social interactions among ‘economic neighbors’, that we denote  $W_{econ}$ . We contrast this against a null hypothesis that states are only influenced by their geographic neighbors,  $W_{geo}$ , as postulated by Besley and Case, 1995 and shown in Figure 1A. With  $W_{econ}$  recovered, we can establish, beyond geography, what predicts the existence and strength of ties between states. Finally, relative to  $W_{geo}$ , we conduct simulations using  $W_{econ}$  to assess the equilibrium propagation of tax setting shocks across mainland US states. Taken together, this body of evidence allows us to provide novel insights related to the role of factor mobility and yardstick competition in driving tax setting behavior across US states.

---

<sup>26</sup>A body of evidence finds that tax bases are mobile in response to tax differentials (Hines, 1996; Devereux and Griffith, 1998; Kleven *et al.*, 2013, 2014)

## 4.1 Data and Empirical Specification

We denote state tax liabilities for state  $i$  in year  $t$  as  $\tau_{it}$ , covering state taxes collected from real per capita income, sales and corporate taxes. We measure this using a series constructed from data published annually in the Statistical Abstract of the United States. Our series covers mainland states ( $N = 48$ ) for years 1962-2015, ( $T = 53$ ), therefore extending the sample used by Besley and Case (1995), that runs from 1962-1988 ( $T = 26$ ).<sup>27</sup> The outcome considered,  $\Delta\tau_{it}$ , is the change in tax liabilities between years  $t$  and  $(t - 2)$  because it might take a governor more than a year to implement a tax program. Their model implies a standard social interactions specification for the tax setting behavior of state governors:

$$\Delta\tau_{it} = \rho \sum_{j=1}^N W_{0,ij} \Delta\tau_{jt} + \gamma \sum_{j=1}^N W_{0,ij} x_{jt} + \beta x_{it} + \alpha_i + \alpha_t + \epsilon_{it}. \quad (11)$$

Tax setting behavior is thus determined by (i) endogenous social effects arising through neighbors' tax changes ( $\sum_{j=1}^N W_{0,ij} \Delta\tau_{jt}$ ); (ii) exogenous social effects arising through the economic/demographic characteristics of neighbors ( $\sum_{j=1}^N W_{0,ij} x_{jt}$ ); (iii) state  $i$ 's characteristics ( $x_{it}$ ), that include income per capita, the unemployment rate, and the proportion of young and elderly. All specifications include state and time effects ( $\alpha_i, \alpha_t$ ), so allowing for time-invariant unobserved heterogeneity across states, and for common (macroeconomic) shocks. Due to the inclusion of the time effects  $\alpha_t$ , we normalize the rows of  $W_{econ}$  to one. Table A7 presents descriptive statistics for the Besley and Case (1995) sample and our extended sample.

Much of the earlier literature focuses on endogenous social effects and ignores exogenous social effects by setting  $\gamma = 0$ . Our identification result allows us to relax this constraint and thus estimate the full typology of social effects described by Manski (1993). This is important because only endogenous social effects lead to social multipliers, and are crucial to identify as they can lead to a race-to-the-bottom or sub-optimal public goods provision (Brennan and Buchanan, 1980; Wilson, 1986; Oates and Schwab, 1988).

After estimating the neighborhood matrix, we follow Besley and Case (1995) and estimate the model instrumenting for  $\Delta\tau_{jt}$  using neighbors' lagged change in income per capita, and neighbors' lagged change in unemployment rate. These instruments are in the spirit of using exogenous social effects to instrument for neighbor's tax changes. However, given our approach allows us to estimate exogenous social effects ( $\gamma \neq 0$ ), these instruments will generally be weaker when estimating the full specification in (11). We thus follow Bramoullé *et al.* (2009) and De Giorgi *et al.* (2010), and also instrument neighbors' tax changes with neighbor-of-neighbor characteristics.

---

<sup>27</sup>Besley and Case (1995) test their political agency model using a two equation set-up: (i) on gubernatorial re-election probabilities; and (ii) on tax setting. Our application focuses on the latter because this represents a social interaction problem. They use two tax series: (i) TAXSIM data (from the NBER) which runs from 1977-88; and (ii) state tax liabilities series constructed from data published annually in the Statistical Abstract of the US that runs from 1962-1988. All their results are robust to either series. We extend the second series.

## 4.2 Preliminary Findings

Table 1 presents our preliminary findings and comparison to Besley and Case (1995). Column 1 shows OLS estimates of (11) where the postulated social interactions matrix is based on geographic neighbors, exogenous social effects are ignored so  $\gamma = 0$  and the panel includes all 48 mainland states but runs only from 1962-1988 as in Besley and Case (1995). Social interactions influence gubernatorial tax setting behavior:  $\hat{\rho}_{OLS} = .375$ . Column 2 shows this to be robust to instrumenting neighbors' tax changes using the instrument set proposed by Besley and Case (1995).  $\hat{\rho}_{2SLS}$  is more than double the magnitude of  $\hat{\rho}_{OLS}$  suggesting tax setting behaviors across jurisdictions are strategic complements, and OLS estimates are heavily downward-biased.

Columns 3 and 4 replicate both specifications over the longer sample period we construct. The evidence confirms Besley and Case's (1995) finding on social interactions to be robust in a longer sample period. We again note that  $\hat{\rho}_{2SLS}$  is more than double the magnitude of  $\hat{\rho}_{OLS}$ . The result in Column 4 implies that for every dollar increase in the average tax rates among geographic neighbors, a state increases its own taxes by 61 cents. This is similar to the headline estimate of Besley and Case (1995).<sup>28</sup>

## 4.3 Endogenous and Exogenous Social Interactions ( $\rho$ and $\gamma$ )

We now move beyond much of the earlier political economy and public economics literature to first establish whether there are endogenous and exogenous social interactions in tax setting behavior. We first focus on the endogenous and exogenous social interaction parameters, and in the next subsection we detail the identified social interactions matrix,  $\hat{W}_{econ}$ . Column 1 of Table 2 shows the initial estimates obtained from the Adaptive Elastic Net procedure where  $\gamma = 0$ . Columns 2 and 3 show the resulting OLS and 2SLS estimates for  $\rho$ :  $\hat{\rho}_{2SLS} = .641 > \hat{\rho}_{OLS} = .378 > 0$ .<sup>29</sup> Columns 4 to 6 estimate the full model in (11). Columns 5 and 6 show the OLS and 2SLS estimates of  $\rho$  are smaller, and less precisely estimated when exogenous social effects are allowed. This is not surprising given that the instrument set is based on neighbors' characteristics, many of which are directly controlled for in (11), thus reducing the effective variation induced by the instrument. Hence, in Column 7, we report 2SLS estimates based on instruments using neighbor-of-neighbor characteristics. This represents our preferred specification:  $\hat{\rho}_{2SLS} = .608$  (with a standard error of .220). This value also meets the requirements on  $\rho$  in Corollaries 3 and 4 for global identification.

In short, there is robust evidence of endogenous social interactions in tax setting behavior of governors across states.<sup>30</sup>

---

<sup>28</sup>Nor is the magnitude very different from earlier work examining fiscal expenditure spillovers. For example, Case *et al.* (1989) find that US state government levels of per-capita expenditures are significantly impacted by the expenditures of their neighbors, with the size of the impact being that a one dollar increase in neighbors' expenditures leads to an increase in own-state expenditures by seventy cents.

<sup>29</sup>We report robust standard errors and so do not adjust them for the fact that  $\hat{W}_{econ}$  is estimated.

<sup>30</sup>Table A8 shows the full set of exogenous social effects (so Columns 1 to 4 refer to the same specifications as

## 4.4 Identified Social Interactions Matrix ( $\hat{W}_{econ}$ )

Figure 1B shows how the structure of economic ( $\hat{W}_{econ}$ ) and geographic networks ( $W_{geo}$ ) differ, where connected edges imply that two states are linked in at least one direction (either state  $i$  causally impacts state taxes in  $j$ , and/or *vice versa*). This comparison makes it clear whether all states geographically adjacent to  $i$  matter for its tax setting behavior and whether there are non-adjacent states that influence its tax rate.

The left-hand panel of Figure 1B shows the network of geographic neighbors (whose edges are colored blue), onto which we have superimposed the edges that are *not* identified as links in  $W_{econ}$ ; these dropped edges are indicated in red. This first implies that not all geographically adjacent states are relevant for tax setting behavior. The right-hand panel of Figure 1B adds new edges identified in  $\hat{W}_{econ}$  that are *not* part of  $W_{geo}$ . These represent non-adjacent states through which social interactions occur. This implies the existence of spatially dispersed social interactions between states. The implication is that for tax-setting behavior, economic distance is imperfectly measured if we simply assume that interactions depend only on geographical distance. As detailed below, this has many implications for the economics of tax competition.

As Table 3 summarizes,  $W_{geo}$  has 214 edges, while  $\hat{W}_{econ}$  has only 144 edges. States are less connected than implied by postulating geographic networks.  $\hat{W}_{econ}$  and  $W_{geo}$  have 79 edges in common. However,  $W_{geo}$  has 135 edges that are absent in  $\hat{W}_{econ}$ . Hence, while geography remains a key determinant of tax competition, the majority of geographical neighbors ( $135/214 = 63\%$ ) are not relevant for tax setting. There are 65 edges that exist only in  $W_{geo}$ , so although there are fewer edges in  $\hat{W}_{econ}$ , the identified social interactions are more spatially dispersed than under the assumption of geographic networks. This is reflected in the far lower clustering coefficient in  $\hat{W}_{econ}$  than in  $W_{geo}$  (.026 versus .194).<sup>31</sup>

## 4.5 Strength of Ties and Reciprocity

Our estimation strategy identifies the continuous strength of ties,  $W_{0,ij}$ , where  $W_{0,ij} > 0$  is interpreted as state  $j$  influencing outcomes in state  $i$ . This is useful because recent developments in tax competition theory, using insights from the social networks literature, suggest links need not be reciprocal or of symmetric strength (Janeba and Osterleh, 2013).

Figure 2A shows the distribution of  $W_{0,ij}$ 's across edges in  $\hat{W}_{econ}$  (conditional on  $W_{0,ij} > 0$ ). The strength of ties between pairs of states varies greatly. The mean strength of ties is .19, that is higher than the median strength, .085, suggesting many weak ties. At the other end of the

---

Columns 4 to 7 in Table 2). Exogenous social effects operate through economic neighbors' income per capita and unemployment rate. Demographic characteristics of economic neighbors to state  $i$  do not impact its tax rate.

<sup>31</sup>The clustering coefficient is the frequency of the number of fully connected triplets over the total number of triplets. Other metrics can also be used to provide a scalar comparison of  $W_{geo}$  and  $\hat{W}_{econ}$ . One way to do so is to reshape both matrices as vectors of length  $(48 \times 47)$  and to compute their correlation. Doing so, we obtain a correlation coefficient of .322.



distribution, the strongest 10% of ties have weight above .6.

On the reciprocity of ties, Table 3 reveals that only 29.2% of edges in  $\hat{W}_{econ}$  are reciprocal (all edges in  $W_{geo}$  are reciprocal by construction). Hence, tax competition is both spatially disperse and highly asymmetric. In most cases where tax setting in state  $i$  is influenced by taxes in state  $j$ , the opposite is not true.

Panels B and C in Figure 2 illustrate this for California, indicating the strength of each tie ( $\hat{W}_{econ,CA,j}$ ). Figure 2B shows the in-network for California: those states causally impacting tax-setting in California. Some geographic neighbors to California influence its tax setting behavior (Nevada and Oregon), although these ties are weak. On the other hand, non-adjacent states influence California (Colorado, Maine), and these in-network ties are stronger than geographically adjacent in-network ties. Figure 2C shows the out-network for California, again indicating each tie strength ( $\hat{W}_{econ,i,CA}$ ): those states whose taxes are influenced by taxes in California. We see that none of the geographic neighbors to California are influenced by its tax setting behavior, whereas a number of non-adjacent states are influenced (including East Coast states such as Virginia, and Southern states, such as Louisiana). When states are influenced by taxes in California, these ties tend to be relatively strong:  $\hat{W}_{econ,i,CA} \geq .19$  for all five in-network ties.

Given common time shocks  $\alpha_t$  in (11), row-sum normalization is required and ensures  $\sum_j W_{0,ij} = 1$ . Hence, for every state  $i$  there will be at least one economic neighbor state  $j^*$  impacts it, so that  $W_{0,ij^*} > 0$ . This just reiterates that social interactions matter. On the other hand, our procedure imposes no restriction on the derived columns of  $\hat{W}_{econ}$ . It could be that a state does not affect any other state. Examining this possibility directly in  $\hat{W}_{econ}$ , we see this occurs for Minnesota, New Jersey, New Mexico, Vermont, and Wisconsin. These states have an out-degree of zero. Their tax rates impact no other states.

Table 3 reports the degree distribution across all nodes (states), splitting for in-networks and out-networks. In  $W_{geo}$ , the in-degree is by construction equal to the out-degree, as all ties are reciprocal. The greater sparsity of the network of economic neighbors is again reflected in the degree distribution being lower for  $\hat{W}_{econ}$  than for  $W_{geo}$ . In  $\hat{W}_{econ}$  the dispersion of in- and out-degree networks is very different (as measured by the standard deviation), being near double for the in-degree. This asymmetry in  $\hat{W}_{econ}$  further suggests that some highly focal or influential states drive tax setting behavior in other states.

Figures 3A and 3B show complete histograms for the in- and out-degree across states. The histogram on the left is for in-degree, and shows that states under  $\hat{W}_{econ}$  generally have lower in-degree than under  $W_{geo}$ . The states that are influenced by the highest number of other states are Utah, Pennsylvania and Ohio. The histogram on the right for out-degree, shows the five states described above that do not impact other states (Wisconsin, Vermont, New Mexico, New Jersey and Minnesota). Delaware is an outlier influential state in its out-degree in determining tax setting in other states: as discussed below, Delaware is a well-known potential tax haven.<sup>32</sup>

---

<sup>32</sup>Dyreng *et al.* (2013) find that taxes play an important role in determining whether firms locate subsidiaries in

## 4.6 Factor Mobility or Yardstick Competition?

We conclude by presenting two strategies to shed light on whether factor mobility and yardstick competition drive these social interactions: (i) exploiting information in the identified social interactions matrix  $\hat{W}_{econ}$ ; (ii) following Besley and Case (1995), using gubernatorial re-election as an indirect test of the relevance of yardstick competition.

In our first strategy we estimate the factors correlated with the existence/strength of links between states  $i$  and  $j$  in  $\hat{W}_{econ}$  using the following dyadic regression:

$$\hat{W}_{econ,ij} = \lambda_0 + \lambda_1 X_{ij} + \lambda_2 X_i + \lambda_3 X_j + u_{ij}.$$

We discretize link strength so  $\hat{W}_{econ,ij} \in \{0, 1\}$  and predict the existence of a link using a linear probability model. We then estimate the correlates of link strength  $\hat{W}_{econ,ij} \in [0, 1]$  using a Tobit model. The elements  $X_{ij}$ ,  $X_i$ , and  $X_j$  correspond to characteristics of the pair of states  $(i, j)$ , of state  $i$ , and state  $j$ , respectively. Covariates are time-averaged over the sample period, and robust standard errors are reported. The sample thus corresponds to  $N \times (N - 1) = 48 \times 47 = 2256$  potential  $ij$  links that could have formed.

Table 4 presents the results. Column 1 controls only for whether states  $i$  and  $j$  are geographic neighbors. This is highly predictive of a link between them. Columns 2 and 3 show that distance between states also negatively correlates with them being linked, but that when both geographic adjacency and distances are included, the former is more predictive. Hence, we control only for whether  $i$  and  $j$  are geographic neighbors in the remaining Columns.

The next set of specifications use the insight that economic neighbors are likely to be based on a mixture of similarity in geography, income per capita, and demography (Case *et al.*, 1989). Column 4 thus adds two  $X_{ij}$  covariates to capture the economic and demographic homophily between states  $i$  and  $j$ . GDP homophily is the absolute difference in the states GDP per capita. Demographic homophily is the absolute difference of the share of young people (aged 5-17) plus the absolute difference of the share of elderly people (aged 65+) across the states. GDP homophily predicts ties, whereas demographic homophily does not.

Columns 5 to 7 then sequentially add in several sets of controls. For labor mobility, we use net state-to-state migration data to control for the net migration flow of individuals from state  $i$  to state  $i$  (defined as the flow from  $i$  to  $j$  minus the flow from  $j$  to  $i$ ).<sup>33</sup> We then add a political

---

Delaware: a Delaware-based state tax avoidance strategy lowers state effective tax rates by around 1 percentage point. They also report that in June 2010, Delaware landed at the top of *National Geographic* magazine's published list of the most secretive tax havens in the world (ahead of foreign tax havens such as Luxembourg, Switzerland, and the Cayman Islands).

<sup>33</sup>We also experimented with alternative measures of labor migration, and results were qualitatively the same. State-to-state migration data are based on year-to-year address changes reported on individual income tax returns filed with the IRS. The data cover filing years 1991 through 2015, and include the number of returns filed, which approximates the number of households that migrated, the number of personal exemptions claimed, which approximates the number of individuals who migrated. The data are available at <https://www.irs.gov/statistics/soi->

homophily variable between states. For any given year, this is set to one if a pair of states have governors of the same political party. As this is time averaged over our sample, this element captures the share of the sample period in which the states have governors of the same party. Lastly, we include whether state  $j$  is considered a tax haven (and so might have disproportionate influence on other states). Based on Findley *et al.* (2012), the following states are coded as tax havens: Nevada, Delaware, Montana, South Dakota, Wyoming and New York. This corroborates earlier evidence in Figure 3B, where Delaware, Wyoming and Nevada were among the states with the highest out-degree.

The specification in Column 7 shows that with this full set of controls, geographic adjacency remains a robust predictor of the existence of links between states. However, the identified economic network highlights additional significant predictors of tax competition between states: political homophily *reduces* the likelihood of a link, suggesting any yardstick competition driving social interactions occurs when voters compare their governor to those of the opposing party in other states. The tax haven states appear to be especially influential in the tax setting behaviors of other states. The strong influence of tax haven states might lead to a race-to-the-bottom. Relative to these factors, the economic and demographic similarity between states play an insignificant role in determining interactions between states.

The final column considers the continuous link strength as an outcome and reports Tobit partial average effect estimates. This reinforces that geography, political homophily, and tax haven status all robustly correlate to the strength of influence states tax setting has on others. Labor mobility between states does not robustly predict either the existence or strength of ties.

Our second strategy to investigate factor mobility and yardstick competition follows the intuition of Besley and Case (1995). They suggest an indirect test of the relevance of yardstick competition is that this mechanism only applies to governors not facing term limits. Therefore we compare our main effects across two subsamples: state-years in which the governor can and cannot run for reelection. The results are reported in Table 5. The 2SLS results suggest that in both samples, endogenous social interaction effects exist, although they are more precisely estimated when governors *can* run for re-election.

Taken together, our evidence suggests that both factor mobility (of both labor and capital, as measured through the influence of tax havens), and yardstick competition (occurring through comparisons to governors of the other party), are important mechanisms driving the existence and strength of interactions in tax-setting behavior across US states.

Finally, in the Appendix, we contrast how shocks to tax setting in a given state propagate under the identified interactions matrix  $\hat{W}_{econ}$ , relative to what would have been predicted under a postulated network structure based on  $W_{geo}$ . As  $\hat{W}_{econ}$  is spatially more dispersed than  $W_{geo}$ , the general equilibrium effects might be very different under the two network structures. We therefore discuss the implications for tax inequality under  $\hat{W}_{econ}$  and the  $W_{geo}$  counterfactual.

---

tax-stats-migration-data (accessed September 2017).

## 5 Discussion

In a canonical social interactions model, we provide sufficient conditions under which the social interactions matrix, and endogenous and exogenous social effects are all globally identified, even absent information on social links. Our identification strategy is novel, and may bear fruit in other areas. We describe how high-dimensional estimation techniques can be used to estimate the model based on the Adaptive Elastic Net GMM method. We showcase our method in Monte Carlo simulations using two stylized and two real world networks: these highlight that even in panels as short as  $T = 5$ , the majority of social ties can be correctly identified. Finally, we employ this estimation strategy to provide novel insights in a classic social interactions problem: tax competition across US states.

Our method is immediately applicable to other classic social interactions problems. For example, in finance a long-standing question has been whether CEOs are subject to relative performance evaluation, and if so, what is the comparison set of firms/CEOs used (Edmans and Gabaix, 2016).<sup>34</sup> Other fields such as macroeconomics, political economy and trade are all obvious areas where social interactions across jurisdictions/countries etc. could drive key outcomes, panel data exist, and the number of nodes is relatively fixed. Our approach can also be applied to new contexts where social interactions determine economic behavior but data on social links is absent. Advances in the availability of administrative data, data from social media or mobile technologies, and high frequency data in finance and from online economic transactions, all offer new possibilities to identify social interactions. For example, van Vliet, 2018 studies the interconnectedness between the largest financial institutions in during the 2008 financial crisis using readily available market data, in which  $N = 13$  and  $T = 500$ .

Three further directions for future research are of note. First, under partial observability of  $W_0$  (as in Blume *et al.*, 2015), the number of parameters in  $W_0$  to be retrieved falls quickly. Our approach can then still be applied to complete knowledge of  $W_0$ , and this could be achieved with potentially weaker assumptions for identification, and in even shorter panels. To illustrate possibilities, Figure 4 shows results from a final simulation exercise in which we assume the researcher starts with partial knowledge of  $W_0$ . We do so for the Banerjee *et al.* (2013) village family network, showing simulation results for scenarios in which the researcher knows the social ties of the three (five, ten) households with the highest out-degree. For comparison we also show the earlier simulation results when  $W_0$  is entirely unknown. This clearly illustrates that with partial knowledge

---

<sup>34</sup>Edmans and Gabaix (2016) overview the theory and empirics of executive compensation. Applying the informativeness principle in contract theory to CEO pay suggests peer performance is informative about the degree to which firm value is due to high CEO effort or luck. In a first generation of studies, Aggarwal and Samwick (1999) and Murphy (1999) showed that CEO pay is determined by absolute, rather than relative performance. However, this conclusion has been challenged by others such as Gong *et al.* (2011) who argue these conclusions arise from identifying relative performance evaluation (RPE) based on an implicit approach, assuming a peer group (e.g. based on industry and/or size). Indeed, when Gong *et al.* (2011) study the explicit use of RPE, based on the disclosure of peer firms and performance measures mandated by the SEC in 2006, they actually find that 25% of S&P 1500 firms explicitly using RPE. We are currently working on using our method to provide novel evidence on the matter.

of the social network, performance on all metrics improves rapidly for any given  $T$ .

Second, we have developed our approach in the context of the canonical linear social interactions model (1). This builds on Manski (1993) when  $W_0$  is known to the researcher, and the reflection problem is the main challenge in identifying endogenous and exogenous social effects. However, as established in Blume *et al.* (2011) and Blume *et al.* (2015), the reflection problem is functional-form dependent and may not apply to many non-linear models. An important topic for future research is thus to extend the insights gathered here to non-linear social interaction settings.

Finally, our approach has taken the network structure as predetermined and fixed. Clearly, an important part of the social networks literature examines endogenous network formation (Jackson *et al.*, 2017; de Paula, 2017). Our analysis allows us to begin probing the issue in two ways. First, the kind of dyadic regression analysis in Section 4 on the correlates of entries in  $W_{0,ij}$  suggests factors driving link formation and dissolution. Second, it is possible to examine whether the identified social interactions matrix is stable over time. To illustrate the possibility in a real world setting, we extend our application on tax competition to investigate the stability of  $\hat{W}_{econ}$  by running the procedure in two subsamples, each with  $T = 26$  periods: 1962-88 and 1989-2015. Panels A and B in Figure 5 shows the resulting estimated economic networks in each subsample, and Panel C provides network statistics for each subsample panel (as well as for the earlier estimated economic network and the network based on geographic neighbors). This highlights that the network structure of tax competition has changed over time, with the later sample network from 1989-2015 having fewer edges, fewer reciprocated edges, lower clustering and lower degree distribution.

This analysis leads naturally to a broad agenda going forward, to address the challenge of simultaneously identifying and estimating time varying models of network formation and social interaction, all in cases where data on social networks is not required.

## References

- ACEMOGLU, D., V. CARVALHO, A. OZDAGLAR, AND A. TAHBAZ-SALEHI (2012). The Network Origins of Aggregate Fluctuations. *Econometrica*, 80, 1977–2016.
- AGGARWAL, R. K. AND A. A. SAMWICK (1999). Executive Compensation, Strategic Competition, and Relative Performance Evaluation: theory and evidence. *The Journal of Finance*, 54.
- AMBROSETTI, A. AND G. PRODI (1972). On the Inversion of Some Differentiable Mappings with Singularities between Banach Spaces. *Annali di Matematica Pura ed Applicata*, 93, 231–46.
- (1995). *A Primer of Nonlinear Analysis*, Cambridge University Press.
- ANSELIN, L. (2010). Thirty Years of Spatial Econometrics. *Papers in Regional Science*, 89, 3–25.

- ATALAY, E., A. HORTACSU, J. ROBERTS, AND C. SYVERSON (2011). Network Structure of Production. *Proceedings of the American Mathematical Society*, 108, 5199–202.
- BALLESTER, C., A. CALVO-ARMENDOL, AND Y. ZENOU (2006). Who’s Who in Networks. Wanted: The Key Player. *Econometrica*, 74, 1403–17.
- BANERJEE, A., A. G. CHANDRASEKHAR, E. DUFLO, AND M. O. JACKSON (2013). The Diffusion of Microfinance. *Science*, 341, 1236498.
- BESLEY, T. AND A. CASE (1994). Unnatural Experiments? Estimating the Incidence of Endogenous Policies. *NBER Working Paper 4956*.
- (1995). Incumbent Behavior: Vote-seeking, Tax-setting, and Yardstick Competition. *American Economic Review*, 85, 25–45.
- BLUME, L., W. A. BROCK, S. N. DURLAUF, AND Y. IOANNIDES (2011). Identification of Social Interactions. in *Handbook of Social Economics*, ed. by J. Behabib, A. Bisin, and M. O. Jackson, North-Holland, vol. 1B.
- BLUME, L. E., W. A. BROCK, S. N. DURLAUF, AND R. JAYARAMAN (2015). Linear Social Interactions Models. *Journal of Political Economy*, 123, 444–96.
- BONALDI, P., A. HORTACSU, AND J. KASTL (2015). An Empirical Analysis of Funding Costs Spillovers in the EURO-zone with Application to Systemic Risk. Princeton University Working Paper.
- BRAMOULLÉ, Y., H. DJEBBARI, AND B. FORTIN (2009). Identification of Peer Effects Through Social Networks. *Journal of Econometrics*, 150, 41–55.
- BRENNAN, G. AND J. BUCHANAN (1980). *The Power to Tax: Analytical Foundations of a Fiscal Constitution*, Cambridge University Press.
- BREZA, E., A. CHANDRASEKHAR, T. MCCORMICK, AND M. PAN (2017). Using Aggregated Relational Data to Feasibly Identify Network Structure without Network Data. Harvard University Working Paper.
- BURSZTYN, L., F. EDERER, B. FERMAN, AND N. YUCHTMAN (2014). Understanding Mechanisms Underlying Peer Effects: Evidence From a Field Experiment on Financial Decisions. *Econometrica*, 82, 1273–301.
- CANER, M. AND H. H. ZHANG (2014). Adaptive Elastic Net for Generalized Method of Moments. *Journal of Business and Economic Statistics*, 32, 30–47.

- CASE, A., J. R. HINES, AND H. S. ROSEN (1989). Copycatting: Fiscal Policies of States and Their Neighbors. *NBER Working Paper 3032*.
- CASE, A., H. ROSEN, AND J. HINES (1993). Budget Spillovers and Fiscal Policy Interdependence: Evidence from the States. *Journal of Public Economics*, 52, 285–307.
- CHANDRASEKHAR, A. AND R. LEWIS (2016). Econometrics of Sampled Networks. Working Paper.
- CHANEY, T. (2014). The Network Structure of International Trade. *American Economic Review*, 104, 3600–34.
- CHIAPPORI, P.-A., I. KOMUNJER, AND D. KRISTENSEN (2015). Nonparametric Identification and Estimation of Transformation Models. *Journal of Econometrics*, 188, 22–39.
- COLEMAN, J. S. (1964). *Introduction to Mathematical Sociology*, London Free Press Glencoe.
- CONLEY, T. G. AND C. R. UDRY (2010). Learning About a New Technology: Pineapple in Ghana. *American Economic Review*, 100, 35–69.
- DE GIORGI, G., M. PELLIZZARI, AND S. REDAELLI (2010). Identification of Social Interactions through Partially Overlapping Peer Groups. *American Economic Journal: Applied Economics*, 2, 241–75.
- DE MARCO, G., G. GORNI, AND G. ZAMPIERI (2014). Global Inversion of Functions: an Introduction. *ArXiv:1410.7902v1*.
- DE PAULA, A. (2017). Econometrics of Network Models. in *Advances in Economics and Econometrics: Theory and Applications*, ed. by B. Honore, A. Pakes, M. Piazzesi, and L. Samuelson, Cambridge University Press.
- DEVEREUX, M. AND R. GRIFFITH (1998). Taxes and the Location of Production: Evidence from a Panel of US Multinationals. *Journal of Public Economics*, 68, 335–67.
- DIEBOLD, F. X. AND K. YILMAZ (2015). *Financial and Macroeconomic Connectedness: A Network Approach to Measurement and Monitoring*, Oxford University Press.
- DYRENG, S., B. LINDSEY, AND J. THORNBOCK (2013). Exploring the Role Delaware Plays as a Domestic Tax Haven. *Journal of Financial Economics*, 108, 751–72.
- EDMANS, A. AND X. GABAIX (2016). Executive Compensation: a modern primer. *Journal of Economic literature*, 54, 1232–87.
- ERDOS, P. AND A. RENYI (1960). On the Evolution of Random Graphs. *Publ. Math. Inst. Hung. Acad. Sci.*, 5, 17–60.

- FARBER, S., A. PÁEZ, AND E. VOLZ (2009). Topology and dependency tests in spatial and network autoregressive models. *Geographical Analysis*, 41, 158–180.
- FINDLEY, M., D. NIELSON, AND J. SHARMAN (2012). Global Shell Games: Testing Money Launderers’ and Terrorist Financiers’ Access to Shell Companies. Griffith University Working Paper.
- GAUTIER, E. AND C. ROSE (2016). Inference in Social Effects when the Network is Sparse and Unknown. (in preparation).
- GAUTIER, E. AND A. TSYBAKOV (2014). High-Dimensional Instrumental Variables Regression and Confidence Sets. Working Paper CREST.
- GONG, G., L. Y. LI, AND J. Y. SHIN (2011). Relative Performance Evaluation and Related Peer Groups in Executive Compensation Contracts. *The Accounting Review*, 86, 1007–43.
- GRANOVETTER, M. (1973). The Strength of Weak Ties. *American Journal of Sociology*, 6, 1360–80.
- HINES, J. (1996). Altered States: Taxes and the Location of Foreign Direct Investment in America. *American Economic Review*, 86, 1076–94.
- HORN, R. A. AND C. R. JOHNSON (2013). *Matrix Analysis*, Cambridge University Press.
- JACKSON, M., B. ROGERS, AND Y. ZENOU (2017). The Economic Consequences of Social Network Structure. *Journal of Economic Literature*, 55, 49–95.
- JANEBA, E. AND S. OSTERLEH (2013). Tax and the City – A Theory of Local Tax Competition. *Journal of Public Economics*, 106, 89–100.
- KENNEDY, J. AND R. EBERHART (1995). Particle Swarm Optimization. *Proceedings of the IEEE International Conference on Neural Networks*, IV, 1942–8.
- KLEVEN, H., C. LANDAIS, AND E. SAEZ (2013). Taxation and International Mobility of Superstars: Evidence from the European Football Market. *American Economic Review*, 103, 1892–924.
- (2014). Migration and Wage Effects of Taxing Top Earners: Evidence from the Foreigners’ Tax Scheme in Denmark. *Quarterly Journal of Economics*, 129, 333–78.
- KLINE, B. AND E. TAMER (2016). Bayesian Inference in a Class of Partially Identified Models. *Quantitative Economics*, 7, 329–366.
- KOMUNJER, I. (2012). Global Identification in Nonlinear Models with Moment Restrictions. *Econometric Theory*, 28, 719–29.



- KRANTZ, S. G. AND H. R. PARKS (2013). *The Implicit Function Theorem*, Birkhauser.
- LAM, C. AND P. C. SOUZA (2016). Detection and Estimation of Block Structure in Spatial Weight Matrix. *Econometric Reviews*, 35, 1347–1376.
- (2019). Estimation and Selection of Spatial Weight Matrix in a Spatial Lag Model. *Journal of Business and Economic Statistics*, forthcoming.
- LEE, L.-F. (2004). Asumptotic Distributions of Quasi-Maximum Likelihood Estimators for Spatial Autoregressive Models. *Econometrica*, 72, 25.
- (2007). Identification and Estimation of Econometric Models with Group Interactions, Contextual Factors and Fixed Effects. *Journal of Econometrics*, 60, 531–42.
- LEE, S. AND A. LEWBEL (2013). Nonparametric Identification of Accelerated Failure Time Competing Risks Models. *Econometric Theory*, 29, 905–19.
- LEWBEL, A., X. QU, AND X. TAN (2019). Social Networks with Misclassified or Unobserved Links. Manuscript.
- MANRESA, E. (2016). Estimating the Structure of Social Interactions Using Panel Data. Manuscript.
- MANSKI, C. F. (1993). Identification of Endogenous Social Effects: the reflection problem. *The Review of Economic Studies*, 60, 531–42.
- MEINSHAUSEN, N. AND P. BUHLMANN (2006). High-Dimensional Graphs and Variable Selection with the Lasso. *The Annals of Statistics*, 34, 1436–1462.
- MIZRUCHI, M. S. AND E. J. NEUMAN (2008). The effect of density on the level of bias in the network autocorrelation model. *Social Networks*, 30, 190–200.
- MURPHY, K. J. (1999). Executive Compensation. *Handbook of Labor Economics*, 3, 2485–563.
- NEUMAN, E. J. AND M. S. MIZRUCHI (2010). Structure and bias in the network autocorrelation model. *Social Networks*, 32, 290–300.
- OATES, W. AND R. SCHWAB (1988). Economic Competition Among Jurisdictions: Efficiency-enhancing or Distortion-inducing?. *Journal of Public Economics*, 35, 333–54.
- ROSE, C. (2015). Essays in Applied Microeconometrics. Ph.D. thesis, University of Bristol.
- ROTHENBERG, T. (1971). Identification in Parametric Models. *Econometrica*, 39, 577–91.

- ROTHENHÄUSLER, D., C. HEINZE, J. PETERS, AND N. MEINSHAUSEN (2015). BACKSHIFT: Learning causal cyclic graphs from unknown shift interventions. in *Advances in Neural Information Processing Systems*, 1513–1521.
- SACERDOTE, B. (2001). Peer Effects with Random Assingment: Results for Dartmouth Roommates. *The Quarterly Journal of Economics*, 116, 681–704.
- SHLEIFER, A. (1985). A Theory of Yardstick Competition. *Rand Journal of Economics*, 16.
- SMITH, T. E. (2009). Estimation bias in spatial models with strongly connected weight matrices. *Geographical Analysis*, 41, 307–332.
- SOUZA, P. C. (2014). Estimating Network Effects without Network Data. PUC-Rio Working Paper.
- TIBSHIRANI, R. J. AND J. TAYLOR (2012). Degrees of freedom in lasso problems. *The Annals of Statistics*, 40, 1198–1232.
- TIEBOUT, C. (1956). A Pure Theory of Local Expenditures. *Journal of Political Economy*, 64, 416–24.
- VAN VLIET, W. (2018). Connections as Jumps: Estimating Financial Interconnectedness from Market Data. Manuscript.
- WANG, W., E. J. NEUMAN, AND D. A. NEWMAN (2014). Statistical power of the social network autocorrelation model. *Social Networks*, 38, 88–99.
- WATTS, D. J. (1999). Networks, Dynamics, and the Small-World Phenomenon. *American Journal of Sociology*, 105, 493–527.
- WILSON, J. (1986). A Theory of Interregional Tax Competition. *Journal of Urban Economics*, 19, 296–315.
- (1999). Theories of Tax Competition. *National Tax Journal*, 52, 269–304.
- YUAN, M. AND Y. LIN (2007). Model Selection and Estimation in the Gaussian Graphical Model. *Biometrika*, 94, 19–35.
- ZOU, H. (2006). The Adaptive Lasso and Its Oracle Properties. *Journal of the American Statistical Association*, 101, 1418–29.
- ZOU, H. AND T. HASTIE (2005). Regularization and Variable Selection via the Elastic Net. *Journal of the Royal Statistical Society: Series B (Statistical Methodology)*, 67, 301–320.

ZOU, H., T. HASTIE, AND R. TIBSHIRANI (2007). On the “Degrees of Freedom” of the LASSO. *The Annals of Statistics*, 35, 2173–2192.

ZOU, H. AND H. H. ZHANG (2009). On the Adaptive Elastic-net with a Diverging Number of Parameters. *Ann. Statist.*, 37, 1733–51.

## A Proofs

### Theorem 1

*Proof.* The local identification result follows Rothenberg (1971). Under the assumptions in our model, the parameter space  $\Theta \subset \mathbb{R}^m$  is an open set (recall that  $m = N(N - 1) + 3$ .) This corresponds to Assumption I in Rothenberg (1971).

We have that,

$$\begin{aligned} \frac{\partial \Pi}{\partial W_{ij}} &= \rho(I - \rho W)^{-1} \Delta_{ij} (I - \rho W)^{-1} (\beta I + \gamma W) + (I - \rho W)^{-1} \gamma \Delta_{ij} \\ \frac{\partial \Pi}{\partial \rho} &= (I - \rho W)^{-1} W (I - \rho W)^{-1} (\beta I + \gamma W) \\ \frac{\partial \Pi}{\partial \gamma} &= (I - \rho W)^{-1} W \\ \frac{\partial \Pi}{\partial \beta} &= (I - \rho W)^{-1}, \end{aligned}$$

where  $\Delta_{ij}$  is the  $N \times N$  matrix with 1 in the  $(i, j)$ -th position and zero elsewhere. Write the  $N^2 \times m$  derivative matrix  $\nabla_{\Pi} \equiv \frac{\partial \text{vec}(\Pi)}{\partial \theta'}$ . By assumption, row  $i$  in matrix  $W$  sums up to one, incorporated through the restriction that  $\varphi \equiv \sum_{j=1, j \neq i}^N W_{ij} - 1 = 0$ , for the unit-normalised row  $i$ . The derivative of the restriction  $\varphi$  is the  $m$ -dimensional vector  $\nabla'_W \equiv \frac{\partial \varphi}{\partial \theta'} = [e'_i \otimes \iota'_{N-1} \ 0_{1 \times 3}]$  (where  $e_i$  is an  $N$ -dimensional vector with 1 in the  $i$ th component and zero, otherwise). Following Theorem 6 of Rothenberg (1971), the structural parameters  $\theta \in \Theta$  are locally identified if, and only if, the matrix  $\nabla \equiv [\nabla'_{\Pi} \ \nabla'_W]'$  has rank  $m$ .<sup>35</sup>

If  $\nabla$  does not have rank  $m$ , there is a nonzero vector  $\mathbf{c} \equiv (c_{W_{12}}, \dots, c_{W_{N,N-1}}, c_{\rho}, c_{\gamma}, c_{\beta})'$  such that  $\nabla \cdot \mathbf{c} = 0$ . This implies that

$$c_{W_{12}} \frac{\partial \Pi}{\partial W_{12}} + \dots + c_{W_{N,N-1}} \frac{\partial \Pi}{\partial W_{N,N-1}} + c_{\rho} \frac{\partial \Pi}{\partial \rho} + c_{\gamma} \frac{\partial \Pi}{\partial \gamma} + c_{\beta} \frac{\partial \Pi}{\partial \beta} = 0 \quad (12)$$

<sup>35</sup>For a parameter vector to be locally identified, Rothenberg (1971) requires that the derivative matrix  $\nabla$  have rank  $m$  at that point and that this vector be (rank-)regular. A (rank-)regular point of the parameter space is one for which there is a neighborhood where the rank of  $\nabla$  is constant (see Definition 4 in Rothenberg, 1971). Because we show that the derivative matrix has rank  $m$  at every point in the parameter space, this also guarantees that every point in the parameter space is (rank-)regular.

and, for the unit-normalized row  $i$  (see A4),

$$\sum_{j \neq i, j=1, \dots, n} c_{W_{ij}} = 0. \quad (13)$$

Premultiplying equation (12) by  $(I - \rho W)$  and substituting the derivatives,

$$\begin{aligned} \sum_{i,j=1, i \neq j}^N c_{W_{ij}} [\rho \Delta_{ij} (I - \rho W)^{-1} (\beta I + \gamma W) + \gamma \Delta_{ij}] + \\ + c_\rho W (I - \rho W)^{-1} (\beta I + \gamma W) + c_\gamma W + c_\beta I = 0. \end{aligned}$$

Define  $C \equiv \sum_{i,j=1, i \neq j}^N c_{W_{ij}} \Delta_{ij}$ . Since the spectral radius of  $\rho W$  is strictly less than one by A2, one can show (by representing  $(I - \rho W)^{-1}$  as a Neumann series, for instance) that  $(\beta I + \gamma W)$  and  $(I - \rho W)^{-1}$  commute. Then, the expression above is equivalent to

$$\rho C (\beta I + \gamma W) (I - \rho W)^{-1} + \gamma C + c_\rho W (\beta I + \gamma W) (I - \rho W)^{-1} + c_\gamma W + c_\beta I = 0.$$

Post-multiplying by  $(I - \rho W)$ , we obtain

$$\rho C (\beta I + \gamma W) + \gamma C (I - \rho W) + c_\rho W (\beta I + \gamma W) + c_\gamma W (I - \rho W) + c_\beta (I - \rho W) = 0$$

which, upon rearrangement, yields

$$(\gamma + \rho\beta) C + c_\beta I + (\beta c_\rho - c_\beta \rho + c_\gamma) W + (c_\rho \gamma - \rho c_\gamma) W^2 = 0. \quad (14)$$

Because  $C_{ii} = 0$  and  $W_{ii} = 0$  (by A1), we have that  $c_\beta + (c_\rho \gamma - \rho c_\gamma) (W^2)_{ii} = 0$  for all  $i = 1, \dots, N$ . Since by assumption A5 there isn't a constant  $\kappa$  such that  $\text{diag}(W_0^2) = \kappa I$ , then  $c_\beta = c_\rho \gamma - \rho c_\gamma = 0$ . Plugging back in (14), we obtain

$$(\gamma + \rho\beta) C + (\beta c_\rho + c_\gamma) W = 0.$$

which implies that  $C = -\frac{\beta c_\rho + c_\gamma}{\gamma + \rho\beta} W$  since  $\gamma + \rho\beta \neq 0$  by assumption A3. Taking the sum of the elements in row  $i$ , we get

$$(\gamma + \rho\beta) \sum_{j \neq i, j=1, \dots, n} c_{W_{ij}} + (\beta c_\rho + c_\gamma) = 0.$$

Note that, by equation (13),  $\sum_{j \neq i, j=1, \dots, n} c_{W_{ij}} = 0$ . So  $\beta c_\rho + c_\gamma = 0$  and  $C = -\frac{\beta c_\rho + c_\gamma}{\gamma + \rho\beta} W = 0$ . This implies that  $c_{W_{ij}} = 0$  for any  $i$  and  $j$ . Combining  $\beta c_\rho + c_\gamma = 0$  with  $c_\rho \gamma - \rho c_\gamma = 0$  obtained above, we get that  $c_\rho (\rho\beta + \gamma) = 0$ . Since  $\rho\beta + \gamma \neq 0$ , then  $c_\rho = 0$ . Given that  $\beta c_\rho + c_\gamma = 0$ , it follows that  $c_\gamma = 0$ . This shows that  $\theta \in \Theta$  is locally identified.  $\square$

### Corollary 1

*Proof.* The parameter  $\theta_0$  being locally identified (see Theorem 1) implies that the set  $\{\theta : \Pi(\theta) = \Pi(\theta_0)\}$  is discrete. If it is also compact, then the set is finite. To establish that we now show that  $\Pi$  is a proper function: the inverse image  $\Pi^{-1}(K)$  of any compact set  $K \subset \mathbb{R}^m$  is also compact (see Krantz and Parks, 2013, p.124).

Let  $\mathcal{A}$  be a compact set in the space of  $N \times N$  real matrices. Since it is a compact set in a finite dimensional space, it is closed and bounded. Since  $\Pi$  is a continuous function of  $\theta$ , the pre-image of a compact set, which is closed, is also closed. Because  $\mathcal{W}$  is bounded and  $\rho \in (-1, 1)$ , their corresponding coordinates in  $\theta \in \Pi^{-1}(\mathcal{A})$  are bounded. Suppose the coordinates for  $\beta$  or  $\gamma$  in  $\theta \in \Pi^{-1}(\mathcal{A})$  are not bounded. So one can find a sequence  $(\theta_k)_{k=1}^\infty$  such that  $|\beta_k| \rightarrow \infty$  or  $|\gamma_k| \rightarrow \infty$ .

Denote the Frobenius norm of the matrix  $A$  as  $\|A\|$ . By the submultiplicative property  $\|AB\| \leq \|A\| \cdot \|B\|$ ,

$$\|\beta I + \gamma W\| \leq \|(\beta I + \gamma W)(I - \rho W)^{-1}\| \cdot \|I - \rho W\|.$$

Note that  $(I - \rho W)^{-1}$  and  $(\beta I + \gamma W)$  commute, and so

$$\|(\beta I + \gamma W)(I - \rho W)^{-1}\| = \|(I - \rho W)^{-1}(\beta I + \gamma W)\| = \|\Pi\|.$$

It follows that

$$\frac{\|\beta I + \gamma W\|}{\|I - \rho W\|} \leq \|\Pi\|.$$

Given  $W$  has zero main diagonal,

$$\|\beta I + \gamma W\|^2 = \beta^2 \|I\|^2 + \gamma^2 \|W\|^2 = \beta^2 N + \gamma^2 \|W\|^2.$$

Also,  $\|I - \rho W\|^2 = N + \rho^2 \|W\|^2 \leq N + \rho^2 C$ , for some constant  $C \in \mathbb{R}$ , since  $W$  is bounded by assumption A2. We then have that

$$\frac{\sqrt{\beta^2 N + \gamma^2 \|W\|^2}}{\sqrt{N + \rho^2 C}} \leq \|\Pi\|.$$

Since  $|\rho| < 1$  by Assumption (A2) the denominator above is bounded. Hence  $|\beta_k| \rightarrow \infty \Rightarrow \|\Pi(\theta_k)\| \rightarrow \infty$ . We now use the fact that  $\sum_j W_{ij} = 1$  to show that there is a lower bound on  $\|W\|^2$ , and so  $|\gamma_k| \rightarrow \infty \Rightarrow \|\Pi(\theta_k)\| \rightarrow \infty$ . To see this, note that

$$\min_{\text{s.t. } \sum_j W_{ij}=1} \|W\|^2 \geq \min_{\text{s.t. } \sum_j W_{ij}=1} \sum_{j=1}^N W_{ij}^2.$$

The Lagrangean for the right-hand side minimization problem is:

$$\mathcal{L}(W_{i1}, \dots, W_{i,i-1}, W_{i,i+1}, \dots, W_{iN}; \mu) = \sum_{j=1}^N W_{ij}^2 - \mu \left( \sum_j W_{ij} - 1 \right).$$

where  $\mu$  is the Lagrangean multiplier for the normalisation constraint. The first-order conditions for this convex minimization problem are:

$$\begin{aligned} \frac{\partial \mathcal{L}}{\partial W_{ij}} &= 2W_{ij} - \mu = 0, \quad \text{for any } j \neq i \\ \frac{\partial \mathcal{L}}{\partial \mu} &= \sum_{j=1}^N W_{ij} - 1 = 0. \end{aligned}$$

The first equation implies that  $W_{ij} = \frac{\mu}{2}$  for  $j = 1, \dots, i-1, i+1, \dots, N$ . Using the fact that  $W_{ii} = 0$ , the second equation implies that  $\mu = 2/(N-1)$ . We have then that  $W_{ij} = \frac{1}{N-1}, j \neq i$  and, consequently,  $\|W\|^2 \geq (N-1) \frac{1}{(N-1)^2} = \frac{1}{N-1}$ . Hence, if  $|\gamma_k| \rightarrow \infty$ , the numerator in the lower bound for  $\|\Pi\|$  above also goes to infinity. Consequently,  $\mathcal{A}$  would not be compact.

Therefore, if  $\mathcal{A}$  is compact the coordinates in  $\theta \in \Pi^{-1}(\mathcal{A})$  corresponding to  $\beta$  and  $\gamma$  are also bounded. Hence,  $\Pi^{-1}(\mathcal{A})$  is bounded (and closed). Consequently it is compact.

For a given reduced form parameter matrix  $\Pi$ , the set  $\{\theta : \Pi(\theta) = \Pi(\theta_0)\}$  is then compact. Since it is also discrete, it is finite.  $\square$

The following lemmas are used in proving Theorem 2.

**Lemma 1.** *Assume (A1)-(A5). If  $\gamma_0 = 0$ ,  $W_0$  is such that  $(W_0)_{1,2} = (W_0)_{2,1} = 1$  and  $(W_0)_{ij} = 0$  otherwise, with  $\rho_0 \neq 0$  and  $\beta_0 \neq 0$ , then  $\theta_0 \in \Theta$  is identified.*

*Proof.* Take  $\theta = (W_{12}, \dots, W_{N,N-1}, \rho, \gamma, \beta) \in \Theta$  possibly different from  $\theta_0$  such that the models are observationally equivalent, so  $\Pi_0 = \Pi$ . Then

$$(I - \rho_0 W_0)^{-1}(\beta_0 I + \gamma_0 W_0) = (I - \rho W)^{-1}(\beta I + \gamma W).$$

Since  $\gamma_0 = 0$  and  $(I - \rho W)^{-1}$  and  $(\beta I + \gamma W)$  commute (see the proof for Theorem 1), it follows that

$$\Pi_0 = \Pi \Leftrightarrow \beta_0(I - \rho_0 W_0)^{-1} = (\beta I + \gamma W)(I - \rho W)^{-1}$$

or, equivalently,

$$\beta_0(I - \rho W) = (I - \rho_0 W_0)(\beta I + \gamma W).$$

This last equation implies that

$$(\beta_0 - \beta)I - (\gamma + \beta_0\rho)W + \rho_0\beta W_0 + \rho_0\gamma W_0W = 0. \quad (15)$$

We first note that  $(W_0W)_{N,N} = 0$  since  $(W_0)_{N,i} = 0$  for any  $1 \leq i \leq N$  and, by Assumption (A1),  $(W)_{N,N} = (W_0)_{N,N} = 0$ . So  $\beta_0 = \beta$ . Taking elements  $(i, j)$  such that  $i \geq 3$  and  $i \neq j$  in equation (15), and using the fact that  $\beta_0 = \beta$ , we find that  $-(\gamma + \beta_0\rho)(W)_{ij} = -(\gamma + \beta\rho)(W)_{ij} = 0$  for any  $(i, j)$  such that  $i \geq 3$  and  $i \neq j$ . By Assumption (A3),  $\gamma + \beta\rho \neq 0$  and it follows that  $(W)_{ij} = 0$  for any  $(i, j)$  such that  $i \geq 3$  and  $i \neq j$ . In fact, since  $(W)_{i,i} = 0$  by Assumption (A1), we get that  $(W)_{ij} = 0$  for any  $(i, j)$  such that  $i \geq 3$ .

Using Assumption (A1) and since  $\beta_0 = \beta$ , elements  $(1, 1)$  and  $(2, 2)$  in equation (15) imply that  $\rho_0\gamma(W)_{2,1} = \rho_0\gamma(W)_{1,2} = 0$ . Given that  $\rho_0 \neq 0$ , we get that  $\gamma(W)_{2,1} = \gamma(W)_{1,2} = 0$ . From element  $(1, 2)$  in equation (15) we find that  $-(\gamma + \beta_0\rho)(W)_{1,2} + \rho_0\beta = 0$  or, equivalently,  $(\rho_0 - \rho(W)_{1,2})\beta_0 - \gamma(W)_{1,2} = 0$ . Given that  $\gamma(W)_{1,2} = 0$  and  $\beta_0 \neq 0$ , it must be that  $\rho_0 - \rho(W)_{1,2} = 0$ . Making the analogous argument for element  $(2, 1)$ , we would also obtain that  $\rho_0 - \rho(W)_{2,1} = 0$ .

If both  $(W)_{1,2}$  and  $(W)_{2,1}$  are equal to zero, using the fact that  $W_{ij} = 0$  for any  $(i, j)$  such that  $i \geq 3$ , we would then obtain that  $W^2$  is equal to

$$\begin{bmatrix} 0 & 0 & (W)_{1,3} & \cdots & (W)_{1,N} \\ 0 & 0 & (W)_{2,3} & \cdots & (W)_{2,N} \\ 0 & 0 & 0 & \cdots & 0 \\ \vdots & \vdots & \vdots & \ddots & \vdots \\ 0 & 0 & 0 & \cdots & 0 \end{bmatrix}^2 = \begin{bmatrix} 0 & 0 & 0 & \cdots & 0 \\ 0 & 0 & 0 & \cdots & 0 \\ 0 & 0 & 0 & \cdots & 0 \\ \vdots & \vdots & \vdots & \ddots & \vdots \\ 0 & 0 & 0 & \cdots & 0 \end{bmatrix},$$

which contradicts Assumption (A5). Hence  $(W)_{1,2} \neq 0$  or  $(W)_{2,1} \neq 0$ . If  $(W)_{1,2} \neq 0$ , using the fact that  $\gamma(W)_{1,2} = 0$ , we get that  $\gamma = 0$ . Equivalently, if  $(W)_{2,1} \neq 0$ , and using the fact that  $\gamma(W)_{2,1} = 0$ , we again get that  $\gamma = 0$ . So, in either case,  $\gamma = \gamma_0 = 0$ .

Taking element  $(1, j)$  in equation (15), with  $j \geq 3$ , we get that  $-(\gamma + \rho\beta_0)W_{1,j} + \gamma\rho_0(W)_{2,j} = -\rho\beta_0W_{1,j} = 0$ . Similarly, element  $(2, j)$ , with  $j \geq 3$  implies that  $-(\gamma + \rho\beta_0)W_{2,j} + \gamma\rho_0(W)_{1,j} = -\rho\beta_0W_{2,j} = 0$ . Then, from  $-\rho\beta_0(W)_{1,j} = -\rho\beta_0(W)_{2,j} = 0$  for  $j \geq 3$ , it follows that  $-\rho(W)_{1,j} = -\rho(W)_{2,j} = 0$  since  $\beta_0 \neq 0$ .

From  $\rho_0 - \rho(W)_{1,2} = 0$ , if  $(W)_{1,2} \neq 0$ , we get that  $\rho = \rho_0/(W)_{1,2} \neq 0$ . Equivalently, if  $(W)_{2,1} \neq 0$ , we get that  $\rho = \rho_0/(W)_{2,1} \neq 0$ . Since  $(W)_{1,2} \neq 0$  or  $(W)_{2,1} \neq 0$ , we obtain that  $\rho \neq 0$ . Then, because  $-\rho(W)_{1,j} = \rho(W)_{2,j} = 0$  for  $j \geq 3$ , we have that  $(W)_{1j} = (W)_{2j} = 0$  for  $j \geq 3$ .

Given that  $\rho_0 - \rho(W)_{1,2} = 0$ ,  $\rho_0 - \rho(W)_{2,1} = 0$  and  $\rho \neq 0$ , we obtain that  $(W)_{1,2} = (W)_{2,1} = \frac{\rho_0}{\rho}$ . Since  $(W)_{1,j} = 0$  for  $j \neq 2$ ,  $(W)_{2,j} = 0$  for  $j \neq 1$  and  $(W)_{ij} = 0$  for  $i \geq 3$ , by Assumption (A5) we get that  $(W)_{1,2} = (W)_{2,1} = 1$  and  $\rho = \rho_0$ . Hence,  $((W)_{1,2}, \dots, (W)_{N,N-1}, \rho, \gamma, \beta) = ((W_0)_{1,2}, \dots, (W_0)_{N,N-1}, \rho_0, \gamma_0, \beta_0)$ .  $\square$

**Lemma 2.** Assume (A1)-(A2) and (A4)-(A5). The image of  $\Pi(\cdot)$ , for  $\theta \in \Theta_+$ , is path-connected and, therefore, connected.

*Proof.* Take  $\theta$  and  $\theta^* \in \Theta_+$ . Consider first the subvectors corresponding to the adjacency matrices  $W$  and  $W^*$ . Without loss of generality, let  $1, \dots, N$  be ordered such that  $(W^2)_{11} > (W^2)_{22}$ . Consider the adjacency matrix  $W_*$  corresponding to the network of directed connections  $\{(1, 2), (2, 1)\}$  and  $\{(3, 4), (4, 5), \dots, (N-1, N), (N, 3)\}$ :

$$W_* = \begin{bmatrix} 0 & 1 & 0 & 0 & \cdots & 0 \\ 1 & 0 & 0 & 0 & \cdots & 0 \\ 0 & 0 & 0 & 1 & \cdots & 0 \\ \vdots & \vdots & \vdots & \ddots & \ddots & \vdots \\ 0 & 0 & 1 & 0 & \cdots & 0 \end{bmatrix}.$$

Note that  $\text{diag}(W_*^2) = (1, 1, 0, \dots, 0)$  and this is an admissible adjacency matrix under assumptions (A1)-(A2) and (A4)-(A5). We first show that  $W$  is path-connected to  $W_*$ .

Consider the path given by

$$W(t) = tW_* + (1-t)W$$

which implies that

$$\begin{aligned} (W(t)^2)_{11} &= (1-t)^2(W^2)_{11} + t^2 + (1-t)t(W_{12} + W_{21}) \\ (W(t)^2)_{22} &= (1-t)^2(W^2)_{22} + t^2 + (1-t)t(W_{12} + W_{21}). \end{aligned}$$

Since  $(W(t)^2)_{11} - (W(t)^2)_{22} = (1-t)^2[(W^2)_{11} - (W^2)_{22}] > 0$  for  $t \in [0, 1)$  and  $W(1) = W_*$ , (A5) is satisfied for any matrix  $W(t)$  such that  $t \in [0, 1]$ . Since all rows in  $W_*$  sum to one and  $(W_*)_{ii} = 0$  for any  $i$ , it is straightforward to see that  $W(t)$  also satisfies (A1) and (A4). Finally,  $\sum_{j=1}^N |W_{ij}(t)| \leq t \sum_{j=1}^N |(W_*)_{ij}| + (1-t) \sum_{j=1}^N |W_{ij}| \leq 1$  for every  $i = 1, \dots, N$  and  $W(t)$  satisfies Assumption (A2).

If  $W^*$  is such that  $(W^{*2})_{11} \neq (W^{*2})_{22}$ , the convex combination of  $W^*$  and  $W_*$  is also seen to satisfy (A1)-(A2) and (A4)-(A5) and a path between  $W$  and  $W^*$  can be constructed via  $W_*$ . If, on the other hand  $(W^{*2})_{11} = (W^{*2})_{22}$ , suppose without loss of generality that  $(W^{*2})_{11} \neq (W^{*2})_{33}$ . In this case, one can construct a path between  $W^*$  and  $W_{**}$  where  $W_{**}$  represents the network of



directed connections  $\{(1, 3), (3, 1)\}$  and  $\{(2, 4), (4, 5), \dots, (N-1, N), (N, 2)\}$ :

$$W_{**} = \begin{bmatrix} 0 & 0 & 1 & 0 & \cdots & 0 \\ 0 & 0 & 0 & 1 & \cdots & 0 \\ 1 & 0 & 0 & 0 & \cdots & 0 \\ \vdots & \vdots & \vdots & \ddots & \ddots & \vdots \\ 0 & 1 & 0 & 0 & \cdots & 0 \end{bmatrix}.$$

Like  $W(t)$  above, this path can be seen to satisfy assumptions (A1)-(A2) and (A4)-(A5). Now note that a path can also be constructed between  $W_*$  and  $W_{**}$  as their convex combination also satisfies (A1)-(A2) and (A4)-(A5). For example, note that  $\hat{W}(t) = tW_* + (1-t)W_{**}$  is such that  $(\hat{W}(t)^2)_{11} = t^2 + (1-t)^2$  and  $(\hat{W}(t)^2)_{NN} = 0$  so  $(\hat{W}(t)^2)_{11} - (\hat{W}(t)^2)_{NN} > 0$  for any  $t \in (0, 1)$  and both  $\hat{W}(0)$  and  $\hat{W}(1)$  satisfy (A5). Hence, we can construct a path  $W(t)$  between  $W$  and  $W^*$  through  $W_*$  and  $W_{**}$ .

Furthermore,  $\rho(t) = t\rho^* + (1-t)\rho$ ,  $\beta(t) = (t\rho^*\beta^* + (1-t)\rho\beta)/(t\rho^* + (1-t)\rho)$ ,  $\gamma(t) = t\gamma^* + (1-t)\gamma$  are such that

$$f(t) \equiv \rho(t)\beta(t) + \gamma(t) = t(\rho^*\beta^* + \gamma^*) + (1-t)(\rho\beta + \gamma) > 0,$$

since  $\theta^*$  and  $\theta \in \Theta_+$ . (Note also that  $|\rho(t)| < 1$  so Assumption (A2) is satisfied.) These facts taken together imply that

$$\theta(t) \equiv (W(t)_{12}, \dots, W(t)_{N,N-1}, \rho(t), \gamma(t), \beta(t)) \in \Theta_+.$$

That is,  $\Theta_+$  is path-connected and therefore connected. Since  $\Pi(\cdot)$  is continuous on  $\Theta_+$ ,  $\Pi(\Theta_+)$  is connected.  $\square$

## Theorem 2

*Proof.* The proof uses Corollary 1.4 in Ambrosetti and Prodi (1995, p. 46),<sup>36</sup> which we reproduce here with our notation for convenience: *Suppose the function  $\Pi(\cdot)$  is continuous, proper and locally invertible with a connected image. Then the cardinality of  $\Pi^{-1}(\bar{\Pi})$  is constant for any  $\bar{\Pi}$  in the image of  $\Pi(\cdot)$ .*

The mapping  $\Pi(\theta)$  is continuous and proper (by Corollary 1), with connected image (Lemma 2), and non-singular Jacobian at any point (as per the proof for Theorem 1) which guarantees local invertibility. Following Corollary 1.4 in Ambrosetti and Prodi (1995, p.46) reproduced above, we obtain that the cardinality of the pre-image of  $\Pi(\theta)$  is finite and constant. Take  $\theta \in \Theta_+$  such that

---

<sup>36</sup>Related results can be found in Ambrosetti and Prodi (1972) and de Marco *et al.* (2014)

$\gamma = 0$ ,  $(W)_{1,2} = (W)_{2,1} = 1$  and  $(W)_{i,j} = 0$  otherwise, with  $\rho \neq 0$  and  $\beta \neq 0$ . By Lemma 1, that cardinality is one.  $\square$

### Corollary 3

*Proof.* Since  $\rho \in (0, 1)$  and  $W_{ij} \geq 0$ ,  $\sum_{k=1}^{\infty} \rho^{k-1} W^k$  is a non-negative matrix. By (5), the off-diagonal elements of  $\Pi(\theta)$  are equal to the off-diagonal elements of  $(\rho\beta + \gamma) \sum_{k=1}^{\infty} \rho^{k-1} W^k$ , the sign of those elements identifies the sign of  $\rho\beta + \gamma$ . By Theorem 2, the model is identified.  $\square$

### Corollary 4

*Proof.* Since  $W_0$  is non-negative and irreducible, there is a real eigenvalue equal to the spectral radius of  $W_0$  corresponding to the unique eigenvector whose entries can be chosen to be strictly positive (i.e., all the entries share the same sign). A generic eigenvalue of  $W_0$ ,  $\lambda_0$ , corresponds to an eigenvalue of  $\Pi_0$  according to:

$$\lambda_{\Pi_0} = \beta_0 + (\rho_0\beta_0 + \gamma_0) \frac{\lambda_0}{1 - \rho_0\lambda_0}$$

If  $\lambda_0 = a_0 + b_0i$  where  $a_0, b_0 \in \mathbb{R}$  and  $i = \sqrt{-1}$ , then

$$\lambda_{\Pi_0} = \beta_0 + (\rho_0\beta_0 + \gamma_0) \frac{a_0(1 - \rho_0a_0) - \rho_0b_0^2}{(1 - \rho_0a_0)^2 + \rho_0^2b_0^2} + (\rho_0\beta_0 + \gamma_0) \frac{b_0}{(1 - \rho_0a_0)^2 + \rho_0^2b_0^2}i.$$

If the eigenvalue  $\lambda_0$  is real,  $b_0 = 0$  and the corresponding  $\lambda_{\Pi_0}$  eigenvalue is also real. Differentiating  $Re(\lambda_{\Pi_0})$ , the real part of  $\lambda_{\Pi_0}$ , with respect to  $Re(\lambda_0) = a_0$ , we get:

$$\frac{\partial Re(\lambda_{\Pi_0})}{\partial a_0} = \frac{(1 - \rho_0a_0)^2 - \rho_0^2b_0^2}{[(1 - \rho_0a_0)^2 + \rho_0^2b_0^2]^2} \times (\rho_0\beta_0 + \gamma_0). \quad (16)$$

If the eigenvalue  $\lambda_0$  is real, the expression (16) becomes:

$$\frac{\partial Re(\lambda_{\Pi_0})}{\partial a_0} = \frac{\partial \lambda_{\Pi_0}}{\partial a_0} = \frac{1}{(1 - \rho_0a_0)^2} \times (\rho_0\beta_0 + \gamma_0).$$

The fraction multiplying  $\rho_0\beta_0 + \gamma_0$  is positive. If  $\rho_0\beta_0 + \gamma_0 < 0$ , the real eigenvalues of  $\Pi_0$  are decreasing on the real eigenvalues of  $W_0$ . Consequently, the eigenvector corresponding to the largest (real) eigenvalue of  $W_0$  will be associated with smallest real eigenvalue of  $\Pi_0$ . If, on the other hand,  $\rho_0\beta_0 + \gamma_0 > 0$  the eigenvector corresponding to the largest real eigenvalue of  $W_0$  will correspond to the largest real eigenvalue of  $\Pi_0$ . Since that eigenvector is the unique eigenvector that can be chosen to have strictly positive entries, the sign of  $\rho_0\beta_0 + \gamma_0$  is identified by the  $\lambda_{\Pi_0}$  eigenvalue it is associated with and whether it is the largest or smallest real eigenvalue. By Theorem 2, the model is identified.

If there is only one real eigenvalue, note that the denominator in the fraction in (16) is positive. The minimum value of the numerator subject to  $|\lambda_0|^2 = a_0^2 + b_0^2 \leq 1$  is given by

$$\min_{a_0, b_0} (1 - \rho_0 a_0)^2 - \rho^2 b_0^2 \text{ s.t. } a_0^2 + b_0^2 \leq 1.$$

The Lagrangean for this minimization problem is given by:

$$\mathcal{L}(a_0, b_0; \mu) = (1 - \rho_0 a_0)^2 - \rho^2 b_0^2 + \mu(a_0^2 + b_0^2 - 1).$$

where  $\mu$  is the Lagrange multiplier associated with the constraint  $a_0^2 + b_0^2 \leq 1$ . The Kuhn-Tucker necessary conditions for the solution  $(a_0^*, b_0^*, \mu^*)$  of this problem are given by:

$$\begin{aligned} (\partial a_0 : ) \quad & \rho_0(1 - \rho_0 a_0^*) - \mu^* a_0^* = 0 \\ (\partial b_0 : ) \quad & (\rho_0^2 - \mu^*) b_0^* = 0 \\ & \mu^* (a_0^{*2} + b_0^{*2} - 1) = 0 \\ & a_0^{*2} + b_0^{*2} \leq 1 \text{ and } \mu^* \geq 0, \end{aligned}$$

Let  $\rho_0 \neq 0$ . (Otherwise, the objective function above is equal to one irrespective of  $a_0$  or  $b_0$  and the partial derivative is  $\rho_0 \beta_0 + \gamma_0$ .) If  $\mu^* = 0$ ,  $\partial b_0$  implies that  $b_0^* = 0$ . Then  $\partial a_0$  would have  $a_0^* = \rho_0^{-1}$  which violates  $a_0^{*2} + b_0^{*2} \leq 1$ .

Hence, a solution should have  $\mu^* > 0$ . In this case, there are two possibilities:  $b_0^* = 0$  or  $b_0^* \neq 0$ . If  $b_0^* \neq 0$ , condition  $\partial b_0$  implies that  $\mu^* = \rho_0^2$  and  $\partial a_0$  then gives  $a_0^* = (2\rho_0)^{-1}$ . Because the constraint is binding,  $b_0^{*2} = 1 - (4\rho_0^2)^{-1}$ . In this case,  $a_0^{*2} \leq 1$  and  $b_0^{*2} \geq 0$  requires that  $|\rho_0| \geq 1/2$ . The value of the minimised objective function in this case  $1/2 - \rho_0^2$ . This is positive if  $|\rho_0| < \sqrt{2}/2$ .

The other possibility is to have  $b_0 = 0$ . Because the constraint is binding,  $a_0 = 1$  and the objective function takes the value  $(1 - \rho_0)^2 > 0$ . Since  $(1 - \rho_0)^2 - 1/2 + \rho_0^2 = 2\rho_0^2 - 2\rho_0 + 1/2 \geq 0$ , this solution is dominated by the previous one when  $|\rho_0| \geq 1/2$ .

Consequently, the fraction multiplying  $\rho_0 \beta_0 + \gamma_0$  is non-negative and it can be ascertained that

$$\text{sgn} \left[ \frac{\partial \text{Re}(\lambda_{\Pi_0})}{\partial a_0} \right] = \text{sgn}[\rho_0 \beta_0 + \gamma_0]$$

as long as  $|\rho_0| < \sqrt{2}/2$ .

If  $\rho_0 \beta_0 + \gamma_0 < 0$ , the real part of the eigenvalues of  $\Pi_0$  is decreasing on the real part of the eigenvalues of  $W_0$ . Consequently, the eigenvector corresponding to the eigenvalue of  $W_0$  with the largest real part will correspond to the eigenvalue of  $\Pi_0$  with the smallest real part. If, on the other hand,  $\rho_0 \beta_0 + \gamma_0 > 0$  the eigenvector corresponding to the eigenvalue of  $W_0$  with the largest real part will correspond to the eigenvalue of  $\Pi_0$  with the largest real part. Since that eigenvector is the unique eigenvector that can be chosen to have strictly positive entries, the sign of  $\rho_0 \beta_0 + \gamma_0$

is identified by the  $\lambda_{\Pi_0}$  eigenvalue it is associated with.

By Theorem 2, the model is identified.  $\square$

### Proposition 1

*Proof.* From equation (6) we observed that  $\Pi_0 v_j = \lambda_{\Pi_0, j} v_j$ , where  $v_j$  is an eigenvector of both  $W_0$  and  $\Pi_0$  with corresponding eigenvalue  $\lambda_{\Pi_0, j} = \frac{\beta_0 + \gamma_0 \lambda_{0, j}}{1 - \rho_0 \lambda_{0, j}}$ . Defining  $c$  as the row-sum of  $\Pi_0$ , we also have that

$$\begin{aligned} \tilde{\Pi}_0(I - H)v_j &= (I - H)\Pi_0(I - H)v_j = (I - H)\Pi_0 v_j - (I - H)\Pi_0 H v_j \\ &= \lambda_{\Pi_0, j}(I - H)v_j - (I - H)cH v_j = \lambda_{\Pi_0, j}(I - H)v_j - (H - H^2)cv_j \\ &= \lambda_{\Pi_0, j}(I - H)v_j - (H - H)c v_j = \lambda_{\Pi_0, j}(I - H)v_j, \end{aligned}$$

where the third equality obtains from  $\Pi_0 H = cH$  and the fifth equality holds since  $H$  is idempotent. So  $\tilde{\Pi}_0$  and  $\Pi_0$  have common eigenvalues, with corresponding eigenvector  $\tilde{v}_j = v_j - \bar{v}_j \iota$  for  $\tilde{\Pi}_0$ , where  $\bar{v}_j = \frac{1}{N} \iota' v_j$ ,  $j = 1, \dots, N$ . Since  $\lambda_{\Pi_0, j}$  and  $\tilde{v}_j$  are observed from  $\tilde{\Pi}_0$ , identification of  $\Pi_0$  is equivalent to identification of  $\bar{v}_j$  (given diagonalizability).

To establish identification of  $\bar{v}_j$ , note that  $W_0(\tilde{v}_j + \bar{v}_j \iota) = \lambda_{0, j}(\tilde{v}_j + \bar{v}_j \iota)$  since  $v_j$  is an eigenvector of  $W_0$ . Consider an alternative constant  $\bar{v}_j^* \neq \bar{v}_j$  that satisfies the previous equation. Then

$$W_0 \iota(\bar{v}_j - \bar{v}_j^*) = \lambda_{0, j}(\bar{v}_j - \bar{v}_j^*).$$

Since  $W_0 \iota = \iota$ ,  $v_j$  must satisfy  $(1 - \lambda_{0, j})(\bar{v}_j - \bar{v}_j^*) = 0$ . For  $j = 2, \dots, N$ ,  $|\lambda_{0, j}| < 1$ . So  $\bar{v}_j = \bar{v}_j^*$  and therefore identified. For  $j = 1$ , it is known that  $\lambda_1 = 1$  with eigenvector  $v_1 = \iota$ .  $\square$

### Proposition 2

*Proof.* Under row-sum normalization and  $|\rho_0| < 1$ ,  $(I - \rho_0 W_0)^{-1} \iota = \iota + \rho_0 W_0 \iota + \rho_0^2 W_0^2 \iota + \dots = \iota + \rho_0 \iota + \rho_0^2 \iota + \dots = \iota \frac{1}{1 - \rho_0}$ , so  $\Pi_{01} \equiv (I - \rho_0 W)^{-1}$  has constant row-sums. If row-sum normalization fails,  $\Pi_{01}$  may not have constant row-sums. Define  $h_{ij}$  as the  $(ij)$ -th element of  $\tilde{H}$ . The first row of the system  $(I - \tilde{H})(I - \rho_0 W)^{-1} \iota = (I - \tilde{H})r_{W_0} = 0$  is  $h_{11}^* r_{W_0, 1} - h_{12} r_{W_0, 2} - \dots - h_{1N} r_{W_0, N} = 0$  where  $h_{11}^* = 1 - h_{11}$  and  $r_{W_0, l}$  is the  $l$ -th element of  $r_{W_0}$ . If there are  $N$  possible  $W_0, W_0^{(1)}, \dots, W_0^{(n)}$ , such that  $[r_{W_0^{(1)}} \dots r_{W_0^{(n)}}]$  has rank  $N$ , then  $h_{11}^* = h_{12} = \dots = h_{1N} = 0$ . Since the same reasoning applies to all rows,  $\tilde{H}$  is the trivial transformation  $\tilde{H} = I$ .  $\square$

## B Estimation

### B.1 Sparsity of $W_0$ and $\Pi_0$

Define  $\tilde{M}$  as the number of non-zero elements of  $\Pi_0$ . We say that  $\Pi_0$  is sparse if  $\tilde{M} \ll NT$ . Denote the number of connected pairs in  $W_0$  via paths of any length as  $\tilde{m}_c$ . We equivalently say that  $W_0$  is "sparse connected" if  $\tilde{m}_c \ll NT$ . We show that sparsity of  $\Pi_0$  is related to sparse connectedness of  $W_0$ .

**Proposition 3.**  $\Pi_0$  is sparse if, and only if, the number of unconnected pairs  $W_0$  is large.

*Proof.* For  $|\rho_0| < 1$ , we have that

$$\Pi_0 = \beta_0 I + (\rho_0 \beta_0 + \gamma_0) \sum_{k=1}^{\infty} \rho_0^{k-1} W_0^k.$$

Given that  $\rho_0 \beta_0 + \gamma_0 \neq 0$ , it follows directly that  $[\Pi_0]_{ij} = 0$  if, and only if, there are no paths between  $i$  and  $j$  in  $W_0$ . Therefore, sparsity of  $\Pi_0$  translates into a large number of  $(i, j)$  unconnected pairs in  $W_0$ .  $\square$

On the one hand, sparsity does not imply sparse connectedness. A circular graph is clearly sparse, but all nodes connect with all other nodes through a path of length at most  $\frac{N}{2}$ . On the other hand, the sparse connectedness implies sparsity and therefore is a stronger requirement. To see this, take any arbitrary network  $G$  with  $\tilde{m}(G)$  non-zero elements and  $\tilde{m}_c(G)$  connected pairs. Now consider the operation of "completing"  $G$ : for every connected  $(i, j)$  pair, add a direct link between  $(i, j)$  if non-existent in  $G$  and denote the resulting matrix as  $\mathcal{C}(G)$ . It is clear that  $\tilde{m}(G) \leq \tilde{m}(\mathcal{C}(G))$ . Yet,  $\tilde{m}(\mathcal{C}(G)) = \tilde{m}_c(G)$ .

## B.2 Adaptive Elastic Net

### B.2.1 Implementation and Initial Conditions

To make our procedure robust to the choice of initial condition, we use the particle swarm algorithm. This is an optimization algorithm tailored to more aptly find global optima, which does not depend on choice of initial conditions. It works as follows. The procedure starts from a large number of initial conditions covering the parameter space, known as "particles" (Kennedy and Eberhart, 1995). Each particle is iterated independently until convergence. The algorithm returns

the optimum calculated across particles.<sup>37,38</sup>

To ensure compliance with row-sum normalization for each row  $i$  of  $W$ , one non-zero parameter  $W_{i,j^*}$  is set to  $1 - \sum_{j=1, j \neq j^*}^N W_{i,j}$ . This avoids making use of constrained optimization routines.<sup>39</sup> We also impose the restriction that  $\rho \geq 0$  and  $W_{ij} \geq 0$  by minimizing the objective function with respect to  $\tilde{\rho}$  with  $\rho = \tilde{\rho}^2$  and  $\tilde{W}_{ij}$  with  $W_{ij} = \tilde{W}_{ij}^2$ .

Optimization of (8) starts from the initial condition selected by the particle swarm algorithm and is minimized with respect to the parameters that were neither set to zero nor were chosen to ensure row-sum normalization. Estimates from the first stage are subsequently used to adjust the penalization, as in the Adaptive Elastic Net GMM objective function (10).<sup>40</sup> The steps above are repeated for different combinations of  $p = (p_1, p_1^*, p_2)$ , selected on a grid. The final estimate is the one that minimizes the BIC criterion.

### B.3 OLS

For the purpose of estimation, it is convenient to write the model in the stacked form. Let  $x = [x_1, \dots, x_T]'$  be the  $T \times N$  matrix of explanatory variables,  $y_i = [y_{i1}, \dots, y_{iT}]'$  be the  $T \times 1$  vector of response variables for individual  $i$  and  $\pi_i^0 = [\pi_{i1}^0, \dots, \pi_{iN}^0]'$  where  $\pi_{ij}^0$  is a short notation for the  $(i, j)$ -th element of  $\Pi_0$ . The concise model is then,

$$y_i = x\pi_i^0 + v_i \quad (17)$$

for each  $i = 1, \dots, N$ , where also  $v_i = [v_{i1}, \dots, v_{iT}]'$ . Model (17) can then be estimated equation-by-equation. Denote  $\pi^0 = [\pi_1^0, \dots, \pi_N^0]'$ . Stacking the full set of  $N$  equations,

$$y = X\pi^0 + v \quad (18)$$

---

<sup>37</sup>We set Caner and Zhang's (2014) suggestion for the initial condition as one of those particles, with minor modifications. The authors suggest calculating the absolute value of the derivative of the unpenalized GMM objective function evaluated at zero,  $\nabla_W$ , and the set parameters smaller than  $p_1$  at zero. The rationale is that if the GMM objective function is invariant with respect to certain parameters, the Elastic Net problem achieves a corner solution (where parameters are set to zero). In our case, allowing only for positive interactions, we set to zero the elements such that  $-\nabla_W \leq p_1$ . All other elements of  $W$  gain equal weights such that row-sum normalization is respected. The derivative  $\nabla_W$  is mechanically zero if  $\rho = \gamma = 0$ . So we set  $\rho = .5$ , given that the parameter space is bounded and  $\rho \in [0, 1)$ . The other parameters that enter the derivative are  $\hat{\beta}$  estimated from a regression of  $y$  on  $x$ , with the full set of fixed effects, and  $\gamma = 0$ .

<sup>38</sup>We also implemented an additional five particles. Particle 2: like Particle 1 but with size proportional to the magnitude of the derivatives conditional on  $-\nabla_W$  being greater than  $p_1$ ; Particle 3: sets to non-zero all positive elements of  $-\nabla_W$  with equal weights; Particle 4: selects 5% highest values of  $-\nabla_W$ , sets all others to zero, and non-zero gain equal weights; Particle 5:  $W$  obtained from the Lasso regression of  $y_t$  on the  $y_t$  of others with penalization  $p_1$ ; Particle 6:  $W$  obtained from the Lasso regression of  $y_t$  on the  $x_t$  of others with penalization  $p_1$ . In all cases, weights are rescaled by row-specific constants such that row-sum normalization is complied with. The remaining 94 particles are uniformly randomly selected by the built-in MATLAB particle swarm algorithm.

<sup>39</sup>At each row, we pick the  $j^*$  closest to the main diagonal of  $W$ .

<sup>40</sup>Note that the Elastic Net penalty  $p_1 \sum |W_{i,j}|$  is invariant with respect to choices of  $W$  if row-sum normalization is imposed. Yet, the penalty affects the initial selection of arguments in which  $W_{i,j}$  is restricted to zero if the derivative of the objective function is smaller than  $p_1$  in absolute value.

where  $y = [y_1, \dots, y_N]$ ,  $X = I_N \otimes x$ ,  $\pi^0 = \text{vec}(\Pi'_0)$ , and  $v = [v_1, \dots, v_N]$ . If the number of individuals in the network  $N$  is fixed and much smaller than data points available,  $N^2 \ll NT$ , equation (18) can be estimated via ordinary least squares (OLS). Under suitable regularity conditions, the OLS estimator  $\hat{\pi} = (X'X)^{-1} X'y$  is asymptotically distributed,

$$\sqrt{NT}(\hat{\pi} - \pi^0) \xrightarrow{d} \mathcal{N}(0, Q^{-1}\Sigma Q^{-1})$$

where  $Q_T \equiv \frac{1}{NT}X'X$ ,  $Q \equiv p \lim_{T \rightarrow \infty} Q_T$ ,  $\Sigma_T \equiv \frac{1}{NT}X'vv'X$  and  $\Sigma \equiv p \lim_{T \rightarrow \infty} \Sigma_T$ . The proof is standard and omitted here. As noted above, in typical applications it is customary to row-sum normalize matrix  $W$ . If no individual is isolated, one obtains that, by equation (5),

$$\begin{aligned} \Pi_0 \iota_N &= \beta_0 \iota + (\rho_0 \beta_0 + \gamma_0) \sum_{k=1}^{\infty} \rho_0^{k-1} W_0^k \iota \\ &= \frac{\beta_0 + \gamma_0}{1 - \rho_0} \iota \end{aligned} \tag{19}$$

where  $\iota_N$  is the  $N$ -length vector of ones. The last equality follows from the observation that, under row-normalization of  $W_0$ ,  $W^k \iota = W \iota = \iota$ ,  $k > 0$ . Equation (19) implies that  $\Pi_0$  has constant row-sums, which implies that row-sum normalization is, in principle, testable. This suggests a simple Wald statistic applied to the estimates of  $\pi^0$ . Under the null hypothesis,

$$\sqrt{NT}R\hat{\pi} \xrightarrow{d} \mathcal{N}(0, RQ^{-1}\Sigma Q^{-1}R')$$

where  $R = [I_{N-1} \otimes \iota'_N; -\iota_{N-1} \otimes \iota'_N]$ . The Wald statistic is  $W = NT(R\hat{\pi})'(Q^{-1}\Sigma Q^{-1})^{-1}(R\hat{\pi}) \sim \chi^2_{N-1}$  which is a convenient expression for testing row-sum normalization of  $W_0$ . We also note that the asymptotic distribution of  $\hat{\theta}$  can be immediately obtained by the Delta Method,

$$\sqrt{T}(\hat{\theta} - \theta_0) \xrightarrow{d} \mathcal{N}(0, \nabla_{\theta}'^{-1}Q^{-1}\Sigma Q^{-1}\nabla_{\theta})$$

where  $\nabla_{\theta}$  is the gradient of  $\hat{\theta}$  with respect to  $\hat{\pi}$ . We note that the derivation of the Wald statistic for testing the row-sum normalization and the asymptotic distribution of  $\hat{\theta}$  does not depend on the OLS implementation, and can be easily adjusted for any estimator for which the asymptotic distribution is known.

## C Simulations

### C.1 Set-Up

The simulations are based on two stylized random network structures, and two real world networks. These networks vary in their size, complexity, and aggregate and node-level features. All four

networks are also sparse. The two stylized networks considered are:

- (i) Erdos-Renyi network: we randomly pick exactly one element in each row of  $W_0$  and set that element to 1. This is a random graph with in-degree equal to 1 for every individual (Erdos and Renyi, 1960). Such a network could be observed in practice if connections are formed independently of one another. With  $N = 30$ , the resulting density of links is 3.45%.
- (ii) Political party network: there are two parties, each with a party leader. The leader directly affects the behavior of half the party members. We assume that one party has twice the number of members as the other. More specifically, we assume individuals  $i = 1, \dots, \frac{N}{3}$  are affiliated to Party A and are led by individual 1; individuals  $i = \frac{N}{3} + 1, \dots, N$  are affiliated to Party B and are led by individual  $\frac{N}{3} + 1$ . This difference in party size allows us to evaluate our ability to recover and identify central leaders, even in the smaller party. To test the procedure further, we add one random link per row to represent ties that are not determined by links to the Party leader. We simulate this network for various choices of  $N$ . If  $N$  is not a multiple of three, we round  $\frac{N}{3}$  to the nearest integer. With  $N = 30$ , this network has a density of 5.17%.
- (iii) Coleman’s (1964) high school friendship network survey: in 1957/8, students in a small high school in Illinois were asked to name, “fellows that they go around with most often.” A link was considered if the student nominated a peer in either survey wave. The full network has  $N = 73$  nodes, of which 70 are non-isolated and so have at least one link to another student. On average, students named just over five friendship peers. This network has density 7.58%. Furthermore, the in-degree distribution shows that most individuals received a small number of links, while a small number received many peer nominations.
- (iv) Banerjee *et al.*’s (2013) village network survey: these authors conducted a census of households in 75 villages in rural Karnataka, India, and survey questions include several about relationships with other households in the village. To begin with, we use social ties based on family relations (later examining insurance networks). We focus on village 10 that is comprised of  $N = 77$  households, and so similar in size to network (iii). In this village there are 65 non-isolated households, with at least one family link to another household. This network has density 5.07%.

For the stylized networks (i) and (ii), we first assess the performance of the estimator for a fixed network size,  $N = 30$ . We later show how performance varies with alternative network sizes. We simulate the real-world networks (iii) and (iv) using non-isolated nodes in each (so  $N = 70$  and 65 respectively). As in Bramoullé *et al.*, 2009, we exclude isolated nodes because they do not conform with row-sum normalization.



Our result identifies entries in  $W_0$  and so naturally recovers links of varying strength. Data limitations often force researchers to postulate some ties to be weaker than others (say, based on interaction frequency). This is in sharp contrast to our approach, that identifies the continuous strength of ties,  $W_{0,ij}$ , where  $W_{0,ij} > 0$  implies node  $j$  influences node  $i$ .

To establish the performance of the estimator in capturing variation in link strength, we proceed as follows for each network. First, for each node we randomly assign one of their links to have value  $W_{0,ij} = .7$ . As the underlying data generating process is assumed to allow for common time effects ( $\alpha_t$ ), we then set the weight on all other links from the node to be equal and such that row-sum normalization (A4') is complied with.<sup>41</sup> As we consider larger networks, we typically expect them to have more non-zero entries in each row of  $W_0$ , but row-sum normalization means that each weaker link will be of lower value. This works *against* the detection of weaker links using estimation methods involving penalization, because they impose small parameter estimates shrink to zero.<sup>42</sup> Finally, to aid exposition, we set a threshold value for link strength to distinguish ‘strong’ and ‘weak’ links. A strong (weak) link is defined as one for which  $W_{0,ij} > (<=) .3$ .

Summary statistics for each network are presented in Panel A of Table A1. Following Jackson *et al.* (2017), we consider the following network-wide statistics: number of edges, number of strong and weak edges, number of reciprocated edges, clustering coefficient, number of components, and the size of the maximal component. In addition, we report the standard deviation calculated across elements of the diagonal of  $W_0^2$ . If this is zero, then the diagonal of  $W_0^2$  is either zero or proportional to the vector of ones, and Assumption A5 would not be satisfied. We can see that for each case this statistic is well above zero.

Following Jackson *et al.* (2017), we consider the following node-level statistics: in- and out-degree distribution (mean and standard deviation), and the three most central individuals. The four networks differ in their size, complexity, and the relative importance of strong and weak ties. For example, the Erdos-Renyi network only has strong ties, the political party network has twice as many strong as weak ties. For the real world networks, the mean out-degree distributions are higher so the majority of ties are weak, with the high school network having around 80% of its edges being weak ties.

Panel data for each of the four simulations is generated as,

$$y_t = (I - \rho_0 W_0)^{-1} (x_t \beta + W_0 x_t \gamma + \alpha_t \iota + \alpha^* + \epsilon_t),$$

where  $\alpha_t$  is a (scalar) time effect and  $\alpha^*$  is a  $N \times 1$  vector of fixed effects, drawn respectively from

---

<sup>41</sup>For example, if in a given row of  $W_0$  there are two links, one will be randomly selected to be set to .7, and the other set to .3. If there are three links one is set to .7 and the other two set to each have weight .15 to maintain row-sum normalization, and so on. For the Erdos-Renyi network, there are thus only strong ties as each node has only one link to another node.

<sup>42</sup>Caner and Zhang (2014) state that “local to zero coefficients should be larger than  $T^{-\frac{1}{2}}$  to be differentiated from zero.”

$N(1, 1)$  and  $N(\iota, I_{N \times N})$  distributions. We consider  $T = \{5, 10, 15, 25, 50, 75, 100, 125, 150\}$ . The true parameters are set to  $\rho_0 = .3$ ,  $\beta_0 = .4$  and  $\gamma_0 = .5$  (thus satisfying Assumption A3). The exogenous variable ( $x_t$ ) and error term ( $\epsilon_t$ ) are simulated as standard Gaussian, both generated from  $N(0_N, I_{N \times N})$  distributions. This is similar to variance terms set in other papers, e.g., Lee (2004). We later conduct a series of robustness checks to evaluate the sensitivity of the simulations to alternative parameters choices, and the presence of common- and individual-level shocks.

For each combination of parameters, we conduct 1,000 simulation runs. On the initial 50 runs, we choose penalization parameters  $p$  that minimize the BIC criteria on a grid. This is computationally intensive because it requires running the optimization procedure described in Section 3.1 as many times as the number of points in the grid for  $p$ .<sup>43</sup> To reduce the computational burden, we do so only in the initial 50 runs and consider these simulation runs as a calibration of  $p$ . For the remaining 950 iterations, the penalization parameter  $p$  is set fixed at the median  $p$  computed over the calibration runs. This only worsens the performance of the estimator, since a sub-optimal  $p$  is chosen for the majority of the iterations.

## C.2 Results

We evaluate the procedure over varying panel lengths (starting from short panels with  $T = 5$ ), using the following metrics. Given our core contribution is to identify the social interactions matrix, we first examine the proportion of true zero entries in  $W_0$  estimated as zeros, and the proportion of true non-zero entries estimated as non-zeros. A global perspective of the proximity between the true and estimated network can be inferred from their average absolute distance between elements. This is the mean absolute deviation of  $\hat{W}$  and  $\hat{\Pi}$  relative to their true values, defined as  $MAD(\hat{W}) = \frac{1}{N(N-1)} \sum_{i,j,i \neq j} |\hat{W}_{ij} - W_{ij,0}|$  and  $MAD(\hat{\Pi}) = \frac{1}{N(N-1)} \sum_{i,j,i \neq j} |\hat{\Pi}_{ij} - \Pi_{ij,0}|$ . The closer these metrics are to zero, more of the elements in the true matrix are correctly estimated. Finally, we evaluate the performance of the procedure using averaged estimates of the endogenous and exogenous social effect parameters,  $\hat{\rho}$  and  $\hat{\gamma}$ . In keeping with the estimation strategy in our empirical application, we report ‘post-Elastic Net’ estimates obtained after having estimated the social interactions matrix by the Elastic Net GMM procedure. We use peers-of-peers’ covariates from the estimated matrix as instrumental variables.

Each Panel in Figure A1 shows a different metric as we vary  $T$  for each simulated network. Panel A shows that for each network, the proportion of zero entries in  $W_0$  correctly estimated as zeros is above 90% even when exploiting a small number of time periods ( $T = 5$ ). The proportion approaches 100% as  $T$  grows. Panel B shows the proportion of non-zeros entries estimated as non-zeros is also high for small  $T$ . It is above 70% from  $T = 5$  for the Erdos-Renyi network, being at least 85% across networks for  $T = 25$ , and increasing as  $T$  grows.

---

<sup>43</sup>In our simulations, we set the penalization grid to  $p_1 = [0, .025, .05, .10]$ ,  $p_1^* = [0, .025, .05, .10]$  and  $p_2 = [0, .025, .05, .10]$ , resulting in  $4^3 = 64$  points per run.

Panels C and D show that for each simulated network, the mean absolute deviation between estimated and true networks for  $\hat{W}$  and  $\hat{\Pi}$  falls quickly with  $T$  and is close zero for large sample sizes. Finally, Panels E and F show that biases in the endogenous and exogenous social effects parameters,  $\hat{\rho}$  and  $\hat{\gamma}$ , also fall quickly in  $T$  (we do not report the bias in  $\hat{\beta}$  since it is close to zero for all  $T$ ). The fact that biases are not zero is as expected for small  $T$ , being analogous to well-known results for autoregressive time series models.

Figure A2 provides a visual representation of the simulated and actual networks under  $T = 100$  time periods. The network size is set to  $N = 30$  in the two stylized networks,  $N = 70$  for the high school network, and  $N = 65$  for the village household network. In comparing the simulated and true network, Figure A2 distinguishes between three types of edges: kept edges, added edges and removed edges. Kept edges are depicted in blue: these links are estimated as non-zero in at least 5% of the iterations and are also non-zero in the true network. Added edges are depicted in green: these links are estimated as non-zero in at least 5% of the iterations but the edge is zero in the true network. Removed edges are depicted in red: these links are estimated as zero in at least 5% of the iterations but are non-zero in the true network. Figure A2 further distinguishes between strong and weak links: strong links are shown in solid edges ( $W_{0,ij} > .3$ ), and weak links are shown as dashed edges.

Consider first Panel A of Figure A2, comparing the simulated and true Erdos-Renyi network. All zero and all non-zero links are correctly estimated. All links are thus recovered and no edges are added to the true network (all edges are in blue). For the political party network, Panel B shows that all strong edges are correctly estimated (it also highlights the party leader nodes). However, around half the weak edges are recovered (blue dashed edges) with the others being missed (red dashed edges). As discussed above, this is not surprising given that shrinkage estimators force small non-zero parameters to zero. Hence, larger  $T$  is needed to achieve similar performance as in the other simulated networks in terms of detecting weak links. Again, we never estimate any added edges (no edges are green).

For the more complex and larger real-world networks, Panel C shows that in the high school network, strong edges are all recovered. However, around half the weak edges are missing (red dashed edges) and there are a relatively small number of added edges (green edges): these amount to 87 edges, or approximately 1.9% of the 4,534 zero entries in the true high-school network. A similar pattern of results is seen in the village network in Panel D: strong edges are all recovered, and here the majority of weak edges are also recovered. A relatively small share of overall edges are added or missed.

Panel B of Table A1 compares the network- and node-level statistics calculated from the recovered social interactions matrix  $\hat{W}$  to those in Panel A from the true interactions matrix  $W_0$ . As Figure A2 showed, the random Erdos-Renyi network is perfectly recovered. For the political party network, the number of recovered edges is slightly lower than the true network (38 vs. 45). This is driven by weak edges: while all the strong edges are recovered (30 out of 30), not all the weak

ones are (8 vs. 15). On node-level statistics, the mean of the in- and out-degree distributions are slightly lower in the recovered network, the clustering coefficient is exactly recovered, and all three nodes with the highest out-degree are correctly captured (nodes 1, 11 and 28), that includes both party leaders (individuals 1 and 11).

Performance in the two real world networks is also encouraging. In the high school network, all strong edges are correctly recovered, as are the majority of weak edges. However, as already noted in Figure A2, because weak edges are not well estimated in the high school network, the average in- and out- degrees are smaller in the recovered network relative to the true network. We recover two out of the three individuals with the highest out-degree (nodes 21 and 69). Finally, in the village network, all strong edges are recovered, the majority of weak edges are recovered, the clustering coefficients are similar across recovered and true networks (.134 vs. .141) and we recover two out of the three households with the highest out-degree (nodes 16, 35, and 57).

### C.3 Robustness

Table A2 presents results for the recovered stylized networks under varying network sizes,  $N = \{15, 30, 50\}$ . Differences between the true and estimated networks are fairly constant as  $N$  increases: even for small  $N = 15$  a large proportion of zeros and non-zeros are correctly estimated. In all cases, biases in  $\hat{\rho}$  and  $\hat{\gamma}$  decrease with larger  $T$ . We also conduct a counterpart robustness check for one of the real work networks. More precisely, we use the savings and insurance networks between households in villages identified in Banerjee *et al.* (2013), that are generally larger than family networks focused on so far. Table A3 shows descriptive statistics on this true village network (Panel A) and the recovered network (Panel B). Relative to the family network, the savings and insurance network has many more edges, a greater proportion of weak edges, is less clustered, with nodes having a higher degree distribution. Despite these differences, the recovered network retains good accuracy on many dimensions: 78% of all edges are recovered, the recovered clustering coefficient is .058 (relative to an actual coefficient of .073) and the three nodes with the highest out-degree are all still identified.

Table A4 conducts robustness checks on the sensitivity of the estimates to parameters choices. We consider true parameters  $\rho_0 = \{.1, .3, .7, .9\}$ ,  $\gamma_0 = \{.3, .7\}$ ,  $\beta_0 = \{.0, .8\}$ . We also introduce a common shock in the disturbance variance-covariance matrix by varying  $q$  in,

$$\epsilon_t \sim N \left( 0, \begin{bmatrix} 1 & q & \cdots & q \\ q & 1 & \cdots & q \\ \vdots & \vdots & \ddots & \vdots \\ q & q & \cdots & 1 \end{bmatrix} \right)$$

where we consider  $q = \{.3, .5, .8, 1\}$ . We find the procedure to be robust to the true values of  $\rho_0$ ,  $\beta_0$ ,  $\gamma_0$ , and  $q$ . For  $\beta_0 = 0$ , performance is slightly worse. This is expected as the exogenous

variation from  $x_t$  no longer affects  $y_t$  directly.

We next probe the procedure by enriching up the structure of shocks across nodes. First, we introduce a common shock correlated with covariates  $x_t$ . To do so, we take  $x_t$  from a Gaussian distribution with mean  $0.5\alpha_t\iota$  and, as before, variance 1. Second, we implement a version where the shock is constant over time but varies at the individual level. In this case, the mean of  $x_t$  is given by  $0.5\alpha^*$ . Third, we implement a version mixing the two types of shocks, with the mean of  $x_t$  given by  $0.5\alpha^* + 0.5\alpha_t\iota$ . In each case, we simulate based on the Erdos-Renyi network as the true  $W_0$ . The results are shown in Figure A3: this shows that for each of the six performance metrics considered, the procedure is highly robust to these richer structures of shocks across individuals and time periods.

The final robustness check demonstrates the gains from using the Adaptive Elastic Net GMM estimator over alternative estimators. Table A5 shows simulation results using Adaptive Lasso estimates of the interaction matrix  $\Pi_0$ , so estimating and penalizing the reduced-form. The Adaptive Lasso estimator performs relatively worse: the mean absolute deviation between  $\hat{W}$  and  $W_0$  is often two to three times larger than the corresponding Adaptive Elastic Net estimates. Appendix Table A6 then shows the performance of the procedure based on OLS estimates of  $\Pi_0$ . Given OLS requires  $m \ll NT$ , we use a time dimension ten times larger,  $T = \{500, 1000, 1500\}$ , and still find a deterioration in performance compared to the Adaptive Elastic Net GMM estimator.

Taken together, these robustness checks suggest the Adaptive Elastic Net GMM estimator is preferred over Adaptive Lasso and OLS estimators. This procedure does well in recovering true network structures, and *a fortiori*, network- and node-level statistics. It does so in networks that vary in size and complexity, and as the underlying social interactions model varies in the strength of endogenous and exogenous social effects, and the structure of shocks.

## D Application: Counterfactuals

We consider a scenario in which California exogenously increases the change in its taxes per capita, so  $\Delta\tau_{it}$  corresponds to an increase of 10%. We measure the differential change in equilibrium state taxes in state  $j$  under the two network structures using the following statistic:

$$\Upsilon_j = \log(\Delta\tau_{jt}|\hat{W}_{econ}) - \log(\Delta\tau_{jt}|W_{geo}), \quad (20)$$

so that positive (negative) values imply taxes being higher (or lower) under  $\hat{W}_{econ}$  than  $W_{geo}$ .<sup>44</sup>

Figure A4 graphs  $\Upsilon_j$  for each mainland US state (including for California itself, the origin of the shock). A wide discrepancy between the equilibrium state tax rates predicted under  $\hat{W}_{econ}$  relative to  $W_{geo}$ : across states  $\Upsilon_j$  varies from  $-3.03$  to  $9.61$ . Only in one state is  $\Upsilon_j$  close to

---

<sup>44</sup>We calculate the counterfactual at  $\hat{\rho}_{2SLS} = .608$ , the endogenous effect parameter estimated in our preferred specification, Column 7 of Table 2.

zero. Table A9 summarizes the general equilibrium effects under both structures. We see that average tax rate increases are 74% higher under  $\hat{W}_{econ}$ . The dispersion of tax rates across states also increases dramatically under  $\hat{W}_{econ}$ . Finally, assuming interactions across states are based solely on geographic neighbors, we miss the fact that many states will have relatively small tax increases.

## Table 1 : Geographic Neighbors

Dependent variable: Change in per capita income and corporate taxes  
Coefficient estimates, standard errors in parentheses

	Besley and Case (1995) Sample		Extended Sample	
	(1) OLS	(2) 2SLS	(3) OLS	(4) 2SLS
Geographic Neighbors' Tax Change (t - [t-2])	.375*** (.120)	.868*** (.273)	.271*** (.075)	.642*** (.152)
Period	1962-1988	1962-1988	1962-2015	1962-2015
First Stage (F-stat)		6.267		27.320
Controls	Yes	Yes	Yes	Yes
State and Year Fixed Effects	Yes	Yes	Yes	Yes
Observations	1,296	1,248	2,592	2,544

Notes: \*\*\* denotes significance at 1%, \*\* at 5%, and \* at 10%. In all specifications, a pair of states are considered neighbors if they share a geographic border. The sample covers 48 mainland US states. In Columns 1 and 2 the sample runs from 1962 to 1988 (as in Besley and Case (1995)). In Columns 3 and 4 the sample is extended to run from 1962 to 2015. The dependent variable is the change in state i's total taxes per capita in year t. OLS regressions estimates are shown in Columns 1 and 3. Columns 2 and 4 show 2SLS regressions where each geographic neighbors' tax change is instrumented by lagged neighbor's state income per capita and unemployment rate. At the foot of Columns 2 and 4 we report the p-value on the F-statistic from the first stage of the null hypothesis that instruments are jointly equal to zero. All regressions control for state i's income per capita in 1982 US dollars, state i's unemployment rate, the proportion of young (aged 5-17) and elderly (aged 65+) in state i's population, and the state governor's age. All specifications include state and time fixed effects. With the exception of governor's age, all variables are differenced between period t and period t-2. Robust standard errors are reported in parentheses.

**Table 2: Economic Neighbors**

**Dependent variable: Change in per capita income and corporate taxes**  
**Coefficient estimates, standard errors in parentheses**

	No Exogenous Social Effects			Exogenous Social Effects			
	(1) Initial	(2) OLS	(3) 2SLS: IVs are Characteristics of Neighbors	(4) Initial	(5) OLS	(6) 2SLS: IVs are Characteristics of Neighbors	(7) 2SLS: IVs are Characteristics of Neighbors-of-Neighbors
<b>Economic Neighbors' Tax Change (t - [t-2])</b>	.886	.378*** (.061)	.641*** (.060)	.645	.145** (.072)	.332* (.199)	.608*** (.220)
<b>Period</b>		1962-2015			1962-2015		
<b>First Stage (F-stat)</b>			19.353			9.571	10.480
<b>Controls</b>	Yes	Yes	Yes	Yes	Yes	Yes	Yes
<b>State and Year Fixed Effects</b>	Yes	Yes	Yes	Yes	Yes	Yes	Yes
<b>Observations</b>	2,952	2,952	2,544	2,952	2,952	2,544	2,592

**Notes:** \*\*\* denotes significance at 1%, \*\* at 5%, and \* at 10%. The sample covers 48 mainland US states running from 1962 to 2015. The dependent variable is the change in state's total taxes per capita in Year t. We allow for exogenous social effects in Columns 4 to 7. In subsequent OLS and IV regressions, the economic neighbors' effect is calculated as the weighted average of economic neighbors' variables. OLS regressions estimates are shown in Column 2, 3 and 5. Column 3 and 6 show the 2SLS regression where each geographic neighbors' tax change is instrumented by lagged neighbors' state income per capita and unemployment rate. Column 7 shows a 2SLS regression where each geographic neighbors' tax change is instrumented by lagged neighbor-of-neighbor's state income per capita and unemployment rate. At the foot of Columns 3, 6 and 7 we report the p-value on the F-statistic from the first stage of the null hypothesis that instruments are jointly equal to zero. All regressions control for state's income per capita in 1982 US dollars, state's unemployment rate, the proportion of young (aged 5-17) and elderly (aged 65+) in state's population, and the state governor's age. All specifications include state and time fixed effects. With the exception of governor's age, all variables are differenced between period t and period t-2. Robust standard errors are reported in parentheses.



**Table 3: Geographic Versus Economic Neighbor Networks**

	Geographic Neighbor Network	Economic Neighbor Network
<b>Number of Edges</b>	214	144
<b>Edges in Both Networks</b>	79	79
<b>Edges in W-geo only</b>	135	
<b>Edges in W-econ only</b>		65
<b>Clustering</b>	.1936	.0259
<b>Reciprocated Edges</b>	100%	29.17%
<b>Degree Distribution Across Nodes (states)</b>		
<b>out-degree</b>	4.458 (1.597)	3.000 (1.185)
<b>in-degree</b>		3.000 (2.073)

**Notes:** This compares statistics derived from the geographic network of US states to those from the estimated economic network among US states. The number of edges, edges in both networks, edges in W-geo only, edges in W-econ only counts the number of edges in those categories. Reciprocated edges is the frequency of in-edges that are reciprocated by out-edges (by construction, this is 100% for geographic networks). The clustering coefficient is the frequency of the number of fully connected triplets over the total number of triplets. The degree distribution across nodes counts the average number of connections (standard deviation in parentheses): we show this separately for in-degree and out-degree (by construction, these are identical for geographic networks).

**Table 4: Predicting Links to Economic Neighbors**

Columns 1-7: Linear Probability Model; Column 8: Tobit  
 Dependent variable (Cols 1-7): =1 if Economic Link Between States Identified  
 Dependent variable (Col 8): =Weighted Link Between States  
 Coefficient estimates, standard errors in parentheses

	(1)	(2)	(3)	(4)	(5)	(6)	(7)	(8)
	Geography	Economic and Demographic Homophily	Labor Mobility	Political Homophily	Tax Havens	Tobit, Partial Avg Effects		
<b>Geographic Neighbor</b>	.699*** (.030)	.701*** (.032)	.701*** (.030)	.698*** (.031)	.698*** (.031)	.697*** (.031)	.068*** (.006)	
<b>Distance</b>	-.453*** (.033)	-.008 (.024)						
<b>Distance sq.</b>	.0949*** (.007)	.003 (.006)						
<b>GDP Homophily</b>			2.409** (1.183)	2.369* (1.186)	2.296* (1.193)	1.046 (1.150)	.322 (.302)	
<b>Demographic Homophily</b>			.222 (.226)	.235 (.226)	.241 (.228)	.256 (.225)	.077 (.067)	
<b>Net Migration</b>			.044* (.025)	.044* (.025)	.044* (.025)	-0.032 (.025)	0.001 (.002)	
<b>Political Homophily</b>			-.057 (.042)	-.083** (.042)	-.025* (.014)	-.025* (.014)	-.025* (.014)	
<b>Tax Haven Sender</b>			.107*** (.024)	.107*** (.024)	.107*** (.024)	.107*** (.024)	.021*** (.005)	
<b>Adjusted R-squared</b>	0.427	0.152	0.427	0.428	0.429	0.429	0.440	-
<b>Observations</b>	2,256	2,256	2,256	2,256	2,256	2,256	2,256	2,256

Notes: \*\*\* denotes significance at 1%, \*\* at 5%, and \* at 10%. The specifications in Columns 1-7 are cross-sectional linear probability models where the dependent variable is equal to 1 if two states are linked, and zero otherwise. In Column 8 the dependent variable is the weighted link between states. Column 8 reports the partial average effects from a Tobit model. A pair of states is considered a first-degree geographic neighbor if they share a border. Distance and distance squared are calculated from the centroids of states' capital cities. GDP homophily is the absolute difference of states' GDP per capita. Demographic homophily is the absolute difference of share of young (aged 5-17) plus the absolute difference of the share of elderly in states' population (aged 65+). Net migration based on individuals tax returns (Source: Internal Revenue Service, <https://www.irs.gov/statistics/soi-tax-stats-migration-data>). Political homophily is equal to one if a pair of states have governors of same party at given year. Nevada, Delaware, Montana, South Dakota, Wyoming and New York are considered tax haven states. Time averages are taken for all explanatory variables. Robust standard errors in parentheses.

## Table 5: Gubernatorial Term Limits

Dependent variable: Change in per capita income and corporate taxes

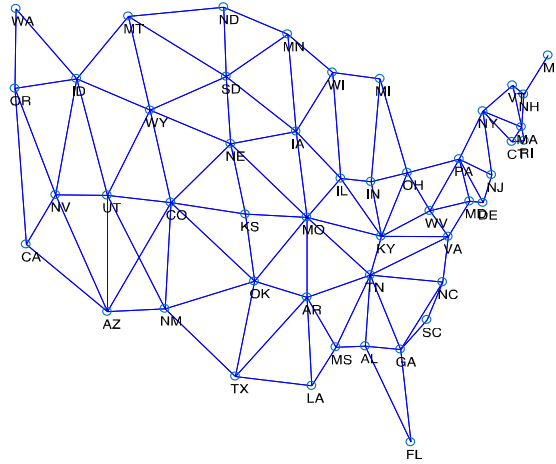
Coefficient estimates, standard errors in parentheses

IVs: Characteristics of Neighbors-of-Neighbors

	All Governors		Governor Cannot Run for Re-election		Governor Can Run for Re-election	
	(1) OLS	(2) 2SLS	(3) OLS	(4) 2SLS	(5) OLS	(6) 2SLS
Economic Neighbors' tax change (t - [t-2])	.145** (.072)	.608*** (.220)	.016 (.105)	.937* (.534)	.182** (.084)	.543** (.237)
Period	1962-2015		1962-2015		1962-2015	
First Stage (F-stat)	10.480		2.835		10.120	
Controls	Yes	Yes	Yes	Yes	Yes	Yes
State and Year Fixed Effects	Yes	Yes	Yes	Yes	Yes	Yes
Observations	2,592	2,592	640	640	1,917	1,917

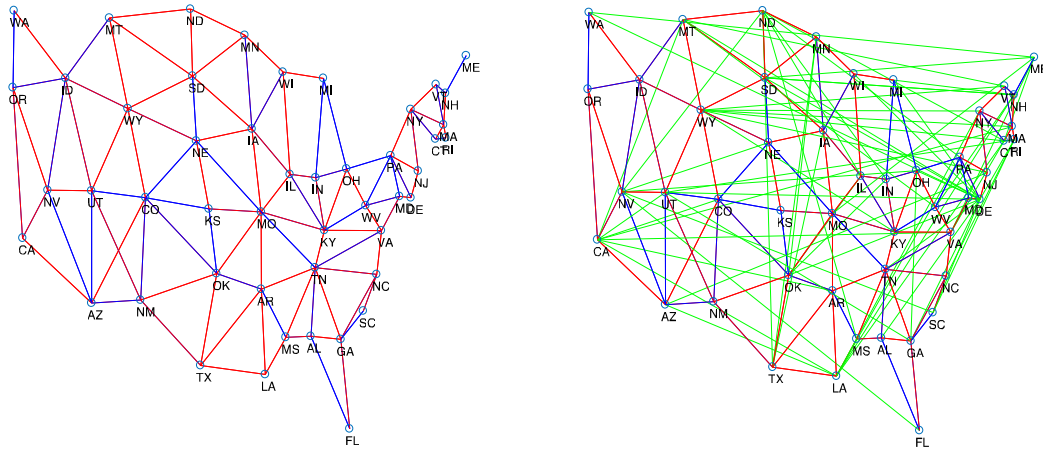
Notes: \*\*\* denotes significance at 1%, \*\* at 5%, and \* at 10%. The sample in Columns 1 and 2 covers 48 mainland US states running from 1962 to 2015. In Columns 3 and 4 we use the subsample of state-years in which the governor that faced term limits in the subsequent gubernatorial election. In Columns 5 and 6 we use the subsample of state-years in which the governor did not face term limits in the subsequent gubernatorial election, and so could run for reelection. The dependent variable is the change in state's total taxes per capita in year t. We first estimate our procedure which outputs parameters and the network of economic neighbors. We penalize geographic neighbors throughout and also allow for exogenous social effects. OLS regressions estimates are shown in Columns 1, 3 and 5. Columns 2, 4 and 6 show a 2SLS regression where each geographic neighbors' tax change is instrumented by lagged neighbor-of-neighbor's state income per capita and unemployment rate. At the foot of Columns 2, 4 and 6 we report the p-value on the F-statistic from the first stage of the null hypothesis that instruments are jointly equal to zero. All regressions control for state's income per capita in 1982 US dollars, state's unemployment rate, the proportion of young (aged 5-17) and elderly (aged 65+) in state's population, and the state governor's age. All specifications include state and time fixed effects. With the exception of governor's age, all variables are differenced between period t and period t-2. Robust standard errors are reported in parentheses.

**Figure 1A: Network Graph of US States, Geographic Neighbors**



**Notes:** Figure 3A represents the continental US states (N=48). An edge is drawn between a pair of states if they share a geographic border. State abbreviations are as used by US Post Office (<http://about.usps.com/who-we-are/postal-history/state-abbreviations.pdf>).

**Figure 1B: Network Graph of US States, Identified Economic Neighbors**

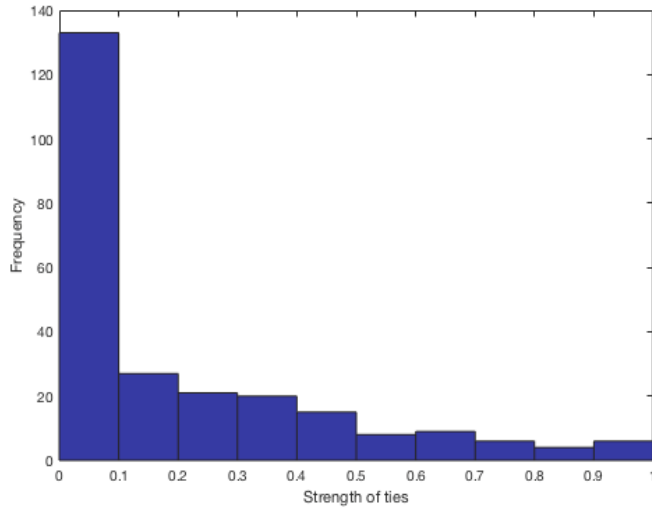


Geographic network edges  
 Removed (geographic) edges in economic network  
 New edges added in economic networks

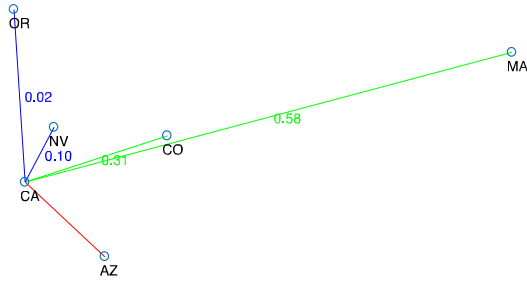
**Notes:** Figure 3B represents the continental United States (N=48). The economic network is derived from our preferred specification, where we penalize geographic neighbors to states and allow for exogenous social effects. A blue edge is drawn between a pair of states if they are geographic neighbors and were estimated as connected. A red edge is drawn between a pair of states if they are geographic neighbors but were not estimated as connected. A green edge is drawn between a pair of states if they are not geographic neighbors and were estimated connected. The left hand side graph just shows read and blue edges. The right hand side shows all three types of edges. State abbreviations are as used by US Post Office (<http://about.usps.com/who-we-are/postal-history/state-abbreviations.pdf>).

**Figure 2: Strength of Ties and Reciprocity**

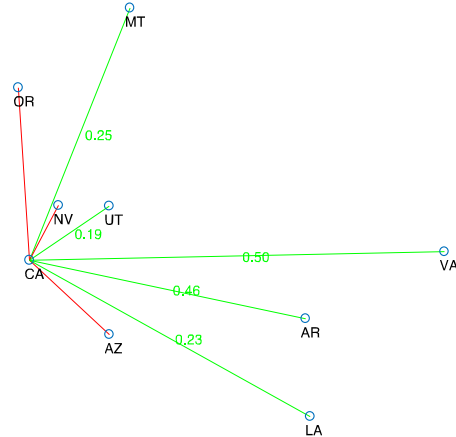
**Panel A: Histogram of Strength of Ties, Conditional on  $W_{0,ij} > 0$**



**Panel B: In-network for California**



**Panel C: Out-network for California**

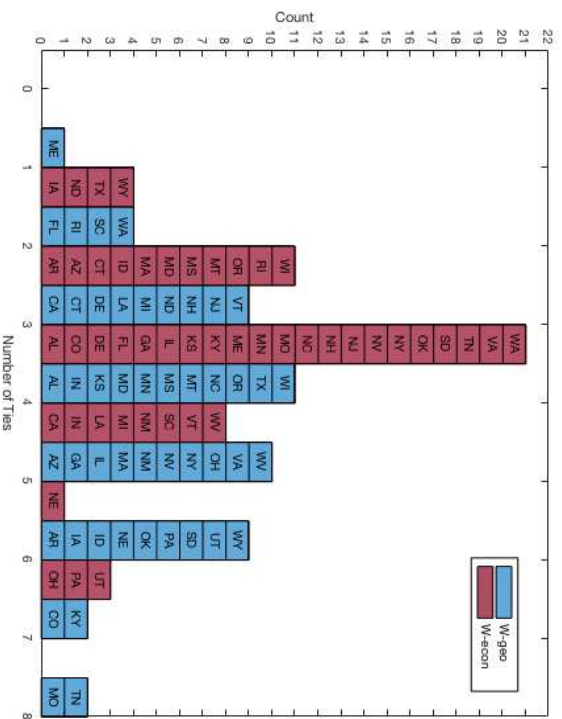


Geographic network edges  
 Removed (geographic) edges in economic network  
 New edges added in economic networks

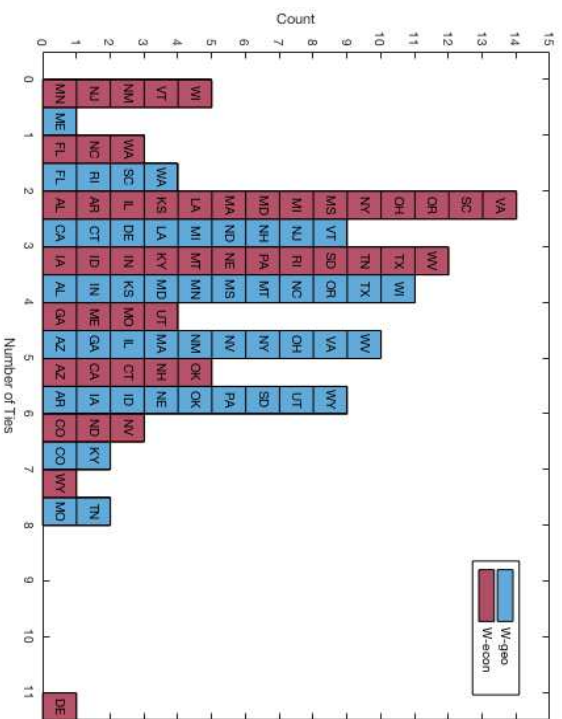
**Notes:** Panel A is the histogram of ties in the economic network, conditional on non-zero ties. Panels B and C show the in-network and out-network of California as derived from our preferred specification, where we penalize geographic neighbors to states, and allow for exogenous social effects. The in-network are the states that determine tax setting in California. The out-network is the states in which taxes are set in direct response to those in California. A blue edge is drawn between a pair of states if they are geographic neighbors and were estimated as connected. A red edge is drawn between a pair of states if they are geographic neighbors but were not estimated as connected. A green edge is drawn between a pair of states if they are not geographic neighbors and were estimated connected. State abbreviations are as used by US Post Office (<http://about.usps.com/who-we-are/postal-history/state-abbreviations.pdf>).

Figure 3: In- and Out-degree Distribution

Panel A: In-degree distribution

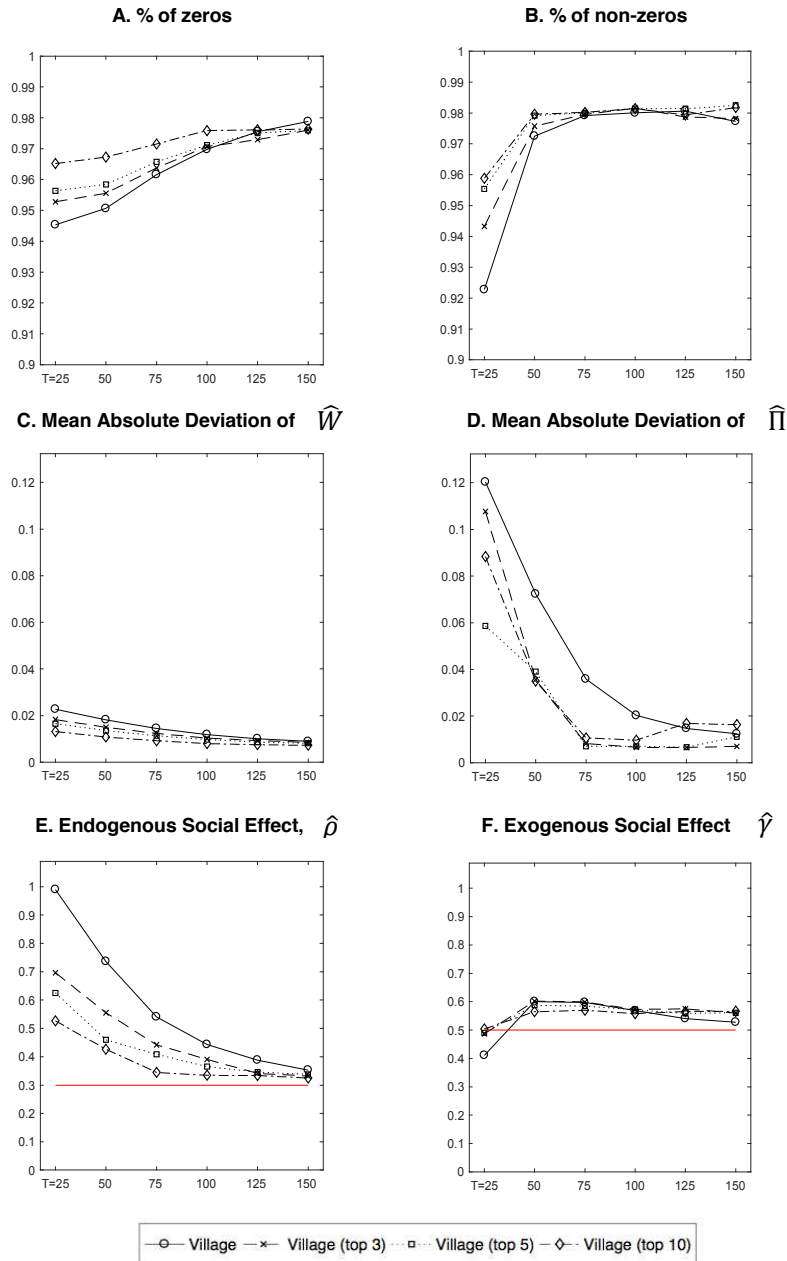


Panel B: Out-degree distribution



Notes: In-degree distribution (Panel A) and out-degree distribution (Panel B). Distribution calculated from geographic neighbors' network (W-geo) in blue. Distribution calculated from economic neighbors' network (W-econ) in red. State abbreviations are as used by US Post Office (<http://about.usps.com/who-we-are/postal-history/state-abbreviations.pdf>).

**Figure 4: Simulation Results, Adaptive Elastic Net GMM**  
**Partial Knowledge of  $W_0$**

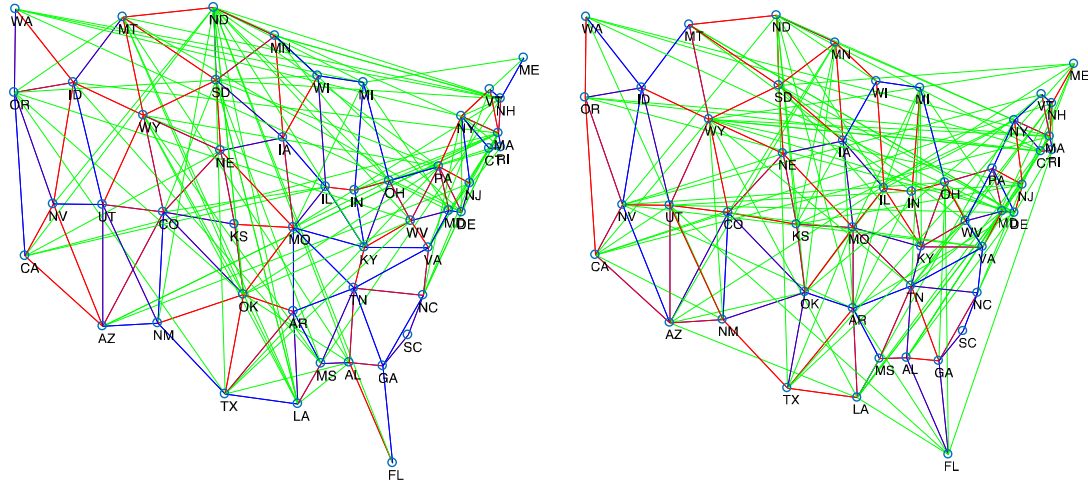


**Notes:** These simulation results are based on the Banerjee et al. (2013) village network, using the Adaptive Elastic Net GMM algorithm, with penalization parameters chosen by BIC, under various assumptions about knowledge of the true network and time periods  $T=25, 50, 100, 125$  and  $150$ . The "Village" case refers to the simulation implemented without knowledge about the true network. "Village (top 3)" refers to the case where all connections of the three households with highest out-degrees are assumed to be known. "Village (top 5)" and "Village (top 10)" are analogously defined. In all cases, 1000 Monte Carlo iterations were performed. The true parameters are  $\rho=0.3$ ,  $\beta=0.4$  and  $\gamma=0.5$ . In Panel A, the % of zeros refers to the proportion of true zero elements in the social interaction matrix that are estimated as smaller than .05. In Panel B, the % of non-zeros refers to the proportion of true elements greater than .3 in the social interaction matrix that are estimated as non-zeros. In Panels C and D, the Mean Absolute Deviations are the mean absolute error of the estimated network compared to the true network for the social interaction matrix  $W$  and the reduced form matrix respectively. In Panels E and F, the true parameter values are marked in the horizontal red lines. The recovered parameter are the estimated parameters averaged across iterations. All specifications include time and node fixed effects.

**Figure 5: Network Graph of US States, Identified Economic Neighbors by Subsamples**

**Panel A: Econ Network, 1962-1988 subsample**

**Panel B: Econ Network, 1989-2015 subsample**



**Notes:** Panels A and B represents the continental United States (N=48). Panel A is estimated with the 1962-1988 subsample. Panel B is estimated with the 1989-2015 subsample. The economic network is derived from our preferred specification, where we penalize geographic neighbors to states, and allow for exogenous social effects. A blue edge is drawn between a pair of states if they are geographic neighbors and were estimated as connected. A red edge is drawn between a pair of states if they are geographic neighbors but were not estimated as connected. A green edge is drawn between a pair of states if they are not geographic neighbors but were estimated connected. The left hand side graph just shows red and blue edges. The right hand side shows all three types of edges. State abbreviations are as used by US Post Office (<http://about.usps.com/who-we-are/postal-history/state-abbreviations.pdf>).

**Panel C: Geographic Versus Economic Neighbor Networks**

	<b>Geographic Neighbor Network</b>	<b>Economic Neighbor Network (Full Sample)</b>	<b>Economic Neighbor Network (1962-1988)</b>	<b>Economic Neighbor Network (1989-2015)</b>
<b>Number of Edges</b>	214	144	197	185
<b>Edges in both W-geo and W-econ</b>		79	108	86
<b>Edges in W-econ only</b>		65	89	99
<b>Edges in W-geo only</b>		135	106	128
<b>Clustering</b>	.1936	.0259	.0389	.0394
<b>Reciprocated Edges</b>	100%	29.17%	35.53%	23.78%
<b>Degree Distribution Across Nodes (states)</b>				
<b>out-degree</b>	4.458 (1.597)	3.000 (1.185)	4.104 (1.704)	3.854 (1.473)
<b>in-degree</b>		3.000 (2.073)	4.104 (2.707)	3.854 (2.518)

**Notes:** This compares statistics derived from the geographic network of US states to those from the estimated economic network among US states, for the three samples ("Full Sample", 1962-2015; 1962-1988; 1989-2015). The number of edges, edges in both networks, edges in W-geo only, edges in W-econ only counts the number of edges in those categories. Numbers are relative to the W-geo network in the first column. Reciprocated edges is the frequency of in-edges that are reciprocated by out-edges (by construction, this is 100% for geographic networks). The clustering coefficient is the frequency of the number of fully connected triplets over the total number of triplets. The degree distribution across nodes counts the average number of connections (standard deviation in parentheses); we show this separately for in-degree and out-degree (by construction, these are identical for geographic networks).



**Table A1: True and Recovered Networks**

	<b>Erdos-Renyi</b>	<b>Political Party</b>	<b>High school</b>	<b>Village</b>
			<i>Coleman (1964)</i>	<i>Banerjee et al. (2013)</i>
<b>A. True Networks</b>				
<b>Number of nodes</b>	<b>30</b>	<b>30</b>	<b>70</b>	<b>65</b>
<b>(a) Network-wide statistics</b>				
<i>Number of edges</i>	30	45	366	240
<i>Number of strong edges</i>	30	30	70	65
<i>Number of weak edges</i>	0	15	296	175
<i>Number of reciprocated edges</i>	2	2	184	240
<i>Clustering coefficient</i>	-	.000	.120	.141
<i>Number of components</i>	12	11	3	3
<i>Size of maximal component</i>	10	16	68	51
<i>Standard deviation of the diagonal of squared W</i>	.254	.254	.167	.239
<b>(b) Node-level statistics</b>				
<i>In-degree distribution</i>	1.00 (0.00)	1.50 (.509)	5.23 (2.04)	3.69 (2.35)
<i>Out-degree distribution</i>	1.00 (1.05)	1.50 (2.49)	5.23 (3.64)	3.69 (2.35)
<i>Nodes with highest out-degree</i>	{ 7, 11, 26 }	{ 1, 11, 28 }	{ 21, 22, 69 }	{ 16, 35, 57 }
<b>B. Recovered Networks</b>				
<b>(a) Network-wide statistics</b>				
<i>Number of edges</i>	30	38	210	194
<i>Number of strong edges</i>	30	30	70	68
<i>Number of weak edges</i>	0	8	140	126
<i>Number of reciprocated edges</i>	2	2	184	170
<i>Clustering coefficient</i>	-	.000	.162	.134
<i>Number of components</i>	12	11	1	4
<i>Size of maximal component</i>	10	14	70	48
<b>(b) Node-level statistics</b>				
<i>In-degree distribution</i>	1.00 (0.00)	1.27 (.450)	3.00 (1.18)	2.99 (1.29)
<i>Out-degree distribution</i>	1.00 (1.05)	1.27 (1.76)	3.00 (1.02)	2.99 (1.15)
<i>Nodes with highest out-degree</i>	{ 7, 11, 26 }	{ 1, 11, 28 }	{ 21, 48, 69 }	{ 16, 35, 57 }

**Notes:** Panel A refers to the true networks. Panel B refers to the recovered networks. In each Panel, the summary statistics are divided into network-wide and node-level statistics. Strong edges are defined as those with strength greater than or equal to .3. For the in-degree and out-degree distribution, the mean is shown and the standard deviation is in parentheses. The nodes with the highest out-degree are those with the greatest influence on others, and are calculated as the column-sum of the social interaction matrix. The recovered networks statistic are calculated over the average network across simulations with T=100.

**Table A2: Simulation Results, Adaptive Elastic Net GMM, Alternative Network Sizes**

	A. Erdos-Renyi										B. Political party																			
	N = 15					N = 30					N = 50					N = 15					N = 30					N = 50				
	T=50	100	150	T=50	100	150	T=50	100	150	T=50	100	150	T=50	100	150	T=50	100	150	T=50	100	150	T=50	100	150	T=50	100	150			
<b>% True Zeros</b>	.954	.976	.973	.957	.992	.997	.947	.965	.979	.950	.977	.979	.943	.978	.989	.943	.961	.976	(.033)	(.031)	(.031)	(.009)	(.004)	(.002)	(.007)	(.006)	(.005)			
	(.033)	(.034)	(.031)	(.009)	(.004)	(.002)	(.007)	(.006)	(.005)	(.034)	(.025)	(.024)	(.009)	(.006)	(.005)	(.007)	(.006)	(.006)	(.031)	(.025)	(.024)	(.009)	(.006)	(.005)	(.007)	(.006)	(.006)			
<b>% True Non-Zeros</b>	.899	.919	.924	.958	.960	.962	.977	.978	.977	.914	.925	.932	.930	.954	.960	.970	.977	.977	(.051)	(.032)	(.026)	(.017)	(.016)	(.011)	(.007)	(.007)	(.008)			
	(.051)	(.032)	(.026)	(.017)	(.016)	(.011)	(.007)	(.007)	(.008)	(.038)	(.022)	(.009)	(.037)	(.023)	(.016)	(.015)	(.009)	(.007)	(.051)	(.032)	(.026)	(.017)	(.016)	(.011)	(.007)	(.007)	(.008)			
<b>MAD(<math>\hat{W}</math>)</b>	.021	.007	.004	.017	.003	.001	.020	.011	.006	.032	.019	.017	.028	.014	.010	.023	.014	.009	(.014)	(.011)	(.008)	(.004)	(.001)	(.002)	(.001)	(.001)	(.001)			
	(.014)	(.011)	(.008)	(.004)	(.001)	(.001)	(.002)	(.001)	(.001)	(.011)	(.007)	(.004)	(.004)	(.002)	(.002)	(.002)	(.001)	(.001)	(.014)	(.011)	(.008)	(.004)	(.001)	(.002)	(.001)	(.001)	(.001)			
<b>MAD(<math>\hat{\Pi}</math>)</b>	.025	.012	.009	.020	.004	.003	.054	.016	.007	.034	.021	.019	.028	.014	.012	.065	.019	.009	(.012)	(.008)	(.006)	(.004)	(.002)	(.001)	(.018)	(.004)	(.002)			
	(.012)	(.008)	(.006)	(.004)	(.002)	(.001)	(.018)	(.004)	(.002)	(.009)	(.006)	(.003)	(.004)	(.002)	(.001)	(.028)	(.004)	(.001)	(.012)	(.008)	(.006)	(.004)	(.002)	(.001)	(.018)	(.004)	(.002)			
$\hat{\rho}$	.262	.270	.276	.286	.286	.283	.667	.398	.270	.235	.245	.241	.209	.228	.223	.700	.383	.242	(.069)	(.044)	(.038)	(.079)	(.026)	(.022)	(.079)	(.050)	(.050)			
	(.069)	(.044)	(.038)	(.079)	(.026)	(.022)	(.079)	(.050)	(.050)	(.078)	(.049)	(.038)	(.084)	(.035)	(.029)	(.100)	(.069)	(.051)	(.069)	(.044)	(.038)	(.079)	(.026)	(.022)	(.079)	(.050)	(.050)			
$\hat{\beta}$	.403	.399	.400	.405	.400	.400	.380	.399	.401	.405	.400	.397	.404	.399	.398	.380	.401	.401	(.039)	(.028)	(.022)	(.028)	(.018)	(.015)	(.025)	(.015)	(.012)			
	(.039)	(.028)	(.022)	(.028)	(.018)	(.015)	(.025)	(.015)	(.012)	(.040)	(.028)	(.022)	(.029)	(.019)	(.015)	(.024)	(.015)	(.012)	(.039)	(.028)	(.022)	(.028)	(.018)	(.015)	(.025)	(.015)	(.012)			
$\hat{\gamma}$	.577	.521	.507	.670	.516	.498	.748	.686	.595	.550	.481	.459	.669	.501	.463	.666	.566	.566	(.094)	(.059)	(.046)	(.054)	(.022)	(.018)	(.118)	(.056)	(.028)			
	(.094)	(.059)	(.046)	(.054)	(.022)	(.018)	(.118)	(.056)	(.028)	(.093)	(.060)	(.050)	(.060)	(.027)	(.021)	(.128)	(.063)	(.032)	(.094)	(.059)	(.046)	(.054)	(.022)	(.018)	(.118)	(.056)	(.028)			

**Notes:** These simulation results are based on the Adaptive Elastic Net GMM algorithm, with penalization parameters chosen by BIC, under various true networks, network sizes and time periods T=50, 100 and 150. In all cases, 1000 Monte Carlo iterations were performed. The true parameters are rho=0=.3, beta=0=.4 and gamma=0=.5. The % of true zeros refers to the proportion of true zero elements in the social interaction matrix that are estimated as smaller than .05. The % of true non-zeros refers to the proportion of true elements greater than .3 in the social interaction matrix that are estimated as non-zeros. The Mean Absolute Deviations are the mean absolute error of the estimated network compared to the true network for the social interaction matrix W and the reduced form matrix respectively. The recovered parameter are the estimated parameters averaged across iterations. All specifications include time and node fixed effects. Standard errors across iterations are in parentheses.

**Table A3: True and Recovered Village Networks**

	Village Family <i>Banerjee et al. (2013)</i>	Village Savings and Insurance <i>Banerjee et al. (2013)</i>
<b>A. True Networks</b>		
<b>Number of nodes</b>	<b>65</b>	<b>65</b>
<b>(a) Network-wide statistics</b>		
<i>Number of edges</i>	240	343
<i>Number of strong edges</i>	65	47
<i>Number of weak edges</i>	175	296
<i>Number of reciprocated edges</i>	240	340
<i>Clustering coefficient</i>	.141	.073
<i>Number of components</i>	3	6
<i>Size of maximal component</i>	51	62
<i>Standard deviation of the diagonal of squared W</i>	.239	.159
<b>(b) Node-level statistics</b>		
<i>In-degree distribution</i>	3.69 (2.35)	4.90 (3.42)
<i>Out-degree distribution</i>	3.69 (2.35)	4.90 (3.43)
<i>Nodes with highest out-degree</i>	{ 16, 35, 57 }	{ 16, 35, 55 }
<b>B. Recovered Networks</b>		
<b>(a) Network-wide statistics</b>		
<i>Number of edges</i>	194	269
<i>Number of strong edges</i>	68	65
<i>Number of weak edges</i>	126	204
<i>Number of reciprocated edges</i>	170	250
<i>Clustering coefficient</i>	.134	.058
<i>Number of components</i>	4	4
<i>Size of maximal component</i>	48	62
<b>(b) Node-level statistics</b>		
<i>In-degree distribution</i>	2.99 (1.29)	3.84 (1.90)
<i>Out-degree distribution</i>	2.99 (1.15)	3.84 (1.98)
<i>Nodes with highest out-degree</i>	{ 16, 35, 57 }	{ 16, 35, 55 }

**Notes:** Panel A refers to the true networks. Panel B refers to the recovered networks. In each Panel, the summary statistics are divided into network-wide and node-level statistics. Strong edges are defined as those with strength greater than or equal to .3. For the in-degree and out-degree distribution, the mean is shown and the standard deviation is in parentheses. The nodes with the highest out-degree are those with the greatest influence on others, and are calculated as the column-sum of the social interaction matrix. The recovered networks statistic are calculated over the average network across simulations with T=100.

**Table A4: Simulation Results, Adaptive Elastic Net GMM, Alternative Parameters**

	A. Erdos-Renyi										B. Political party													
	$p_0$	$\beta_0$	$\gamma_0$	$q$	$p_0$	$\beta_0$	$\gamma_0$	$q$	$p_0$	$\beta_0$	$\gamma_0$	$q$	$p_0$	$\beta_0$	$\gamma_0$	$q$								
<b>% True Zeros</b>	.986	.994	.991	.979	.986	.987	.974	.997	.996	.997	.997	.997	.971	.983	.982	.966	.978	.977	.959	.986	.985	.992	.996	.997
	(.005)	(.004)	(.004)	(.005)	(.005)	(.007)	(.006)	(.002)	(.002)	(.003)	(.002)	(.002)	(.008)	(.005)	(.006)	(.007)	(.008)	(.007)	(.007)	(.005)	(.004)	(.004)	(.004)	(.003)
<b>% True Non-Zeros</b>	.951	.963	.963	.956	.806	.967	.961	.961	.963	.962	.961	.959	.772	.813	.836	.864	.469	.856	.741	.834	.803	.808	.816	.832
	(.028)	(.011)	(.011)	(.017)	(.096)	.000	(.015)	(.016)	(.012)	(.013)	(.013)	(.018)	(.045)	(.036)	(.034)	(.031)	(.147)	(.035)	(.044)	(.036)	(.037)	(.035)	(.034)	(.027)
<b>MAD(<math>W</math>)</b>	.005	.002	.003	.007	.014	.004	.011	.001	.001	.001	.000	.000	.017	.012	.012	.018	.029	.012	.023	.010	.011	.009	.008	.007
	(.002)	(.001)	(.001)	(.002)	(.005)	(.002)	(.003)	(.001)	(.001)	(.001)	(.001)	(.001)	(.003)	(.002)	(.002)	(.003)	(.007)	(.002)	(.003)	(.002)	(.002)	(.001)	(.001)	(.001)
<b>MAD(<math>\hat{\eta}</math>)</b>	.005	.006	.013	.077	.013	.007	.009	.004	.003	.003	.002	.002	.011	.021	.043	.208	.021	.017	.016	.016	.013	.011	.010	.009
	(.002)	(.002)	(.005)	(.051)	(.004)	(.003)	(.002)	(.002)	(.001)	(.001)	(.001)	(.001)	(.002)	(.002)	(.004)	(.026)	(.004)	(.003)	(.002)	(.002)	(.002)	(.001)	(.001)	(.001)
<b><math>\hat{\rho}</math></b>	.081	.487	.709	.917	.318	.244	.287	.286	.285	.285	.288	.292	.046	.403	.598	.847	.298	.171	.221	.225	.224	.222	.218	.218
	(.034)	(.027)	(.025)	(.012)	(.047)	(.076)	(.036)	(.023)	(.023)	(.020)	(.017)	(.009)	(.038)	(.031)	(.040)	(.040)	(.071)	(.067)	(.048)	(.030)	(.030)	(.028)	(.025)	(.018)
<b><math>\hat{\beta}</math></b>	.401	.399	.397	.364	(.008)	.801	.402	.399	.401	.400	.400	.400	.400	.399	.398	.380	-.015	.801	.402	.400	.399	.398	.398	.398
	(.018)	(.019)	(.019)	(.023)	(.025)	(.018)	(.019)	(.019)	(.016)	(.012)	(.009)	(.001)	(.019)	(.020)	(.020)	(.026)	(.029)	(.020)	(.020)	(.019)	(.016)	(.014)	(.009)	(.003)
<b><math>\hat{\gamma}</math></b>	.532	.512	.517	.509	.432	.552	.376	.698	.503	.495	.493	.492	.519	.489	.488	.469	.305	.548	.391	.638	.474	.454	.440	.431
	(.023)	(.022)	(.024)	(.028)	(.070)	(.033)	(.027)	(.021)	(.018)	(.015)	(.012)	(.007)	(.030)	(.027)	(.031)	(.050)	(.117)	(.038)	(.036)	(.025)	(.023)	(.019)	(.015)	(.010)

**Notes:** These simulation results are based on the Adaptive Elastic Net GMM algorithm, with penalization parameters chosen by BIC, under various true networks, network sizes, time periods T=100 and parameter values. In all cases, 1000 Monte Carlo iterations were performed. The % of true zeros refers to the proportion of true zero elements in the social interaction matrix that are estimated as non-zeros. The Mean Absolute Deviations are the mean absolute error of the estimated network compared to the true network for the social interaction matrix W and the reduced form matrix respectively. The recovered parameter are the estimated parameters averaged across iterations. All specifications include time and node fixed effects. Standard errors across iterations are in parentheses.

**Table A5: Simulation Results, Adaptive Lasso**

	A. Erdos-Renyi										B. Political party									
	N = 15		N = 30		N = 50		N = 15		N = 30		N = 50									
	T=50	100	150	T=50	100	150	T=50	100	150	T=50	100	150	T=50	100	150					
<b>% True Zeros</b>	.728	.798	.842	.737	.848	.878	.845	.846	.913	.730	.799	.840	.737	.849	.880	.846	.846	.921		
	(.023)	(.024)	(.022)	(.012)	(.008)	(.008)	(.005)	(.006)	(.027)	(.024)	(.025)	(.023)	(.013)	(.009)	(.009)	(.006)	(.006)	(.008)		
<b>% True Non-Zeros</b>	.996	1.000	1.000	.497	1.000	1.000	.494	.496	.930	.992	1.000	1.000	.507	1.000	1.000	.498	.501	.996		
	(.039)	(.000)	(.000)	(.096)	(.001)	(.000)	(.071)	(.074)	(.177)	(.023)	(.002)	(.000)	(.105)	(.004)	(.001)	(.074)	(.076)	(.042)		
<b>MAD(<math>\bar{W}</math>)</b>	.071	.050	.039	.064	.039	.033	.039	.039	.027	.070	.050	.039	.063	.038	.032	.039	.038	.025		
	(.005)	(.005)	(.004)	(.002)	(.002)	(.002)	(.000)	(.002)	(.005)	(.005)	(.004)	(.004)	(.002)	(.002)	(.002)	(.000)	(.002)	(.001)		
<b>MAD(<math>\hat{\Pi}</math>)</b>	.092	.056	.042	.084	.049	.036	.071	.045	.032	.093	.057	.044	.084	.050	.036	.071	.045	.033		
	(.008)	(.005)	(.004)	(.005)	(.003)	(.002)	(.004)	(.003)	(.002)	(.008)	(.005)	(.003)	(.005)	(.003)	(.002)	(.004)	(.002)	(.002)		
$\hat{\rho}$	.962	.815	.535	.998	.988	.965	1.000	.993	.995	.970	.783	.512	.998	.993	.979	1.000	.994	.995		
	(.112)	(.186)	(.231)	(.040)	(.066)	(.095)	(.000)	(.075)	(.054)	(.106)	(.199)	(.236)	(.041)	(.050)	(.077)	(.000)	(.069)	(.054)		
$\hat{\beta}$	.131	.285	.330	.000	.158	.254	.000	.000	.121	.144	.292	.336	.000	.177	.259	.000	.000	.167		
	(.079)	(.049)	(.038)	(.000)	(.053)	(.030)	(.000)	(.000)	(.066)	(.081)	(.049)	(.039)	(.000)	(.047)	(.030)	(.000)	(.000)	(.044)		
$\hat{\gamma}$	.996	.998	.968	.000	1.000	.999	.000	.000	.863	1.000	.995	.942	.000	1.000	.999	.000	.000	.992		
	(.063)	(.015)	(.051)	(.000)	(.000)	(.007)	(.000)	(.000)	(.344)	(.000)	(.023)	(.066)	(.000)	(.000)	(.014)	(.000)	(.000)	(.089)		

**Notes:** These simulation results are based on the Adaptive Lasso algorithm, with penalization parameters chosen by BIC, under various true networks, network sizes and time periods T=50, 100 and 150. In all cases, 1000 Monte Carlo iterations were performed. The true parameters are  $\rho=0=3$ ,  $\beta=0=4$  and  $\gamma=0=5$ . The % of true zeros refers to the proportion of true zero elements in the social interaction matrix that are estimated as smaller than .05. The % of true non-zeros refers to the proportion of true elements greater than .3 in the social interaction matrix that are estimated as non-zeros. The Mean Absolute Deviations are the mean absolute error of the estimated network compared to the true network for the social interaction matrix W and the reduced form matrix respectively. The recovered parameter are the estimated parameters averaged across iterations. All specifications include time and node fixed effects. Standard errors across iterations are in parentheses.

**Table A6: Simulation Results, OLS**

	A. Erdos-Renyi				B. Political party				
	N = 15		N = 30		N = 50		N = 50		
	T=500	1000	1500	T=500	1000	1500	T=500	1000	1500
<b>% True Zeros</b>	.825 (.018)	.878 (.020)	.911 (.021)	.884 (.007)	.928 (.007)	.958 (.006)	.936 (.019)	.966 (.003)	.979 (.002)
<b>% True Non-Zeros</b>	1.000 (.000)	1.000 (.000)	1.000 (.000)	1.000 (.000)	1.000 (.000)	1.000 (.000)	.977 (.107)	1.000 (.000)	1.000 (.000)
<b>MAD(<math>\bar{W}</math>)</b>	.039 (.003)	.032 (.004)	.028 (.004)	.031 (.001)	.025 (.001)	.022 (.001)	.025 (.000)	.021 (.000)	.019 (.000)
<b>MAD(<math>\hat{\Pi}</math>)</b>	.038 (.002)	.027 (.001)	.022 (.001)	.039 (.001)	.027 (.001)	.022 (.001)	.040 (.001)	.027 (.000)	.022 (.000)
<b><math>\hat{\rho}</math></b>	.488 (.114)	.381 (.117)	.362 (.108)	1.000 (.000)	.981 (.051)	.617 (.064)	1.000 (.000)	1.000 (.000)	1.000 (.000)
<b><math>\hat{\beta}</math></b>	.394 (.017)	.398 (.009)	.399 (.006)	.343 (.017)	.372 (.025)	.400 (.003)	.256 (.064)	.350 (.002)	.353 (.013)
<b><math>\hat{\gamma}</math></b>	.964 (.046)	.871 (.079)	.809 (.083)	1.000 (.000)	1.000 (.000)	.998 (.009)	.956 (.205)	1.000 (.000)	1.000 (.000)

**Notes:** These simulation results are based on OLS estimates, under various true networks, network sizes and time periods T=500, 1000 and 1500. In all cases, 1000 Monte Carlo iterations were performed. The true parameters are rho=0=3, beta=0=4 and gamma=0=5. The % of true zeros refers to the proportion of true zero elements in the social interaction matrix that are estimated as smaller than .05. The % of true non-zeros refers to the proportion of true elements greater than .3 in the social interaction matrix that are estimated as non-zeros. The Mean Absolute Deviations are the mean absolute error of the estimated network compared to the true network for the social interaction matrix W and the reduced form matrix respectively. The recovered parameter are the estimated parameters averaged across iterations. All specifications include time and node fixed effects. Standard errors across iterations are in parentheses.

## Table A7: Summary Statistics, Tax Competition Application

	Obs	Mean	SD	Min	q25	Median	q75	Max
<b>A. Besley and Case sample (1962-1988)</b>								
State total tax per capita	1296	.371	.266	.036	.145	.300	.530	1.345
State income per capita	1296	9.951	2.130	4.105	8.585	9.919	11.375	18.808
Unemployment rate	1296	5.885	2.242	1.800	4.200	5.500	7.000	18.000
Proportion of young	1296	.234	.033	.160	.210	.240	.260	.310
Proportion of elderly	1296	.106	.020	.040	.090	.110	.120	.190
State governor's age	1296	51.088	7.441	33.000	45.000	50.000	56.000	73.000
Governor term limit dummy	1296	.258	.438	.000	.000	.000	1.000	1.000
<b>B. Extended sample (1962-2014)</b>								
State total tax per capita	2688	0.983	0.803	0.036	0.037	0.813	1.557	4.298
State income per capita	2736	13.268	4.016	4.147	10.348	12.960	15.879	27.974
Unemployment rate	2688	5.764	2.026	1.800	4.300	5.400	6.800	17.800
Proportion of young	2688	0.236	0.033	0.170	0.210	0.230	0.260	0.340
Proportion of elderly	2688	0.117	0.023	0.050	0.100	0.120	0.130	0.190
State governor's age	2736	53.557	8.134	33.000	47.000	53.000	59.000	78.000
Governor term limit dummy	2638	0.249	0.433	0.000	0.000	0.000	0.000	1.000

**Notes:** Summary statistics of variables (in levels) used in subsequent regressions. Besley and Case sample runs from 1962 to 1988 and extended sample until 2014. State total tax per capita is the sum of sales, income and corporation tax in thousands of 1982 US dollars. State income per capita in thousands of 1982 US dollars. Proportion of young is the proportion of the population between 5 and 17 years. Proportion of elderly is the proportion of the population aged 65 or older. State governor's age in years. Governor term limit dummy is equal to 1 if governor faces term limits in the current mandate. Data sources: State total tax per capita, Census of Governments (1972, 1977, 1982, 1987, 1992-2016) and Annual Survey of Government Finances (all other years); State income per capita, Bureau of Economic Analysis; Unemployment rate, Bureau of Labor Statistics; Proportion of young (aged 5-17) and elderly (aged 65+), Census Population & Housing Data; State governor's age and political variables manually sourced from individual governor's webpages on Wikipedia.

**Table A8: Exogenous Social Effects**

Dependent variable: Change in per capita income and corporate taxes  
Coefficient estimates, standard errors in parentheses

	(1) Initial	(2) OLS	(3) 2SLS: IVs are Characteristics of Neighbors	(4) 2SLS: IVs are Characteristics of Neighbors-of-Neighbors
Economic Neighbors' tax change (t - [t-2])	.645	.145** (.072)	.332* (.199)	.608*** (.220)
Economic Neighbors' income per capita	.090	.098*** (.011)	.091*** (.012)	.080*** (.014)
Economic Neighbors' unemployment rate	37.200	9.899*** (3.443)	11.780*** (2.856)	13.714*** (3.022)
Economic Neighbors' population aged 5-17	1378.1	376.2 (399.0)	478.5 (414.2)	596.6 (401.7)
Economic Neighbors' population aged 65+	-4304.5	-842.8 (504.3)	-769.7* (450.2)	-641.3 (468.6)
Economic Neighbors' governor age	-2.158	-0.311 (.281)	-0.293 (.285)	-0.263 (.294)
Period			1962-2015	
First Stage (F-stat)			9.571	10.480
Controls	Yes	Yes	Yes	Yes
State and Year Fixed Effects	Yes	Yes	Yes	Yes
Observations	2,952	2,952	2,544	2,592

Notes: \*\*\* denotes significance at 1%, \*\* at 5%, and \* at 10%. The sample covers 48 mainland US states running from 1962 to 2015. The dependent variable is the change in state's total taxes per capita in year t. In all Columns, we penalize geographic neighbors in all Columns and allow for exogenous social effects. In OLS and IV regressions, the economic neighbors' effect is calculated as the weighted average of economic neighbors' variables. OLS regressions estimates are shown in Column 2. Column 3 shows the 2SLS regression where each geographic neighbors' tax change is instrumented by lagged neighbor-of-neighbor's state income per capita and unemployment rate. Column 4 shows a 2SLS regression where each geographic neighbors' tax change is instrumented by lagged neighbor-of-neighbor's state income per capita and unemployment rate. At the foot of Columns 3 and 4 we report the p-value on the F-statistic from the first stage of the null hypothesis that instruments are jointly equal to zero. All regressions control for state's income per capita in 1982 US dollars, state's unemployment rate, the proportion of young (aged 5-17) and elderly (aged 65+) in state's population, and the state governor's age. All specifications include state and time fixed effects. With the exception of governor's age, all variables are differenced between period t and period t-2. Robust standard errors are reported in parentheses.

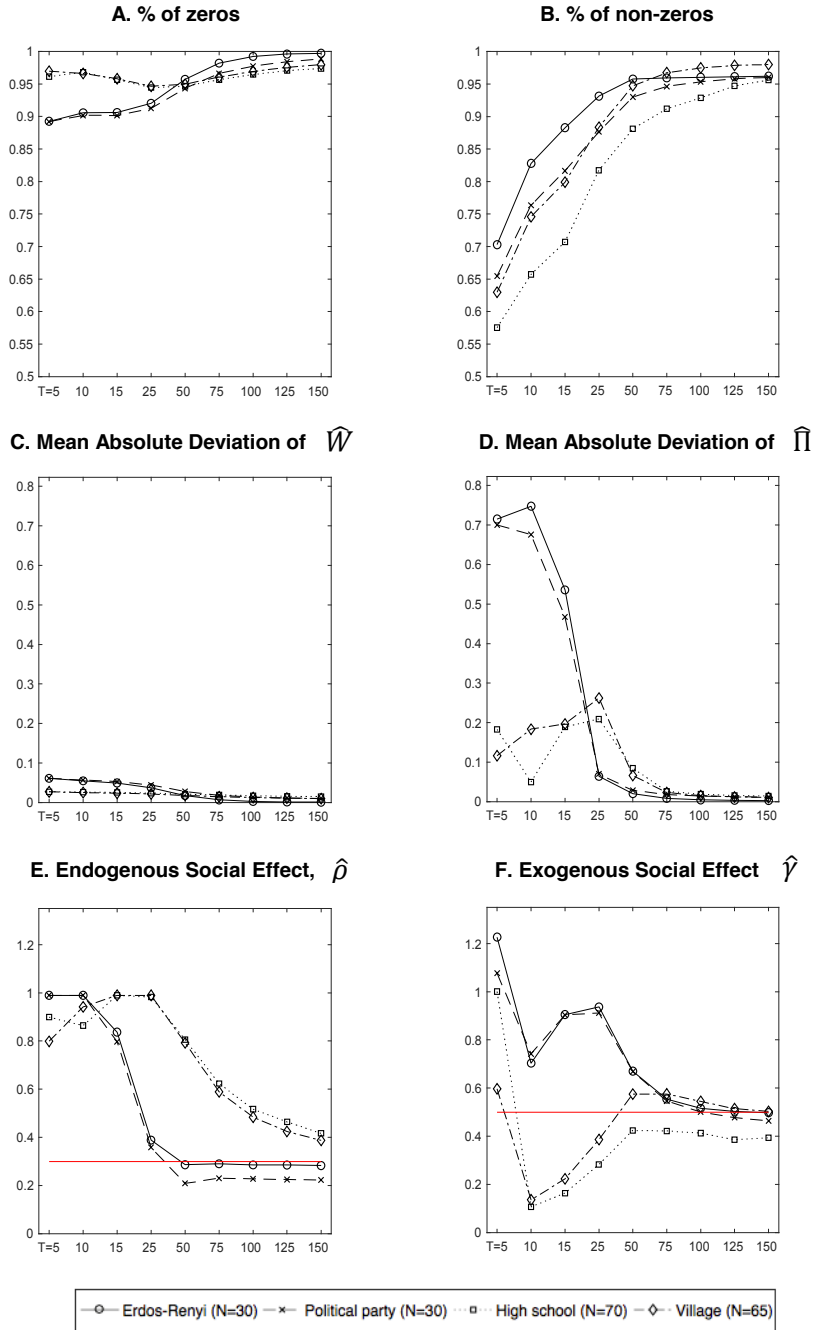


**Table A9: General Equilibrium Impacts of California Tax Rise**

	<b>Geographic Neighbor Network</b>	<b>Economic Neighbor Network</b>	<b>Ratio</b>
<b>Average tax increase</b>	0.0038	0.0066	1.74
<b>Variance tax increase</b>	0.0160	0.0153	0.96
<b>Tax dispersion</b>	0.0053	0.0141	2.66
<b>States with tax increase</b>	48	48	1.00
<b>States with tax increase &gt; 0.05%</b>	11	44	4.00
<b>States with tax increase &gt; 0.5%</b>	5	11	2.20
<b>States with tax increase &gt; 1%</b>	4	8	2.00
<b>States with tax increase &gt; 2.5%</b>	1	3	3.00
<b>States with tax increase &gt; 5%</b>	1	1	1.00

**Notes:** This shows the equilibrium impulse responses in taxes set in each state as a result of California increasing its tax change by 10%. The rho coefficient is derived from our preferred specification to estimate the economic network, where we penalize geographic neighbors to states, and allow for exogenous social effects (based on a sample of 48 mainland US states running from 1962 to 2015). We compare these derived tax changes under the identified economic network structure, relative to that assumed under a geographic neighbors structure. The final Column shows the ratio of the same statistic derived under each network.

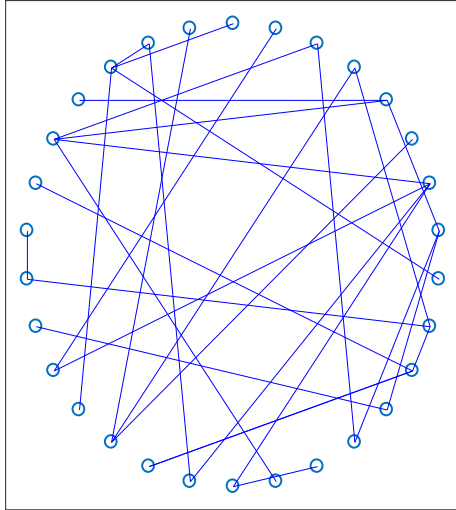
**Figure A1: Simulation Results, Adaptive Elastic Net GMM**



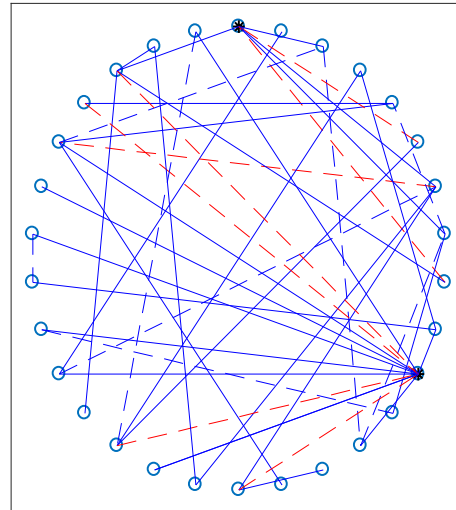
**Notes:** These simulation results are based on the Adaptive Elastic Net GMM algorithm, with penalization parameters chosen by BIC, under various true networks and time periods  $T=5, 10, 15, 25, 50, 100, 125$  and  $150$ . In all cases, 1000 Monte Carlo iterations were performed. The true parameters are  $\rho=0.3$ ,  $\beta=0.4$  and  $\gamma=0.5$ . In Panel A, the % of zeros refers to the proportion of true zero elements in the social interaction matrix that are estimated as smaller than  $.05$ . In Panel B, the % of non-zeros refers to the proportion of true elements greater than  $.3$  in the social interaction matrix that are estimated as non-zeros. In Panels C and D, the Mean Absolute Deviations are the mean absolute error of the estimated network compared to the true network for the social interaction matrix  $W$  and the reduced form matrix respectively. In Panels E and F, the true parameter values are marked in the horizontal red lines. The recovered parameter are the estimated parameters averaged across iterations. All specifications include time and node fixed effects.

## Figure A2: Simulated and True Networks

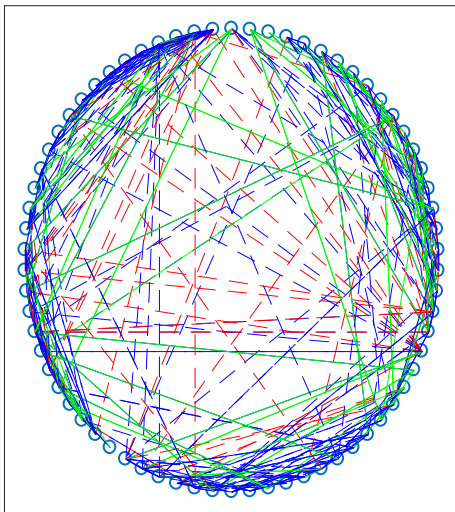
A. Erdos-Renyi



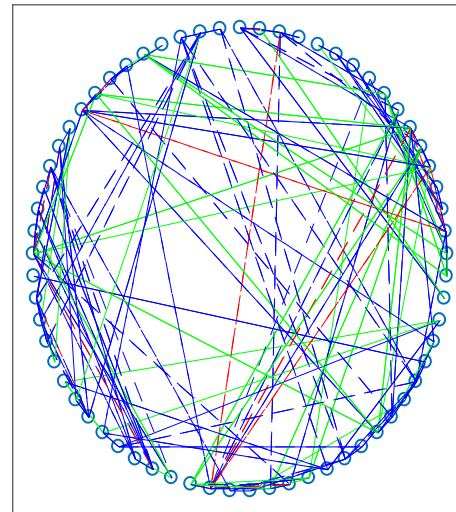
B. Political Party



C. High-school



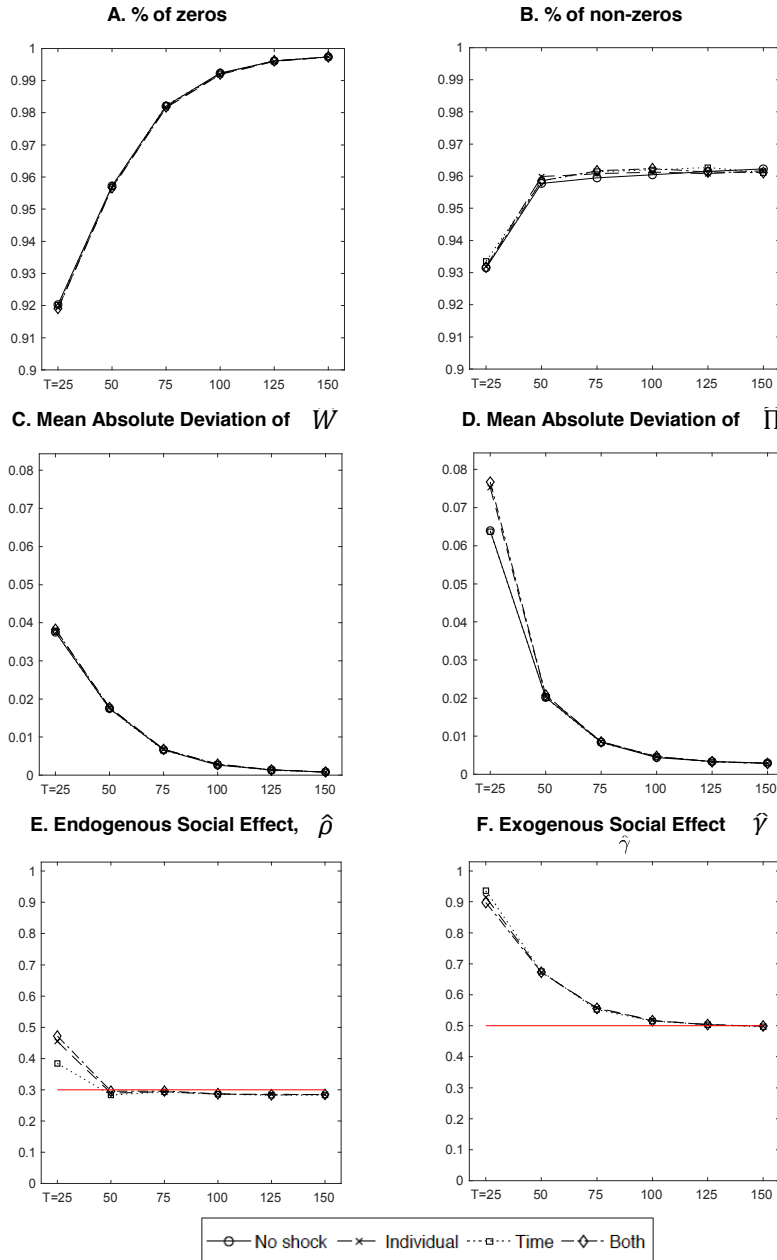
D. Village



**Notes:** These simulation results are based on the Elastic Net algorithm, with penalization parameters chosen by BIC, under various true networks and time periods  $T=50, 100$  and  $150$ . In the two stylized networks (Erdos-Renyi and political party), we set  $N=30$ , and the real world networks, the high school friendship and village network are based on  $N=65$  and  $70$  non-isolated nodes respectively. Party leaders in the political party network are marked in black in Panel B. In all cases, 1,000 Monte Carlo iterations were performed. The true parameters are  $\rho_0=0.3$ ,  $\beta_0=0.4$  and  $\gamma_0=0.5$ . All specifications include time and node fixed effects. Kept edges are depicted in blue: these links are estimated as non-zero in at least 5% of the iterations and are also non-zero in the true network. Added edges are depicted in green: these links are estimated as non-zero in at least 5% of the iterations but the edge is zero in the true network. Removed edges are depicted in red: these links are estimated as zero in at least 5% of the iterations but are non-zero in the true network. The figures further distinguish between strong and weak links: strong links are shown in solid edges (whose strength is greater than or equal to  $.3$ ), and weak links are shown as dashed edges.

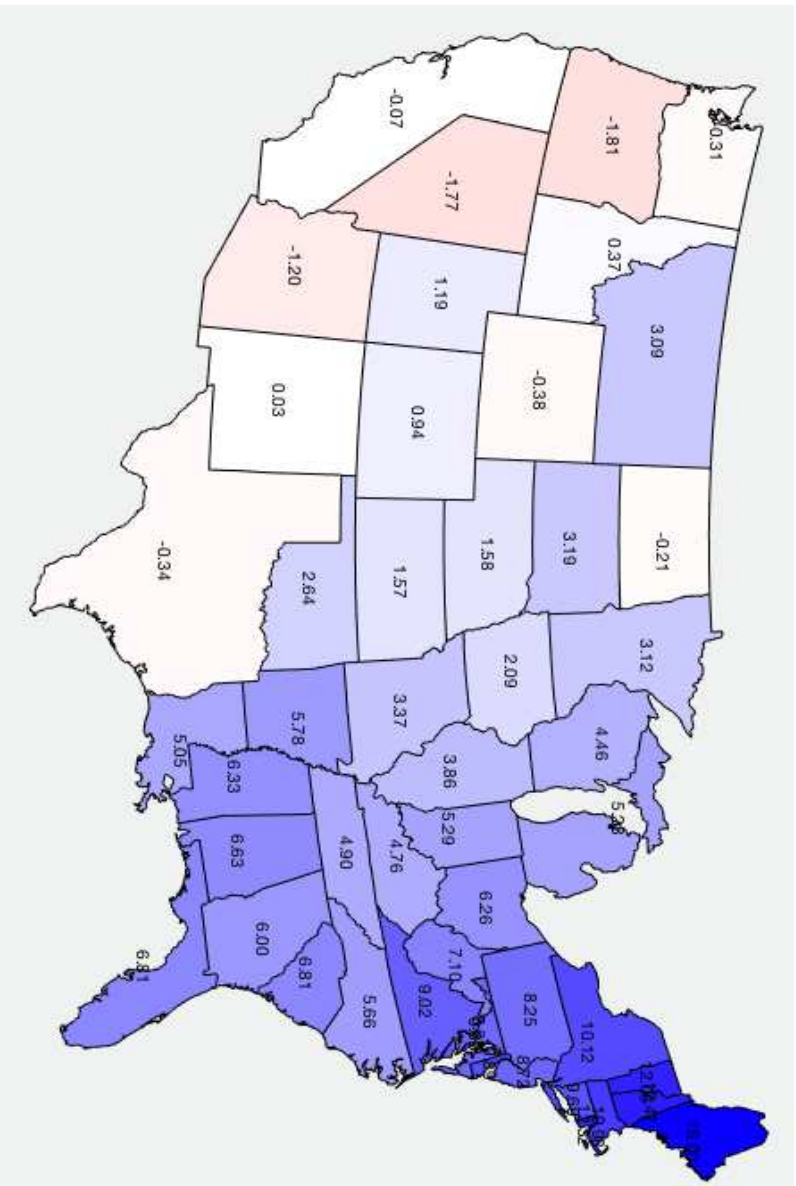
**Figure A3: Simulation Results, Adaptive Elastic Net GMM**  
**Alternative Structures of Shocks**

Erdos-Renyi graph (N=30)



**Notes:** Simulations with common shocks between the exogenous variable and the error term: time-constant and varying at the individual level ("individual"), constant across individuals and varying over time ("time") and both types of shocks. These simulation results are based on the Adaptive Elastic Net GMM algorithm, with penalization parameters chosen by BIC, under various true networks and time periods T=25, 50, 100, 125 and 150. In all cases, 1000 Monte Carlo iterations were performed. The true parameters are  $\rho=0.3$ ,  $\beta=0.4$  and  $\gamma=0.5$ . In Panel A, the % of zeroes refers to the proportion of true zero elements in the social interaction matrix that are estimated as smaller than .05. In Panel B, the % of non-zeros refers to the proportion of true elements greater than .3 in the social interaction matrix that are estimated as non-zeros. In Panels C and D, the Mean Absolute Deviations are the mean absolute error of the estimated network compared to the true network for the social interaction matrix  $W$  and the reduced form matrix respectively. In Panels E and F, the true parameter values are marked in the horizontal red lines. The recovered parameter are the estimated parameters averaged across iterations. All specifications include time and node fixed effects.

**Figure A4: General Equilibrium Impacts of CA Tax Rise Shocks**  
**State's Reaction to 10% increase in CA taxes**



**Log(equilibrium taxes under W-econ) - Log(equilibrium taxes under W-geo)**

**Positive values indicate higher equilibrium taxes under Economic neighbors than geographic neighbors**

**Negative values indicate low equilibrium taxes under Economic neighbors than geographic neighbors**

**Notes:** This shows the equilibrium impulse responses in taxes set in each state as a result of California increasing its tax change by 10%. This is as derived from our preferred specification, where we penalize geographic neighbors to states, and allow for exogenous social effects. We compare these derived tax changes under the identified economic network structure, relative to that assumed under a geographic neighbors structure. We graph the log change in equilibrium taxes under economic neighbors, minus the log change in equilibrium taxes under geographic neighbors. Positive values (red shaded) states indicate higher equilibrium taxes under economic neighbors than geographic neighbors, and negative values (blue shaded) states indicate lower equilibrium taxes under economic neighbors than geographic neighbors.